Understanding HIV-1- Neuropathogenesis Using 3D Brain Organoids: Role of Host and Viral Factors in Neuronal Dysregulation

by

Roberta Souza dos Reis

PharmD, Federal University of Rio Grande do Sul, 2007

MS.in Cell and Molecular Biology, Federal University of Rio Grande do Sul, 2011

Submitted to the Graduate Faculty of the

Graduate School of Public Health in partial fulfillment

of the requirements for the degree of

Doctor of Philosophy

University of Pittsburgh

2021

UNIVERSITY OF PITTSBURGH

GRADUATE SCHOOL OF PUBLIC HEALTH

This dissertation was presented

by

Roberta Souza dos Reis

It was defended on

January 21, 2021

and approved by

Amy Lynn Hartman, PhD, Associate Professor, Department of Infectious Diseases and Microbiology, Graduate School of Public Health, University of Pittsburgh

Amantha Thathiah, PhD, Assistant Professor, Department of Neurobiology, School of Medicine, University of Pittsburgh

Andrea Jeanne Berman, PhD, Associate Professor, Department of Biological Sciences, Molecular, Cellular, and Developmental Biology, University of Pittsburgh

Quasar Padiath, PhD, Assistant Professor, Department of Human Genetics, Graduate School of Public Health, University of Pittsburgh

Dissertation Director: Velpandi Ayyavoo, PhD, Professor, Department of Infectious Diseases and Microbiology, Graduate School of Public Health, University of Pittsburgh

Copyright © by Roberta Souza dos Reis

2021

Understanding HIV-1-Neuropathogenesis using 3D Brain Organoids: Role of Host and Viral Factors in Neuronal Dysregulation

Roberta Souza dos Reis, PhD

University of Pittsburgh, 2021

Abstract

Dendritic pruning and synapses loss are the major pathological hallmarks of HIV-1 associated neurocognitive disorders (HAND). However, the underlying mechanisms remain elusive mainly because of the lack of human representative *in vitro* models. Neurogranin (Nrgn) is a post-synaptic protein that is enriched in dendritic spines of neurons in healthy cortex and hippocampus. Interestingly, our group has identified that Nrgn expression is altered in *postmortem* tissue from HIV-1 positive individuals cognitively impaired, suggesting a role for this protein in the development of HAND. We hypothesized that HIV-1 induced inflammatory factors and/or viral proteins differentially regulate Nrgn levels in HIV-1, resulting in synaptic dysfunction and cognitive impairment. To address this hypothesis, we firstly developed a brain organoid as a more physiologically relevant tool to further HIV-1 neuropathogenesis studies *in vitro*. The incorporation of HIV-1 infected microglia to brain organoids resulted in a tri-culture that recapitulated the pathological hallmarks of HIV-1 neuropathogenesis as neuroinflammation, astrogliosis, synaptodendritic damage and neurodegeneration. Secondly, we showed that Nrgn is dysregulated in frontal cortex tissue from HIV-1 positive individuals at mRNA and protein levels before the emergence of cognitive symptoms. Further studies demonstrated that HIV-1 infection of macrophages/microglia alters the inflammatory milieu, leading to a transient downregulation of Nrgn mRNA in neurons, which in turn might disrupts the synaptic integrity. Lastly, we have identified a long noncoding RNA transcript (RP11-677M14.2) from the antisense strand of NRGN

locus which is up-regulated in *postmortem* tissue from HIV-1 positive individuals. Our *in vitro* results pointed out to a plausible role for RP11-677M14.2 in modulating Nrgn expression, and the lncRNA dysregulation may be mechanistic link between Nrgn loss and early stages of HAND.

This study contributes to public health because it describes a new brain-representative *in vitro* model with improved physiological relevance over standard 2D experimental models for investigating host-viral interactions. Our findings also shed new light on the molecular mechanism(s) underlying the dysregulation of synaptodendritic integrity, in particular those involved in decreased levels of neurogranin observed in HAND. Restoring neurogranin levels in neurons can potentially prevent or revert the synaptic injury alleviating the cognitive deficits in patients with HAND.

.

Table of Contents

List of Tables

List of Figures

Preface

This work would have not been possible without the support of a number of people to who I will be forever grateful. To begin with, I would like to thank my PhD advisor and mentor, Dr. Velpandi Ayyavoo. I deeply appreciate the opportunity you have given to me to be part of your lab and for dedicating so much of your time to make me a real scientist. You continually pushed me to overcome my limits and gave me all the opportunities to succeed, supporting me until the very end. I am also thankful for my co-worker Marc Wagner for always keeping Dr. Ayyavoo's lab a joyful and positive environment for everyone to work in. I appreciate your support and friendship over the years. Your passion for the HIV-1 research has always been very inspiring to me. I also thank to all the students in Dr. Ayyavoo's lab that have given to me the opportunity to participate in their projects, enriching my PhD experience.

I would like to thank my committee members: Dr. Amy Hartman, Dr. Amantha Thathiah, Dr. Andrea Berman and Dr. Quasar Padiath. You were all great committee members, helping me at different times and for various reasons over the years. I am grateful not only for your support in the timely and successful completion of my program but also for providing invaluable advice and suggestions. I also thanks to Dr. Shilpa Sant for her huge contribution to the 3D brain organoids model. This chapter of my dissertation would have not been possible without your guidance and persistance.

Finally, I would like to give a huge thanks to my entire family. To my mom, for being the force of my life, for giving your unwavering support and endless love throughout these crazy years. To my dad, for supporting my education and never accepting less than the best of me. My brothers, Rafael and Roberto for your love and support when I needed the most, even if it meant babysitting

Pedro during the school brakes while I had to work. To my husband Dover, my partner in this endeavor, my rock, my love, I could not have made it without you. I know it has not been easy, but I am deeply thankful for your immense patience, love and daily encouragement. To my son Pedro, my angel, my all. You have made me stronger, better and more fulfilled that I could have ever imagined. You are the reason this started, and I would never be here today without you.

1.0 Introduction

1.1 The HIV-1 Burden

Since early 1980's, Human Immunodeficiency Virus (HIV) has moved from a single report of an infection cluster to a global pandemic (1). There are currently 38 million adults and children living with the HIV-1 worldwide. These include the approximately 1.7 million individuals newly infected in 2019 (2).

HIV subtype 1 (HIV-1), the predominant agent of HIV pandemic, can be transmitted via the exchange of body fluids such as blood, breast milk, semen and vaginal secretions. The virus primarily targets subsets of CD4+ T cells and macrophages that are abundant in mucosal tissues. As the virus destroys or impairs the function of immune cells, infected individuals gradually become immunodeficient. The most advanced stage of HIV-1 infection is the Acquired Immunodeficiency Syndrome (AIDS), which can take from 2 to 15 years to develop. AIDS is defined by the development of certain cancers, infections, or other severe clinical manifestations (3-5).

There is no cure for HIV-1 infection and vaccination remains elusive. However, effective combination of antiretroviral therapies (ART) has drastically improved the health and survival outcomes by controlling the viral replication and by helping to prevent transmission. Global coverage of ART reached 67% at the end of 2019 and the gains in treatment are largely responsible for the decline in AIDS-related death in the last decade. Nevertheless, approximately 690,000 people died from HIV-1 related causes globally just in 2019 (2,6).

Although ART prolongs life and prevents AIDS-related complications, people living with HIV-1 (PLWH) have a disproportionate risk of developing comorbidities compared to HIV-1-negative people (7,8). Cardiovascular diseases, cancer and chronic diseases driven by liver, bone and kidney complications have been described as common comorbidities associated with HIV-1, including the individuals receiving ART (9). Among these complications that still impact health and quality of life of PLWH, HIV-1-associated neurocognitive disorders (HAND) pose unique challenges. Despite the prevalence of dementia due to HIV-1 infection has markedly reduced since the advent of ART, less severe forms continue to increase. It has been suggested that as many as 70% of HIV-1-infected individuals might have some degree of cognitive impairment despite long term ART. While the precise pathogenesis surrounding these disorders is still unclear, effective diagnostic and treatment options for HAND are limited. As such, efforts to better understand the mechanisms underlying neurodegeneration in HAND will be paramount in the improvement of HIV-1 therapy (10,11).

1.2 HIV-1 Neuropathogenesis and HAND

1.2.1 HIV-1 Neuroinvasion

Circulating monocytes enter the brain and differentiate into infiltrating and perivascular macrophages to replace those macrophages that have undergone injury. HIV-1 is believed to ride into the central nervous system (CNS) via the infected circulating monocytes early in the course of infection. Once the infected monocyte has crossed the blood-brain barrier and entered the central nervous system, it then differentiates into an infected brain macrophage. These brain macrophages

are the cell type most commonly infected by HIV-1 in CNS. The infected infiltrating and perivascular macrophages can then carry productive HIV-1 infection within the CNS. Thus, by using this "Trojan horse" mechanism, HIV-1 has found a way to evade the host immune system and enter the brain to establish infection (12).

1.2.2 Neuropathological Manifestations Associated with HIV-1

It usually takes 3 to 6 weeks to become seropositive after HIV-1 infection. During the early stage, known as seroconversion stage, most of HIV-1 infected individuals experience transient "acute HIV-1 syndrome" characterized for mild cognitive complaints, motor findings and neuropathy that tend to cease with early ART intervention (13,14). After the seroconversion period, HIV-1 infection enters a phase called the asymptomatic period which can last for years. During this period of clinical latency, neuropathological abnormalities are not consistent and often restricted to microglial proliferation and activation, and vascular inflammation. No significant neuronal loss is observed in the frontal cortex during this stage (15). On the other hand, non-apoptotic neuronal injuries, including dendritic pruning or aberrant sprouting, axonal disruption and synaptic degeneration were observed (16,17).

During advanced stage of HIV-1 infection, a myriad of pathological manifestations can be found within the CNS and are termed HIV-1 associated encephalitis (HIVE) (18). HIVE is characterized by widespread reactive astrogliosis, myelin pallor, and infiltration of peripheral monocytes that differentiate into brain macrophages and multinucleated giant cells as indicative of active viral replication. In addition, significant neuronal loss via apoptosis has been reported in the frontal cortex of AIDS patients (15).

Although pathological features of encephalitis associate with full blown dementia, these do not correlate well with milder forms of cognitive impairment (19). By contrast, synaptic alteration and dendritic loss in the brain of HIV-1 patients appear to correlate well with the clinical signs and severity of cognitive impairment (20,21).

1.2.3 HIV-1 Associated Neurocognitive Disorders (HAND)

HAND refers to a spectrum of neurological disorders ranging from asymptomatic neurocognitive impairment (ANI), an intermediate form termed mild neurocognitive disorder (MND) and the severe form, HIV-1 associated dementia (22). In the pre-ART era, HAD was the most common form of HAND and was almost invariably fatal. However, the prevalence of HAD has substantially declined with the widespread implementation of ART. As a result, HAD, the most severe form of HAND, is rare in the developed world today. Despite that, HAND remains a major cause of morbidity: 40% to 70% of HIV-1 seropositive individuals are estimated to have HAND (23-25). This proportion remains similar to that in the pre-ART era. It should be noted, however, that these HAND cases primarily represent the milder forms of the neurocognitive changes. Left undetected, they have the potential to significantly impact patient well-being, adherence to antiretroviral treatment and overall health outcomes. Currently, the diagnostic is clinical with neuropsychological performance testing, neuroimaging, and measurement of viral RNA in cerebral spinal fluid providing additional information (10,19,26). Unfortunately, despite its success in controlling systemic viral load, ART does not provide complete protection from the development and progression of HAND, probably due to poor penetration of drugs across the blood brain barrier. In addition, the prevalence of HAND is expected to increase as infected individuals have now longer lifespan. Although a variety of potential biomarkers for HAND have

been identified (25), the majority of these are actually markers associated with HAD rather than ANI and MND, which currently represent much more common forms of cognitive impairment.

To date, research has focused on uncovering biological mechanisms underlying the HAND onset and progression. A more complete understanding of the pathogenesis of HAND will help identify biomarkers and therapeutic targets for its prevention and treatment.

1.2.3.1 Neuropathogenesis of HAND

Neurons are not infected by HIV-1. However, neurons are vulnerable to indirect damage triggered by infected macrophages and microglia in the brain. (10). Though neuro- pathogenesis of HIV remains a puzzle, the consensus model of HIV-1 induced neurodegeneration is shown in **Figure 1** (18). Briefly, infected macrophages or microglia release virus particles, viral proteins, cytokines (for example TNF-α and IL-1β) and chemokines, which in turn activate uninfected macrophages and microglia. Once immune activated, these cells, together with activated astrocytes, release neurotoxic factors (for example, excitatory amino acids, free radicals, TNF-α) which promote neuroinflammation (reviewed in [18]). The neuroinflammatory milieu is thought to lead to excessive activation of glutamate receptor N- methyl-D-aspartate (NMDAR) on neurons (27). Potentiation of NMDAR is a common step that initiates synaptic changes. However, hyperactivation of NMDAR alters calcium influx to potentially lethal levels. In order to keep homeostasis, neurons can adapt to NMDAR overactivation by down regulation and loss of excitatory synapses. Moreover, this type of homeostatic plasticity may be reversible in neurons during the early stages of HAND (20). If the viral load is not controlled, the neuroinflammation may, in turn, amplify the direct effects of HIV-1, by facilitating HIV-1 replication or reseeding.

Once the pro-viral DNA has been integrated and the viral reservoir has been established in the brain, ART does not impact the production of viral proteins (28-30). Therefore, multiple mechanisms have been proposed as to how low level of viral proteins released from infected cells into the extracellular milieu can lead to neuropathogenesis even in virally suppressed individuals. These include the activation of uninfected glial cells by gp120, Vpr and Tat as the direct injury caused interaction of these molecules with neurons without any intermediate role of non-neuronal cells (31). The envelope protein gp120 has been shown to affect neuronal cell metabolism (32-34) via CXCR4 (35) and/or NMDA receptors (36,37) resulting in cell death. Additionally, gp120 and the accessory protein Vpr have been shown to directly induce neuronal apoptosis *in vitro* through activation of caspase 8 (38) and *in vivo* through activation of caspase 9 (39). Tat, an important regulator of viral transcription, can trigger neurodegeneration through NMDA receptors (40-42).

The mechanisms involved in HIV-1 neurodegeneration are complex and the effects are not mutually exclusive. Most of evidence thus far point to the hypothesis of chronicity and cumulative neuronal injury due to a combination of direct and indirect effects of HIV-1 infected and/or activated microglia/macrophages (20,21).

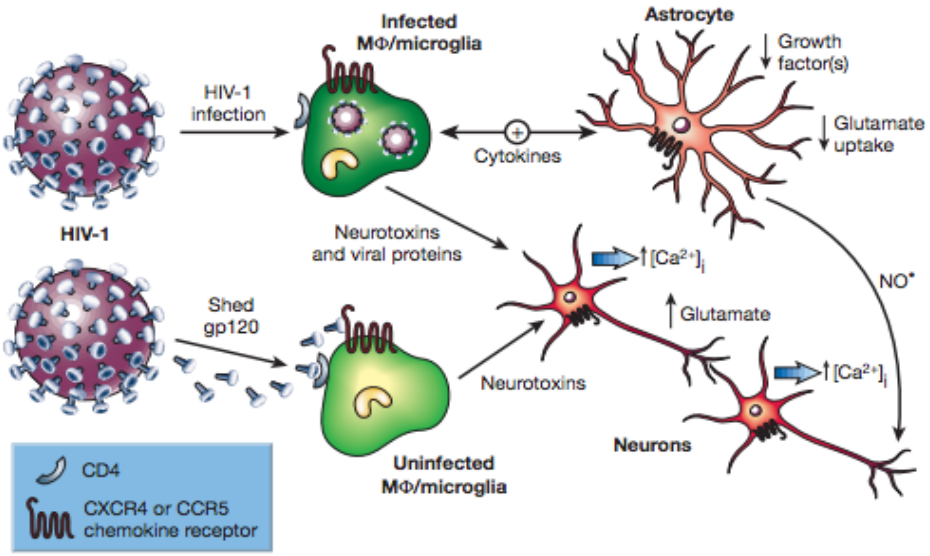

Figure 1. Current model of HIV-1-related neuronal injury (adapted from Ref. 18)

1.3 Modeling HIV-1 Neuropathogenesis *in vitro*

To better investigate the molecular mechanisms of HAND-related pathologies, a physiologically relevant model is crucial. Much of our current understanding of HAND has been derived from examination of post-mortem brains, supported by observations of SIV-infected non-human primates and experimental studies focused largely on tissue cultures. However, these model systems cannot recapitulate the unique and dynamic features of the interaction between the human brain and the human-specific virus as HIV-1.

One strategy to circumvent this limitation is the use of 3D brain organoids. The human brain organoids have the capacity to differentiate into different cells, self-organize and form complex interactions which make them ideal *in vitro* models to study the pathogenesis of neurological diseases (43). The neuropathology of HAND correlates with glial cells (microglia and astrocytes) activation and its consequences on neurons. Neuronal and synaptic damage could

be detected by immunohistochemical staining of various neuronal and synaptic markers. Thus, mixed cultures of human neurons and glial cells using the organoids technology would provide a promising *in vitro* setting to investigate molecular mechanisms during the HIV-1 induced neuropathogenesis.

1.4 Synaptic Plasticity Dysregulation and the Role of Neurogranin

Loss of synaptic elements as a result of activity or some pathology is thought to affect the plasticity of the remaining synapses in the network (20). The term synaptic plasticity is attributed to the ability of neurons to change the strength of synaptic transmission in response to changes in synaptic activity during learning and memory formation as well as the brain's ability to recover from injury or insult. Our current knowledge on learning and memory at the molecular level is based on what we know about long-term potentiation (LTP) and long-term depression (LTD) mechanisms, which dictate the signaling context that leads to neurotransmission amplification or attenuation. LTP induction requires the activation of NMDA receptors and a relatively large increase in Ca^{2+} concentration within the dendritic spines. This increase in local Ca^{2+} concentration within the dendritic spines (few seconds) causes a conformational change in Calmodulin (CaM) allowing it to activate Ca^{2+}/CaM-dependent protein Kinase II (CaMKII), which mediates AMPA receptor delivery to synapses. Interestingly, a small increase in postsynaptic Ca2+ causes CaM to activate calcineurin, resulting in the expression of LTD. Thus, through activation of two different prominent pathways within the same spine, CaM can lead to either LTP or LTD (44).

Neurogranin (Nrgn) is a post synaptic protein, enriched in dendritic spines (45), whose the main function is to sequester and bind the Ca^{2+}-free form of CaM (apo-CaM) (46,47). On rise of

the intracellular Ca^{2+} concentration, Nrgn releases CaM, freeing it to bind Ca^{2+} and to activate downstream signaling molecules as CaMKII. Indeed, overexpression of Nrgn increases CaMKII activation and enhances synaptic strength (48). Importantly, Nrgn mutants that are incapable of binding to CaM, or those that constitutively bind to CaM even in the high Ca2+ levels, are incapable of enhancing synaptic strength. Also, Nrgn-knockout mice suffer from learning and memory deficits (48,49). On the other hand, increase in CaM levels does not enhance synaptic plasticity. Thus, Nrgn acts as a potent regulator of postsynaptic signal transduction pathways and plays an important role in synaptic LTP (Summarized in **Figure 2** (50)). Of particular relevance, Nrgn highest expression during development coincides with the period characterized by rapid dendritic growth and formation of the majority of cortical synapses (51,52). Thus, it is widely thought that Nrgn expression play an important role in neuroplasticity and learning and memory.

In the attempt to address these questions and to better understand the molecular pathways underlying synaptic dysfunction, our group has recently found that Nrgn is dysregulated in HAND (53). Also, Nrgn levels in brain from HIV-1 infected individuals were shown to be correlated with the cognitive decline and pathology of HAND: lowest level of Nrgn was found in the most severe form of HAND. Further, co-immunoprecipitation assay showed reduced Nrgn-CaM interaction without significant difference in CaM expression. Thus, a more precise knowledge of the mechanisms involved in Nrgn dysregulation by HIV-1 will contribute to a better understanding of

the neuronal plasticity and consequently the molecular basis of synapses loss and dendritic pruning observed in *post-mortem* HAND brain.

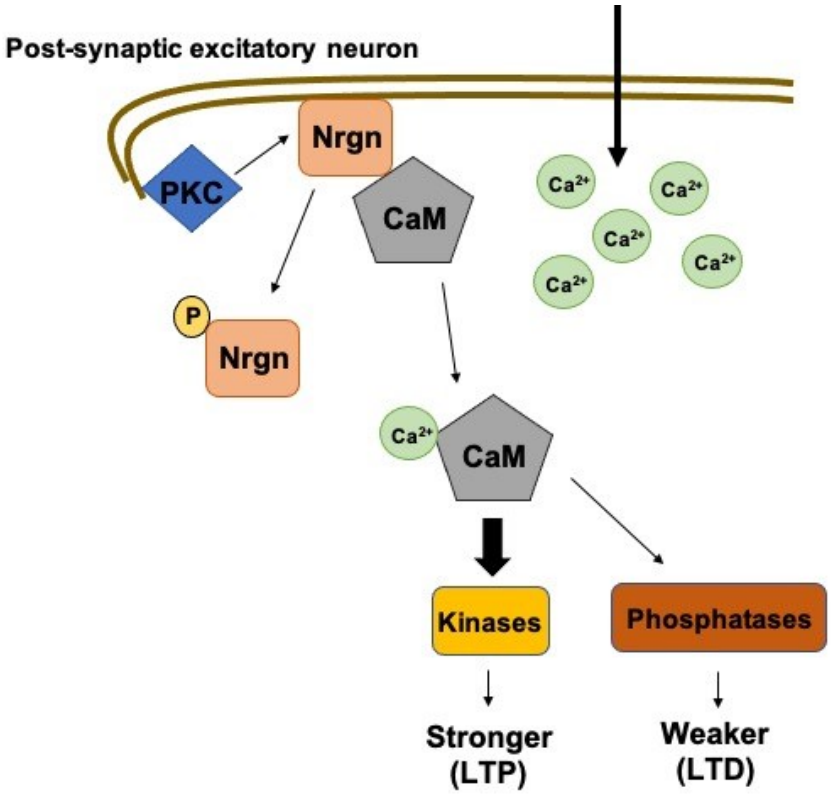

Figure 2. Schematic diagram illustrating the role of Nrgn in post-synaptic signaling pathway (adapted from Ref. 50)

1.5 Non-Coding RNAs in neurodegenerative diseases

Non-coding RNAs (ncRNAs) are functional RNA transcripts that do not encode proteins. Excluding structural housekeeping RNAs such as ribosomal, spliceosomal and transfer RNAs, ncRNAs can be generally divided into three classes according to the size of transcripts: ncRNAs with less than 50 nucleotides are considered as small ncRNAs, which include microRNA (miRNA)

and small interfering RNAs (siRNAs). Medium ncRNAs (50-200 nts) and longer ncRNA (>200 nts) are collectively referred to as large or long ncRNAs (lncRNAs) (54).

Unlike short RNAs and proteins, the function of lncRNAs cannot simply be inferred from their sequence or structure or even localization. Although, it has been shown that, like translated proteins, lncRNA have one or several modular domains that can bind either proteins and/or pair to nucleic acid sequences. Hence, lncRNAs are emerging as important components of gene regulatory networks, working in concert with transcription factors and epigenetic regulators of gene expression. Interestingly, many lncRNAs are highly expressed in the adult and developing brain, often showing precise temporal and spatial patterns of expression. This specificity of expression and growing awareness of the importance of lncRNAs suggest that they play key roles in CNS development and function (55).

Diverse available evidence shows the involvement of lncRNAs in neurodegenerative diseases. 17A, a lncRNA embedded in the GABA B receptor 2 (GABBR2) locus is dysregulated in brain tissues from patients with Alzheimer Dementia. 17A influences intracellular signaling pathways downstream of the associated GABA receptor by regulating its alternative splicing. In addition, 17A is expressed in response to inflammatory stimuli, and it promotes Aβ secretion and increases the pathologic Aβ42:Aβ40 ratio (56). Another lncRNA linked to AD is BACE1-AS, which is transcribed in an antisense orientation to the β-secretase-1 (BACE1) gene and modulates the expression of this enzyme (57). BACE-1 is essential for the generation of beta-amyloid, and the consequent amyloid plagues, which are central to the pathophysiology of Alzheimer. Exposure to harmful stimuli, including reactive oxygen species, chronic hypoxia and Aβ42, enhanced expression and nuclear–cytoplasmic translocation of BACE1-AS. lncRNAs are associated with cognitive and behavioral disorders in addition to Alzheimer dementia. For example, HAR1

expression is decreased in the striatum of patients with Huntington's disease, mediated by REST lncRNA (58). Furthermore, disrupted in schizophrenia 2 (DISC2) is implicated in neuropsychiatric disorders, such as schizophrenia, mood disorders and autism spectrum disorder (59).

We have identified a lncRNA transcript localized in the antisense strand in the NRGN locus. Although its biological role and putative mechanisms have yet to be investigated, preliminary data suggest that it is involved in Nrgn expression/translation regulation. Understanding the role of this lncRNA in Nrgn dysregulation during HAND onset and progression will help to develop new strategies to prevent or alleviate the cognitive deficits associated to HIV-1.

2.0 Hypothesis and Specific Aims

The **overall goal** of this work is to understand Nrgn dysregulation in HIV-1 neuropathogenesis to provide insights into HIV-1 induced cognitive impairment by using human relevant models. *My central hypothesis is that HIV-1 induced inflammatory factors and/or viral proteins differentially regulate non-coding RNAs and Nrgn levels in HIV-1 individuals, resulting in synaptic dysfunction and cognitive impairment*. My hypothesis was addressed through the completion of three specific aims that are summarized in **Figure 3**.

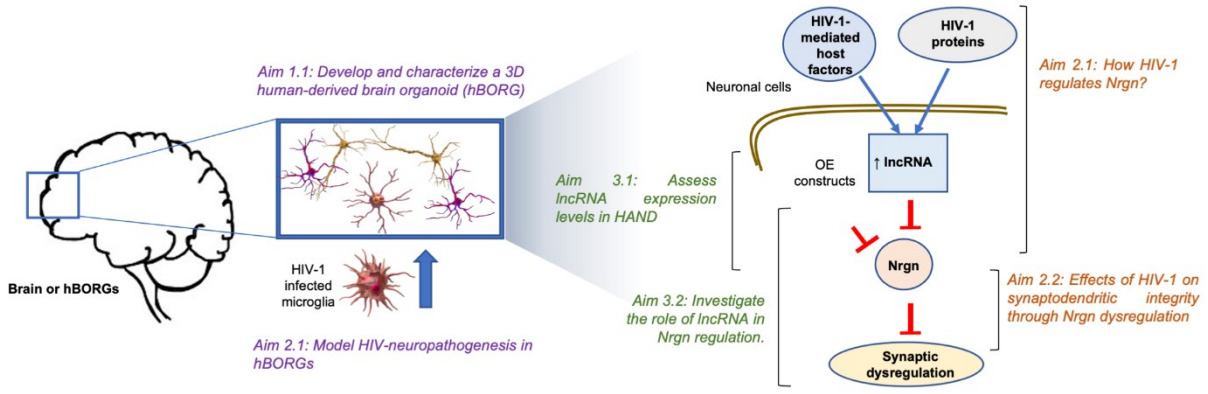

Figure 3. Schematic of Specific Aims hBORGs (human-derived brain organoids); lncRNA (long non-coding RNA); Nrgn (neurogranin), OE (overexpression)

2.1 Aim1: Develop a three-dimensional (3D) brain organoid tool to study HIV-1 neuropathogenesis

HIV-1 associated neurocognitive disorder (HAND) is characterized by neuroinflammation and glial activation that, together with the release of viral proteins, trigger the pathogenic cascade resulting in synaptodendritic damage and neurodegeneration, leading to cognitive impairment. However, the molecular events underlying HIV-1 neuropathogenesis remain elusive, mainly due to lack of brain-representative experimental systems to study HIV-1-CNS pathology. To fill this gap, I developed and characterized a 3D human brain organoid (hBORG) model. This model was further used to incorporation of HIV-1 infected microglia to mimic HIV-1 neuropathogenesis *in vitro*. The triculture system generated recapitulated hallmarks of HIV-1 neuropathology as neuroinflammation and neurodegeneration.

2.2 Aim 2: Elucidate how HIV-1 dysregulated Nrgn and correlates to synaptic dysregulates Nrgn and correlates to synaptic dysfunction and loss of dendrites

The underlying mechanism of early cognitive impairment is the synaptic dysregulation. One of the proteins that is directly involved in the efficiency of synaptic signal is Nrgn (50). Our data showed that Nrgn is dysregulated both at protein and mRNA levels upon HIV-1 infection of human frontal cortex. In addition, our preliminary results showed that Nrgn levels are depleted in brain before the loss of dendrites integrity, and consequently before the emergence of clinical symptoms. *In vitro* results showed that viral/host factors released by infected

macrophages/microglia contribute to Nrgn dysregulation in neurons. Moreover, our results indicated that this dysregulation is reversible.

2.3 Aim 3: Investigate putative mechanisms by which Nrgn is dysregulated- role of ncRNAs

In our pursuit to identify molecular mechanisms by which Nrgn expression is dysregulated in HIV-1, we have identified a lncRNA gene (RP11-677M14.2) of 1,704 base pair lengths, which is localized in the antisense strand in NRGN locus. We hypothesized that this lncRNA was transcribed and it was most likely involved in the regulation of Nrgn expression. The assessment of RP11-677M14.2 transcript levels in frontal cortex indicated that this lncRNA is significantly enriched in HAND-positive and HIV-1-positive individuals, respectively. We also investigated the correlation between the expression levels of both Nrgn and its anti-sense transcripts in frontal cortex and cerebellum and observed that RP11-677M14.2 transcript levels inversely correlates with Nrgn transcript levels specifically in the frontal cortex. To confirm the negative regulatory effect of RP11-677M14.2 on Nrgn transcription, we overexpressed this lncRNA in neuronal cells and found reduced Nrgn levels.

3.0 Development of the Three-Dimensional (3D) Human-Derived Brain Organoid Tool to Study HIV-1 Neuropathogenesis

This chapter includes results that were published in "*Dos Reis, R.S., et al., Modeling HIV-1 neuropathogenesis using three-dimensional human brain organoids (hBORGs) with HIV-1 infected microglia. Sci Rep, 2020.* ***10****(1): p. 15209."*

3.1 Introduction

Following systemic infection, human immunodeficiency virus-1 (HIV-1) infiltrates the brain by crossing the blood brain barrier (BBB) through infected monocytes from periphery (25,60,61). These infected monocytes differentiate to resident macrophages, release infectious particles to infect and expose permissive bystander resident cells, such as microglia and other glial cells(12,18). Neurons are not infected (62-64), yet these cells are most susceptible to dysfunction due to the presence of HIV-1 in the CNS(12,65-67). It has been proposed that low level of viremia along with inflammatory factors released by infected and/or exposed microglia and macrophages are implicated in selective synaptodendritic damage in neurons in the prefrontal cortex, which slowly evolves to CNS pathology (65-70). The neuronal dysfunction manifests as impaired cognitive function, a syndrome collectively called HIV-1 associated neurocognitive disorders (HAND), which affects more than 50% of HIV-1 positive individuals regardless of antiretroviral treatment (12,25,71,72).

Studies to delineate the mechanisms underlying early stages of HIV-1 neuropathogenesis are hampered due to the lack of brain-representative models available to study HIV-1 CNS disease. Although a variety of potential molecular players for HAND have been identified (25,68), much of our current understanding has been derived from examination of *post-mortem* brain tissue with HIV-1 associated dementia (22) (73). However, the less severe forms of disease, such as asymptomatic neurocognitive impairment (ANI) and mild neurocognitive disorder (MND), currently represent much more common forms of cognitive impairment, and *post-mortem* tissues do not allow the study of early stages of infection and disease progression. *Post-mortem* evaluations have been further supported by observations in the simian immunodeficiency virus (SIV)-infected non-human primates (74,75) and *in vitro* experimental studies utilizing two-

dimensional (2D) tissue cultures models (76-80). However, these approaches do not reflect the unique and dynamic features of the human brain physiology and inter-individual differences, notably those including the interaction with a human-specific virus as HIV-1. Therefore, developing an appropriate experimental model with relevant human neuronal cell lineages remains a high priority, since no therapeutic treatments are available to ameliorate the comorbid neurodegenerative disease.

Our strategy to circumvent these limitations is to develop a three-dimensional (3D) human brain organoid (hBORG) model built from human neural progenitor cells (NPCs). Human NPCs have the capacity to differentiate into distinct cell types in the brain and to self-organize to form brain-specific cellular architecture, making them ideal for use in developing a 3D *in vitro* brain organoid model to study neurological diseases (43,81,82). However, most of the available protocols for 3D brain organoids require complex and time-consuming protocols (82-86), and lack of microglia in the 3D organoids, the essential neuroinflammatory component of the associated pathological events required to accurately model HIV-1 neuropathogenesis (18,25,87).

Human microglia stem from myeloid precursor cells that originate from the embryonic yolk sac (88,89). These precursor cells migrate through the bloodstream to infiltrate the developing brain, where they undergo maturation (88,90). In the healthy adult brain, microglia constitute about 0.5-17% of total cells, depending on the brain region (91). Any disturbance that affects brain homeostasis such as infection, trauma or altered neuronal activity can elicit rapid and pronounced changes in microglial morphology, gene expression, and functionality that are associated with inflammation (88,89,92). Microglia and macrophages are the major cell types that are productively infected by HIV-1 in the brain (63,64). Although little is known about the exact pathological role of microglia in HIV-1 neuropathogenesis, its activation due to HIV-1 infection likely contributes

to neurotoxicity observed during HAND (25,26,68). While infection of astrocytes still remains controversial, astrocytosis is an important event in the HIV-1 associated CNS pathology (25,93). Thus, a 3D tri-culture experimental model is critical to investigate the mechanisms of HIV-1 induced neuropathogenesis; however, such model has not yet been explored for HIV-1 infection to the best of our knowledge.

Here, we have developed a 3D hBORG model using NPCs as precursor cells, which can self-organize and differentiate into major cell types found in the brain, including neurons and astrocytes. We further tested the ability of these hBORGs to support HIV-1 infection as well as to recapitulate the hallmarks of CNS pathology seen in HIV-1 patients by incorporating HIV-1 infected primary microglia. Our hBORG model displays both neuronal and glial characteristics, where cells self-organize in a complex network. To further model HIV-1 neuropathogenesis, we have successfully engineered a tri-culture system incorporating microglia into hBORGs recapitulating their natural infiltration process (88). Incorporation of HIV-1 infected microglia into hBORGs (MG-hBORGs) resulted in inflammatory response and induced damage to neurons and astrocytes, major hallmark features seen in the CNS of HIV-1 infected individuals. Collectively, our results suggest that this novel microglia-incorporated hBORGs (MG-hBORGs) provide a valid brain-representative *in vitro* model with improved physiological relevance over standard 2D experimental models for investigating the pathogenesis of HIV-1 in the human brain.

3.2 Materials and Methods

3.2.1 Isolation, culture of NPCs and differentiation of neurons and astrocytes

Primary human NPC cultures were adapted from the method developed by Hammond *et al*., 2002 (76) and Lu *et al*., 2011 (94). Human fetal cortical tissue (gestational age of 18-20 weeks) was obtained from medically or elective indicated termination of pregnancy through Magee-Women's Hospital of UPMC via the University of Pittsburgh, Health Sciences Tissue Bank. Written informed consent of the maternal donors was obtained in all cases, under IRB of the University of Pittsburgh guidelines and federal/state regulations. The use of human fetal cells to build human brain organoids was reviewed and approved by human individuals' institutional review board (IRB) of the University of Pittsburgh, in accordance with regulations of Declaration of Helsinki. Briefly, fetal cortical tissues were mechanically dissociated by pipetting. The tissue homogenate was passed through a 40 μm strainer to isolate single neuroprogenitor cells (NPCs). Cells were counted and plated on Poly-D-Lysine/Laminin-coated plates and kept in defined 2D differentiation media: Knockout DMEM/F12 (Invitrogen) supplemented with B27 plus (50x, Invitrogen) in serum-free media for neuronal differentiation or 1% FBS for astrocyte differentiation. For differentiation of mixed brain culture, we combined both B27 plus and 1% FBS in the basal media for culturing. Six weeks post culturing on tissue culture plates, more than 90% of the cells were differentiated and exhibited mature neuronal and/or astrocytic differentiation.

3.2.2 Fabrication of hydrogel microwell arrays

Non-adhesive hydrogel microwell arrays containing 70-80 microwells per 1x1 cm^2 were microfabricated using polyethylene glycol dimethacrylate (PEGDMA, 1000Da, Sigma) and polydimethyl siloxane (PDMS) molds as described previously (95-99). Each microwell was 600 μm in diameter and 600 μm in depth. First, PDMS molds were fabricated as described below. A prepolymer silicone elastomer base solution and curing agent were combined in a ratio of 10:1 (Sylgard 184; Dow Corning Corporation). After removal of bubbles by degassing, the mixture was poured onto a silicon master patterned with an SU-8 photoresist and cured at 75°C for 45 min. PDMS stamps containing micropillars were peeled from the silicon masters. The PDMS stamps were used to generate non-adhesive PEGDMA microwell arrays. PDMS stamps were placed on a PEGDMA 1000 (20% w/v) solution containing photoinitiator Irgacure-1959 (1% w/w; Sigma) and then photo-crosslinked by exposure to UV light (350−500 nm wavelength, 5 W/cm^2) for 45 seconds using the OmniCure Series 2000 curing station (EXFO). The PDMS stamp was then peeled from the substrate. The hydrogel microwell devices were sterilized in 70% isopropanol under UV for 1h, were washed three times with phosphate buffer saline (PBS) to remove isopropanol and observed under microscope for any imperfections/air bubbles. The sterilized devices were used to generate size-controlled neurospheres and hBORGs as described below.

3.2.3 Generation of neurospheres and human brain organoids (hBORGs)

Isolated NPCs were expanded in 175 mm flasks in NPC media (StemPro® NSC SFM media (Gibco) supplemented with 20 ng/mL of both human recombinant FGF and EGF (Gibco)). Half of the media was exchanged every 4 days with fresh media. Cultures were kept in a humidified

incubator at 37℃ and an atmosphere of 5% CO_2. NPCs were cultured statically in suspension until they formed loose aggregates (4-7 days). To generate size controlled neurospheres, NPCs (20 x 10^6 cells/device/50 μL NPCs media) were seeded on top of each microwell device (1x1 cm^2) and were allowed to settle inside the microwells (30 min), followed by addition of NPC media. The devices were incubated at 37℃ and an atmosphere of 5% CO_2. After 24h, the NPC media was changed to remove floating cells. Optimum compaction of neurospheres was observed when the borders were smooth and optically translucent, as observed by light microscopy (circa 4 days). When neurospheres were formed, the media was aspirated and replaced according to the four treatments to be tested. One set of devices was replenished with NPC media only (NS); another set of devices was replenished with mixed differentiation media (100) only (NS+DM). To test the effect of matrigel on boosting differentiation, two additional set of devices were prepared. Forty μL of matrigel (Corning) was applied on the top of the two sets of devices to cover all the neurospheres (70-80/1x1 cm^2 device) and allowed to gel by incubating for 30 min at 37˚C and culture media was replaced with either fresh NPC media (NS+M) or differentiation media (NS+DM+M). Half of media was routinely replenished every other day until the hBORGs were harvested for downstream analysis.

3.2.4 Cell culture of primary and immortalized microglia

HEK293T, U87MG $CD4^+$ $CCR5^+$ and immortalized HMC-3 microglia (ATCC® CRL-3304) were grown in DMEM supplemented with 10% FCS, 1% glutamine and 1% penicillin-streptomycin. All cell lines were kept in at 37℃ and 5% CO_2. Primary adult human microglia were obtained from Dr. Changiz Geula from Northwestern University. Briefly, microglia were isolated from the prefrontal cortex of a 71-year-old Caucasian male (*postmortem* interval of 31 hours).

Experiments were conducted with passages between 8 to 10. Brain tissue from this patient was obtained from Northwestern University Alzheimer's Disease Center Brain Bank (AG13854). The study was approved by the Northwestern University Institutional Review Board and conducted in accordance with the Helsinki Declaration. Written informed consent was obtained for the collection of human tissue. Culture was maintained as previously published (101).

3.2.5 Viral preparation

HIV-1 virus stocks were generated using the neurotropic proviral DNA construct pNL43-YU2-Env with enhanced green fluorescent protein (EGFP) as reporter gene. HEK293T cells ($2x10^6$) were transfected with 3.5 μg of proviral construct and 1.5 μg of vesicular stomatitis virus G (VSV-G)-Envelope expression plasmid using 15 μL PolyJet transfection reagent (SignaGen Laboratories) as described before (102). Viruses were collected 48h post transfection, centrifuged at 3000g and filtered (0.2 μm) followed by ultracentrifugation for 60 min at 20,000 rpm (4˚C) and stored at -80˚C until further use. Viruses were tittered using U87MG $CD4^+$ $CCR5^+$ permissive cells to determine the infectivity and plotted as infectious units/mL (IP/mL).

3.2.6 Infection of microglia and incorporation into hBORGs

Human primary microglia and immortalized HMC3 microglial cell line (ATCC CRL-3304) were infected with HIV-1 strain NLYU2-eGFP at a multiplicity of infection (MOI) of 1.0. Mock infection was performed using equal amount of PBS. Mock and infected cells were maintained in culture until infected cells expressed EGFP (72h p.i.). The proportion of cells expressing EGFP was estimated to be 30% using an inverted fluorescence microscope. Microglia

(both mock and infected) were detached from the flasks and labeled with tracking dye CellVue Claret Far red as a second color to distinguish between the uninfected microglia (red) and infected microglia (green+red). In parallel, two-week old hBORGs originated from NS+DM+M treatment were rinsed with PBS, and nuclei were labeled with Hoechst (1:1000 in PBS) for 1h. We have standardized the optimal density of microglia added to the hBORGs as 5% of total number of NPCs (1 microglia to 20 NPCs) based on previous studies on microglial density in the normal adult cortex(91,103). Labelled infected and mock-infected microglia ($1x10^6$ microglia/well) were added to the Hoechst-labeled hBORGs and were incubated without agitation for 24h to allow attachment of microglia to the hBORG surface. The MG-hBORGs were then carefully transferred to a new plate with fresh differentiation media to remove unattached MGs and were maintained in culture in differentiation media for an additional 15 days. Half of the media was changed every other day and supernatants stored in -80˚C until assayed.

3.2.7 Histology and Immunofluorescence

NPC-derived neurons and astrocytes were stained as described (76) to assess the differentiation into neuronal and/or astrocytic lineages. Antibodies and concentrations were the same as described for 3D immunostaining (Table S1). Staining of the hBORGs was carried out in 4-well or 8-well chambered cover glass (LabTek, Thermo Scientific Nunc). hBORGs were transferred from the original well followed by wash with PBS and fixation in 4% paraformaldehyde overnight at 4˚C. After fixation, hBORGs were either embedded and sectioned at 10 mm on a microtome as described(104), or followed by their immersion in 95% chilled methanol for 15 min on ice and another washing step in PBS for whole organoid staining. Permeabilization buffer was prepared by diluting Triton X-100 (0.1% v/v) in PBS. hBORGs were

incubated in permeabilization buffer for 1.5 h at room temperature, followed by washing with PBST (0.1% v/v Tween20 in PBS) 3 times for 5 min, each. Blocking/dilution buffer was prepared by adding BSA (3% w/v) in permeabilization buffer. hBORGs were incubated in blocking solution for 1h at room temperature followed by washing with PBST 3 times for 5 min each. Further, hBORGs were incubated with primary antibodies diluted in blocking buffer at 4˚C overnight followed by species-specific secondary antibodies at 4˚C overnight (**Table S1**). Post staining with secondary antibodies, hBORGs were washed 3 times with PBST and counterstained with 1x HOECHST (in PBS) at 4˚C overnight and washed with PBS and immersed in glycerol for storage and imaging. Paraffin sections were hydrated in a descending series of alcohol, followed by PBS. Finally, sections were circled with a Liquid Blocker Mini Pap Pen (Life Technologies), blocked, permeabilized and stained as previously described (104).

3.2.8 Confocal Microscopy

Confocal imaging was carried out using a Z-stacking function on the Olympus FV1000 inverted confocal microscope using step size of 5-10μm to allow visualization of the entire hBORGs and 0.5-1.5 μm for coverslips and paraffin sections. Maximum intensity Z-projections were generated using Olympus Fluoview FV10-ASW 4.2 software. For supplementary movie S1 generation, Z-stacks of the entire hBORG were acquired and exported as mp4 format in an interval of 500 ms between. Images shown are representative of cultures generated from 3 independent experiments and from 2 independent tissue donors derived NPCs.

Table 1: Antibodies resources

Antibody to:	Host species	Dilution	Manufacturer
βIII-Tubulin (clone Tuj-1)	mouse	1:200	R&D Systems
MAP2	mouse	1:200	Merck
GFAP	chicken	1:500	Abcam
SOX2	rabbit	1:200	Bioss
Nestin	mouse	1:200	R&D Systems
NeuN	rabbit	1:200	Proteintech
VGlut1	rabbit	1:200	Sigma-Millipore
VGAT	rabbit	1:100	Proteintech
TH	mouse	1:100	Proteintech
PSD95	rabbit	1:100	Abcam
Synaptophysin	mouse	1:100	Novus Biologicals

3.2.9 Cell viability assay and image analysis

Cell viability of neurospheres and hBORG was checked using the LIVE/DEAD staining kit (488/570, Molecular Probes, Life Technologies) as per manufacturer's specifications. Images were taken on the inverted Olympus FV1000 microscope, with identical acquisition settings and processed using ImageJ 1.52q (National Institutes of Health, USA).

3.2.10 ELISA

Levels of IL-1β and TNF-α were measured in the supernatants from MG-hBORGs containing HIV-1 and mock-infected microglia and hBORGs alone by standard sandwich ELISA using human DuoSet ELISA kit (R&D Systems) following the manufacturer's protocol.

3.2.11 Cytotoxicity

LDH activity was measured to assess cell damage/cell death in supernatants from HIV-1 infected MG-hBORGs compared to mock-infected MG-hBORGs by CyQUANT LDH Cytotoxicity assay kit, as per manufacturer's protocol. Results were plotted as percentage of cytotoxicity using the following formula: [sample LDH activity-spontaneous LDH activity/Maximum LDH activity-spontaneous LDH activity] x 100.

3.2.12 RNA extraction and quantitative real time PCR

RNA was isolated from hBORGs using the MirVana kit (ThermoFisher) as per manufacturer's recommendations. The concentration and purity of the RNA were measured by NanoDrop p2000 spectrophotometer (ThermoFisher Scientific) and RNA quality by Bioanalyzer (RIN values between 8 and 9.7). cDNA was prepared from 200 ng to 400 ng of total RNA using a high-capacity cDNA reverse transcription kit (ThermoFisher) in 20 µL total volume reaction. Quantitative real time PCR was performed using TaqMan Universal PCR master mix and the appropriate TaqMan assays or primers (**Table 2**) with 2 µL of the cDNA reaction mixture. Assays were conducted using an ABI Vii7 real time PCR system in the following cycling conditions:

activation of Taq DNA polymerase at 95°C for 10 min, followed by 40 cycles of amplification at 95°C for 15 s and 60°C for 1 min. Results were normalized to the expression of the endogenous control Ribosomal Protein Lateral Stalk Subunit P0 (RPLP0).

3.2.13 Statistical analysis

Expression level of specific transcripts in hBORGs and cells were calculated by the $2^{-\Delta\Delta Ct}$ method and expressed as fold change to undifferentiated NPCs or mock-infected hBORGs. Statistical analysis was performed using GraphPad Prism, version 7.0 (GraphPad Software, La Jolla, CA, USA). Statistical significance was calculated using unpaired t-test and $P<0.05$ was considered significant.

Table 2: RT-PCR primer sets and probes used in this study

mRNA	Description	5'-3' sequence
Nestin	Assay ID	Applied Biosystems TaqMan® Gene Expression Assays ID: Hs04187831_g1
βIII-Tubulin	Assay ID	Applied Biosystems TaqMan® Gene Expression Assays ID: Hs00801390_s1
MAP2	Assay ID	Applied Biosystems TaqMan® Gene Expression Assays ID: Hs00258900_m1
GFAP	Assay ID	Applied Biosystems TaqMan® Gene Expression Assays ID: Hs00909233_m1
Iba1 (AIF1)	Assay ID	Applied Biosystems TaqMan® Gene Expression Assays ID: Hs00610419_g1
SS-Gag	Primer F	TCTCTAGCAGTGGCGCCCGAACA
	Primer R	TCTCCTTCTAGCCTCCGCTAGTC
	Probe	CGGGAGTACTCACCAGTCGCCGCCCCTCGCCCTCCCG
MS-Gag	Primer F	CTTAGGCATCTCCTATGGCAGGAA
	Primer R	TTCCTTCGGGCCTGTCGGGTCCC
	Probe	GGGCCTTCTCTATCAAAGCAACCCACCTCCAGGCCC

3.3 Results

3.3.1 Optimized mixed culture protocol efficiently drives differentiation of both neurons and astrocytes simultaneously

NPCs are self-renewing and multipotent cells that can give rise to almost any cell type of developing brain (105). Here, we tested the generation of 2D mixed brain cultures from NPCs by using the combination of neuronal media and astrocyte differentiation media in comparison with single lineage differentiation media. Immunostaining was performed in mixed brain cultures using specific neuronal (TuJ-1, a βIII-Tubulin epitope) and astrocyte (GFAP) markers along with the single differentiation cultures at week 2, 4 and 6 post differentiation (**Figure 4A**). Single neuronal and astrocyte cultures expressed TuJ-1 and GFAP, respectively as early as two weeks (**Figure 4A, neurons and astrocytes panels**). On the other hand, in mixed cultures, a TuJ-1-positive signal appeared on week 4 and increased by week 6 while a GFAP-positive signal was observed as early as 2 weeks (**Figure 4A, mixed culture panel**). Similar results were obtained by assessing mRNA expression of these markers. Comparison of the expression of the neuron-specific cytoskeletal marker βIII-Tubulin between single **(Figure 4B)** and mixed culture **(Figure 4C)** differentiation protocols indicated that both protocols lead to peak expression of βIII-Tubulin on day 28 in culture (3.9-fold and 3.3-fold change from monoculture and mixed cultures, respectively, compared to NPCs). Expression of the astrocytic marker GFAP increased by 38.8-fold at the initial phase of single culture differentiation (day 7), peaked on day 28 and plateaued afterwards (**Figure 4D**).

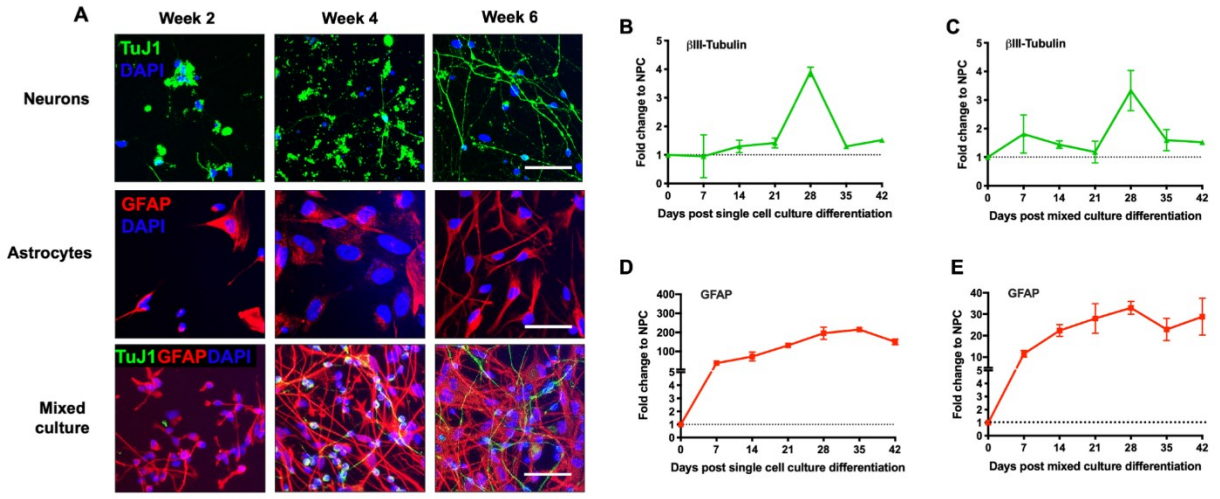

Figure 4. Differentiation and characterization of mixed 2D primary brain cultures. (A) NPCs were differentiated into either single culture or mixed cultures according to the protocol described and characterized for expression of cell specific markers by immunofluorescence. Representative images comparing single cell and mixed culture differentiation are depicted. Neurons were stained with βIII Tubulin Tuj1 (green) and astrocytes were stained with GFAP (red) and nucleus with Dapi (blue) at week 2, 4 and 6 post differentiation. Scale bar, 50 µm. (B & C) Time-course RNA analysis of the neuronal marker βIII Tubulin expression during differentiation in monocultures compared to mixed culture by RT-qPCR. (D & E) Time-course analysis of GFAP RNA, astrocyte marker expression during differentiation in monocultures compared to mixed culture by RT-qPCR. Fold change was calculated by normalizing expression level in undifferentiated NPCs in (N=3) independent experiments.

Although less robust, the increase in GFAP expression in mixed culture followed the same trend as single culture (**Figure 4E**). Together, our results suggest that the optimized mixed culture protocol is equally efficient as single culture differentiation protocol to drive differentiation of both neurons and astrocytes simultaneously. Moreover, neurons in the mixed culture express markers of mature neurons such as MAP2 (**Figure 5A)** and markers of synaptic activity including synaptophysin (SYN) and PSD95 (**Figure 5B**) at week 6, suggesting that our mixed culture differentiation protocol results in mature neurons.

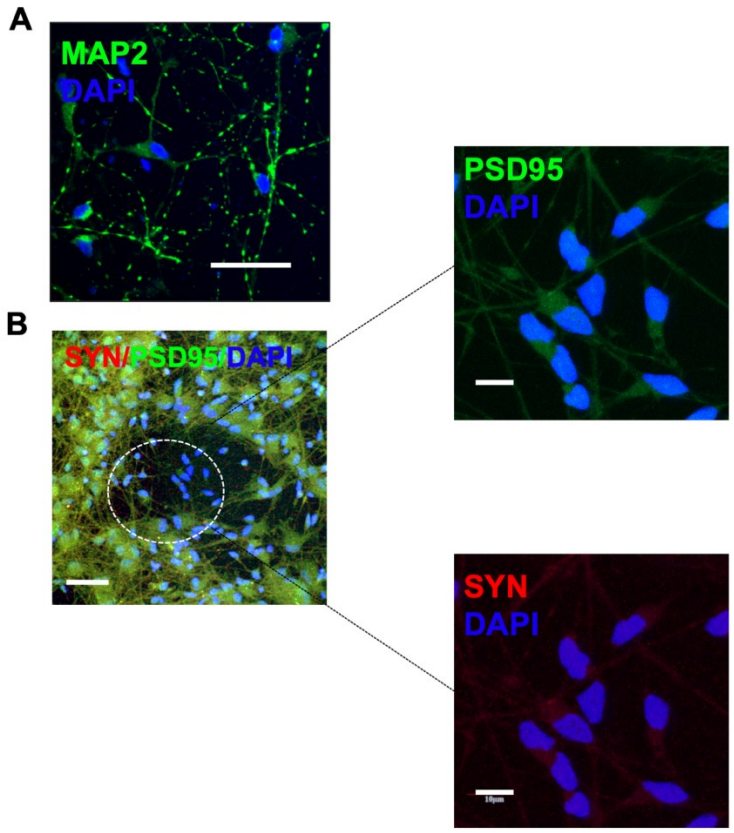

Figure 5. Characterization of neuronal population in 2D mixed primary cultures. NPCs were differentiated to neurons for 6 weeks according to protocol and characterized by immunofluorescence for expression of (A) MAP2 (green) as mature neuronal marker; (B) Synaptophysin (red) and PSD95 (green) as markers of synaptic integrity. Nucleus was stained with Dapi (blue). Scale bar, 50 μm.

3.3.2 Human NPCs aggregate to form human brain organoids (hBORGs) upon treatment with mixed differentiation media

Based on the results obtained with our mixed differentiation of brain cells from primary NPCs in 2D monolayers, we next developed a 3D culture platform to generate brain organoids.

Therefore, we adapted a hydrogel microwell platform previously described for generation of uniform size microtumors to generate uniform size brain organoids in a high throughput manner(95-99). NPCs were seeded onto the hydrogel devices containing multiple 600μm microwells that enabled formation of aggregates, referred henceforth as neurospheres (NS) within 24-48h (**Figure 6A**). Each 1x1 cm^2 device generated 70-80 NS simultaneously. NS were grown in NPC media until they were compacted (4 days). To determine the size variations of the NS, their diameters were measured 4 days post culture. Overall, the average size of the neurospheres were ~369±36μm (**Figure 6B**). Assessing the viability of compacted NS indicated that cells were viable at least for 4 weeks (**Figure 7).** To generate human brain organoids (hBORGs) from these NS, we tested two different protocols for differentiation: culturing NS in mixed differentiation media only (NS+DM, **Figure 6A, panel c**) or NS overlaid in matrigel matrix and supplemented with mixed differentiation media (NS+DM+M, **Figure 6A, panel d**). To tease out the contribution of the matrigel to cell differentiation, we carried out cultures of NS only as a negative control **(Figure 6A, panel a**) and NS overlaid with matrigel supplemented with NPC media **(Figure 6A, panel b)**. We monitored these four culture conditions for morphological changes for 7-14 days. Results suggest that NS only and NS+DM treatment triggered retraction of NS boundaries (**Figure 6A, panels a and c**), whereas the addition of matrigel with or without differentiation media triggered spontaneous outgrowth of projections from NS resembling neurites within the first 24h (**Figure 6A, panels b and d, and Figure 8, panels A and B)**. Continuation of culture for 14 days in differentiation media along with matrigel showed that these neurites appeared to fuse to neurites of adjacent organoids that became tightly interconnected (**Figure 6A, panel d and Figure 8, panels C and D**). To further characterize the differentiation capabilities of the organoids, we first assessed the expression of neuronal progenitor marker, Nestin, both at mRNA and protein levels.

Compared to non-differentiation conditions (NS only and NS+M), both differentiation treatments (NS+DM and NS+DM+M) led to a significant decrease (3.4-fold and 7.5-fold, respectively, compared to NPCs) in levels of Nestin mRNA over time (**Figure 6C**), suggesting the transition of progenitor cells to differentiated phenotypes. Similarly, a significant reduction of Nestin positive cells was also observed in NS+M and NS+DM+M at day 7 by Nestin-specific staining, which virtually disappeared at day 14 in NS+DM+M cultures (**Figure 6D**) indicating a transition from a proliferating to a post-mitotic state.

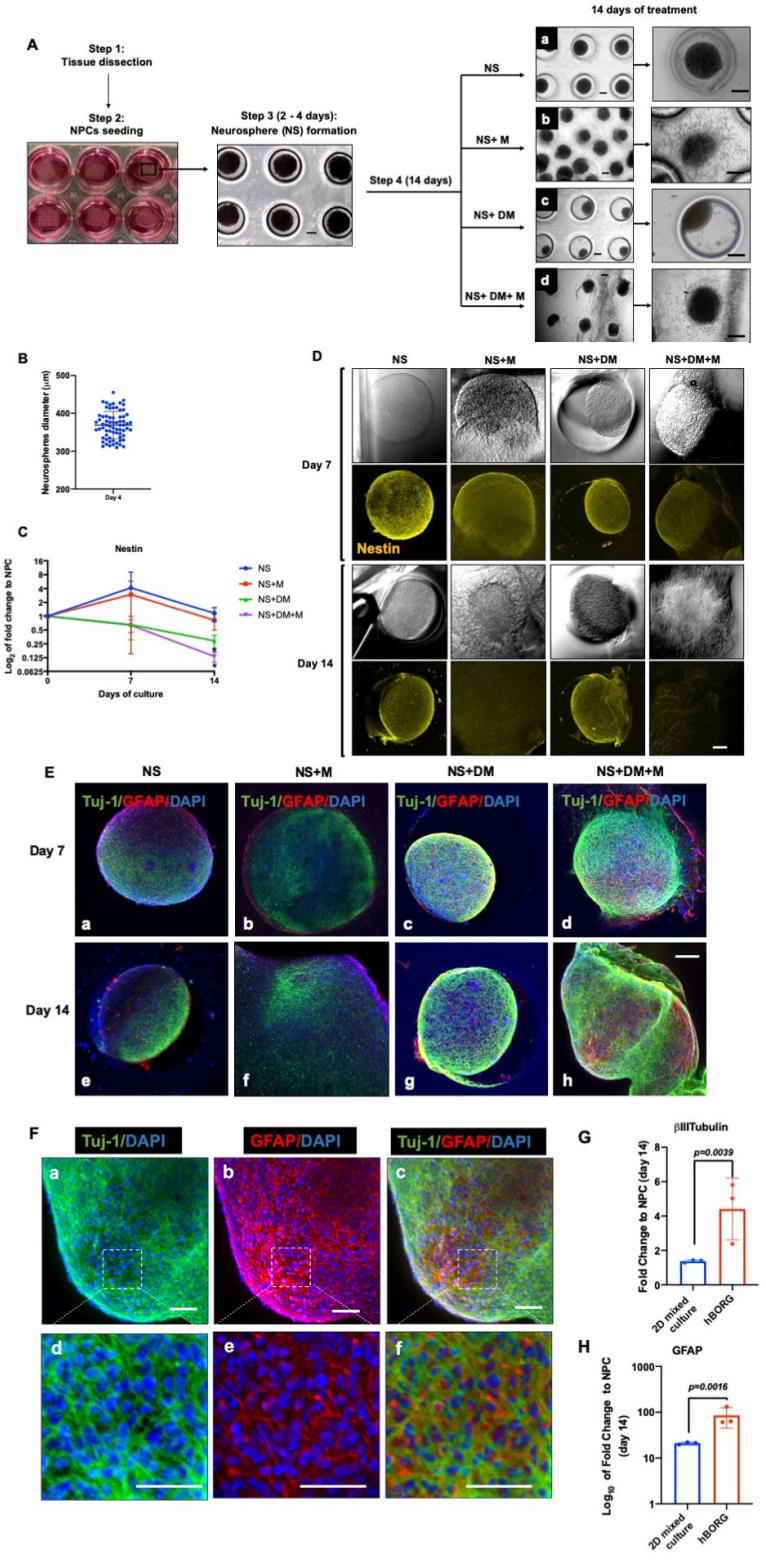

Figure 6. Generation and characterization of size controlled hBORGs from human NPCs. (A) Schematics to illustrate the hydrogel devices and experimental design to generate neurospheres from NPCs (step 2). Bright field

images show formation of uniform-sized neurons. neurospheres in the microwells 2 to 4 days post culture (step 3). Step 4: Phase-contrast images of neurospheres captured 14 days post treatment in different culture conditions: neurospheres in medium only (panel a), neurospheres in medium plus matrigel overlay (panel b), neurospheres in differentiation medium only (panel c), and neurospheres in differentiation medium plus matrigel overlay (panel d). Scale bar, 100 μm. Higher magnification of resulting organoids are shown at the right panel. Scale bar, 200 μm. (B) Size distribution of neurospheres on day 4 post seeding, size of multiple neurospheres (N=70) from 5 different devices were calculated as described in methods and the size distribution is presented. (C) Expression of the neuroprogenitor marker, Nestin was measured by RT-qPCR on 14 days post differentiation in different treatments conditions as indicated. NS, neurospheres in culture medium; NS+M, neurospheres in culture medium and martigel; NS+DM, neurospheres in differentiation medium; NS+DM+M, neurospheres in differentiation medium with matrigel. Amount of Nestin RNA transcripts in organoids was normalized to undifferentiated NPCs. Statistical significance was determined by unpaired Student's t tests, *$p<0.05$ of three independent experiments (N=3). (D) Expression of Nestin was assessed by immunofluorescence using anti-Nestin antibody. Representative confocal images validate decreased level of Nestin (yellow). Scale bar, 100 μm. (E) Expression of neuronal marker, βIII-Tubulin Tuj-1, (green) and glial marker, GFAP (red) was determined in all four different treatments by immunofluorescence on day 7 and 14 post differentiation. Nucleus was stained with Dapi (blue) Scale bar, 100 μm. (F) Expression of neuronal marker, βIII-Tubulin Tuj1 (green) and astrocyte marker, GFAP (red) was measured in neurospheres cultured in differentiation medium with matrigel on day 14 post differentiation. Scale bar in panel a, b and c is 50 μm and in panel d, e and f is 100 μm. Orthogonal analysis of Z-stack is shown in panel f. (G & H) Expression level of βIII-Tubulin (G) and GFAP (H) RNA transcripts in hBORGs compared to 2D mixed culture 14 days post differentiation (N=3). Fold change was calculated by comparing the level of RNA in undifferentiated NPCs. Statistical significance was calculated using unpaired Student's t test and the p value is indicated in the figure. (I) Cell viability in hBORGs was assessed by live/dead assay and imaged. Images represent live cells (green) and dead cells (red) are shown from one of the representative experiments (N=3). Scale bar, 100 μm.

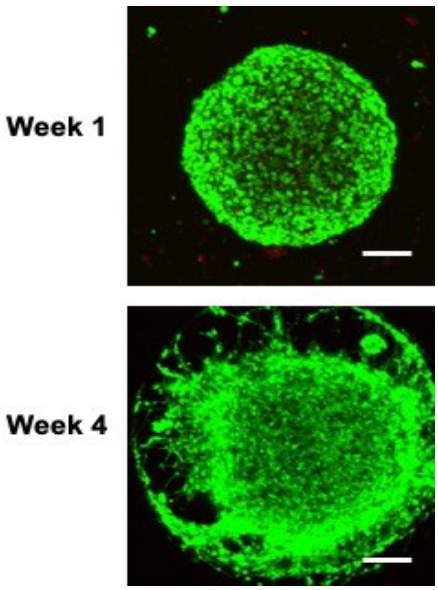

Figure 7. Determination of the viability of neurospheres before differentiation by live/dead staining. NPCs were seeded on hydrogel devices to form uniform size neurospheres. Cell viability in neurospheres was assessed by live/dead assay and imaged. Images represent live cells (green) and dead cells (red). Scale bar, 100 μm.

Next, to characterize the differentiated cell lineages within the organoids, we stained the organoids from all four groups for specific neuronal (TuJ-1) and astrocyte (GFAP) markers. As expected, qualitative assessment of the staining intensity on day 7 post treatment exhibited a strong signal for TuJ-1-positive neurons, when NS were cultured with differentiation media (**Figure 6E**, **panels c and d**). However, distinct neuronal and glial cell populations could be clearly observed only in matrigel embedded organoids treated for 7 days with mixed differentiation media (**Figure 6E**, **panel d**). Additionally, the same treatment (DM+M) led to accumulation of GFAP-positive signal 14 days post differentiation (**Figure 6E, panel h**). In contrast, NS cultured in non-differentiation conditions (NS and NS+M) induced less differentiation into TuJ-1-positive neurons by day 7 without further improvement by day 14 **(Figure 6E, panels a, b, e and f)**. Similarly, lower levels of GFAP+ astrocytes were observed by day 14 in non-differentiation conditions

(**Figure 6E**, **panels a, b, e and f**). Immunostaining results also suggested that addition of matrigel may have shifted the ratio of neurons/astrocytes towards neuronal population (**Figure 6E, panel h**). Overall, addition of matrigel to the culture containing differentiation media (NS+DM+M) produced the best response in terms of expression of neuronal and astrocytic markers. Higher magnification images of the NS+DM+M-treated cultures revealed an intricate network of neurons and astrocytes **(Figure 6F, a-e)** as revealed by orthogonal projection of zoomed confocal images (**Figure 6F, panel f)**. To compare the efficacy of simultaneous differentiation of the 2D vs. 3D cultures (NS+DM+M treatment), towards neuronal and astrocyte lineages, we quantified βIII-Tubulin and GFAP expression by RT-qPCR at day 14 (**Figure 6G and 6H**). Comparison between 2D mixed cultures and hBORG cultures demonstrated that both neuronal and astrocytic differentiation were promoted significantly (2.9-fold and 4-fold, respectively) in 3D cultures, reflecting the ability of 3D microenvironment to promote faster NPCs differentiation *in vitro*. Taken together, these results suggest that 3D-NPC cultures treated with matrigel and differentiation media displayed decreased NPC stemness, enhanced simultaneous differentiation into both neuronal and astrocytic lineages, and induced spatial organization with intricate cellular networks in each individual organoid while simultaneously generating 70-80 human brain organoids (hBORGs) in one device.

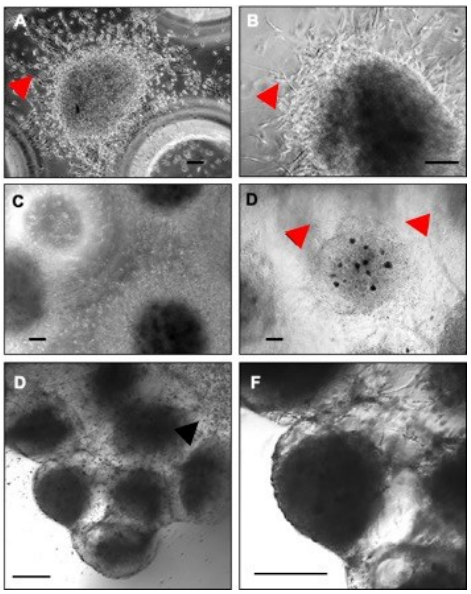

Figure 8. Morphological chnages of hBORGs in culture over time. Bright field images of neurospheres (NS) with and without differentiation medium (100) with Matrigel (M) were captured on day 7 and 14. Red arrow heads point to neurites extension that are seen after 7 days NS+M culture (A) and NS+DM+M (B). Connection among the neurospheres were seen after 14 days in NS+M culture (C) and NS+DM+M condition (D). Images from Differential Interference contrast (DIC) microscopy evidence neurites networks connecting adjacent organoids in (E) and (F). Scale bar 200 μm.

3.3.3 hBORGs express differentiated and mature cell types and remained viable for at least 12 weeks

To characterize differentiation and maturation process of cells in the organoids, hBORGs were harvested on 14, 28 and 180 days, sectioned and sections were stained for specific neuronal and glial markers. Neurons were positive for the neuron-specific cytoskeletal marker β-III-tubulin (Tuj1) (**Figure 9A, panels a and b**). Further confocal microscopy analysis of sections revealed that hBORGs protocol resulted in the generation of dense neural networks (**Figure 9A, panel b,**

and Figure 10). GFAP+ cells constituted 39% of all DAPI+ nuclei (**Figure 9A, panel a and c, and Figure 10**) and can be identified among neurons in direct proximity of neuronal bodies. Additionally, hBORGs harvested on day 28 (**Figure 10**) and day 180 (**Figure 10**) stained for Tuj1 and GFAP also demonstrated consistent cytoarchitecture over time. Although no signal for the neuroprogenitor marker, SOX2 (Sex-determining region Y-box 2) was observed at day 14, few Nestin positive cells were observed in the most superficial layer of hBORGs (**Figure 9A, panels d and e**) suggesting loss of stem cell identity and enhanced differentiation towards mature brain organoids.

Since HIV-1 neuropathogenesis is generally known to affect glutamatergic circuits(106-108), we sought to evaluate the presence of glutamatergic neurons in the hBORGs by assessing the expression of vesicular glutamate transporter 1 (VGLUT1) (**Figure 9B, panel a**) on day 14. Majority of differentiated neurons (Tuj1+) are VGLUT1 positive (**Figure 9B, panel b**), consistent with a glutamatergic lineage identity. Furthermore, tyrosine hydroxylase (TH), that is exclusively expressed in dopaminergic neurons, was observed only on day 180, suggesting that this neuronal subtype is spontaneously generated in longer term culture (**Figure 9B, panels c-f**). In contrast, minimal expression of vesicular GABA transporter (VGAT) over time confirmed that a small population of differentiated neurons in hBORGs were GABAergic (**Figure 9B, panels c, d and e**). Next, to test the majority of hBORG- glutamatergic neurons, we evaluated the expression of pre-synaptic synaptophysin (SYN) and post-synaptic PSD95 markers (**Figure 9C, panels a and b**). Indeed, colocalization of SYN and PSD puncta is suggestive of synaptic network connectivity (**Figure 9C, panel c**).

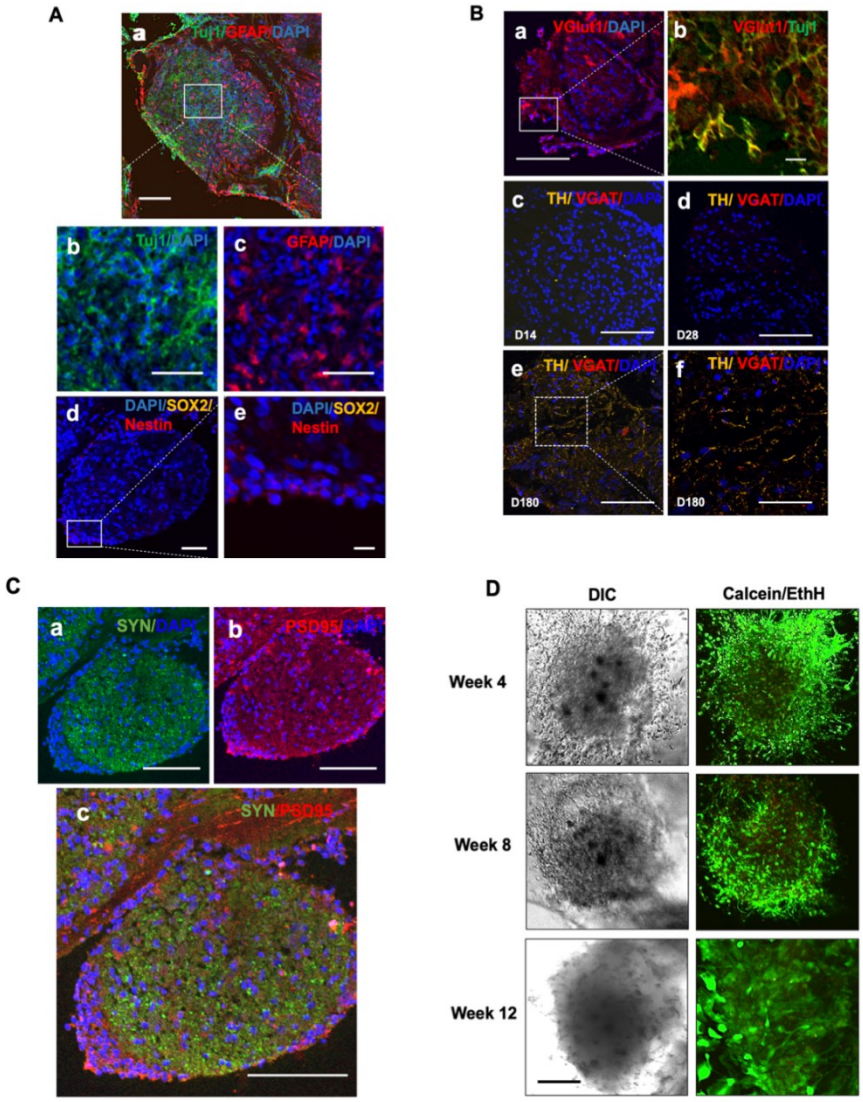

Figure 9. Expression of selected neuronal markers in hBORGs. (A) Representative images of comparison of neuronal and glial markers expression by co-immunostaining in hBORGs sections in panel a. At day 14 after differentiation, βIII-Tubulin Tuj1+ neurons (panel b) and GFAP+ astrocytes (panel c) were identified without a preferential localization. At day 14, few cells were Nestin+/SOX2+ (panel d and e). Scale bar in panel a and d is 100 µm, in panel b and c is 50 µm and in panel e is 10 µm. (B) Representative images of neuronal lineage markers. hBORGs sections from day 14 showed that most of differentiated neurons expressed VGlut1 (panel a and b), marker of glutamatergic neuronal lineage. Minimal expression of VGAT, marker of GABAergic neuronal lineage, was observed in hBORGs sections from day 28 and was maintained up to day 180 (panels c, d and e), whereas the

expression of tyrosine hydroxylase (TH), marker of dopaminergic neuronal lineage, is evident only at day 180 (panels e and f). Scale bar in panels a, c, d and e is 100 µm and in panels b is 10 µm and and f is 50 µm. (C) Expression of synaptic markers synaptophysin (SYN), PSD95 were observed as early as day 14 of differentiation (panel a-c) (D) Cell viability in hBORGs was assessed by live/dead assay followed by confocal microscopy. Images represent live cells (green) and dead cells (red) from one of the representative experiments (N=3). Scale bar is 100 µm.

Finally, we assessed the viability of hBORGs, which is important to validate the applicability of this model for further experiments. hBORGs were stained with Calcein AM to detect live cells and Ethidium homodimer to detect dead cells at different time points (**Figure 9D**). With appropriate maintenance, we observed that hBORGs are viable for more than 12 weeks with minimal cell death as indicated by live/dead staining.

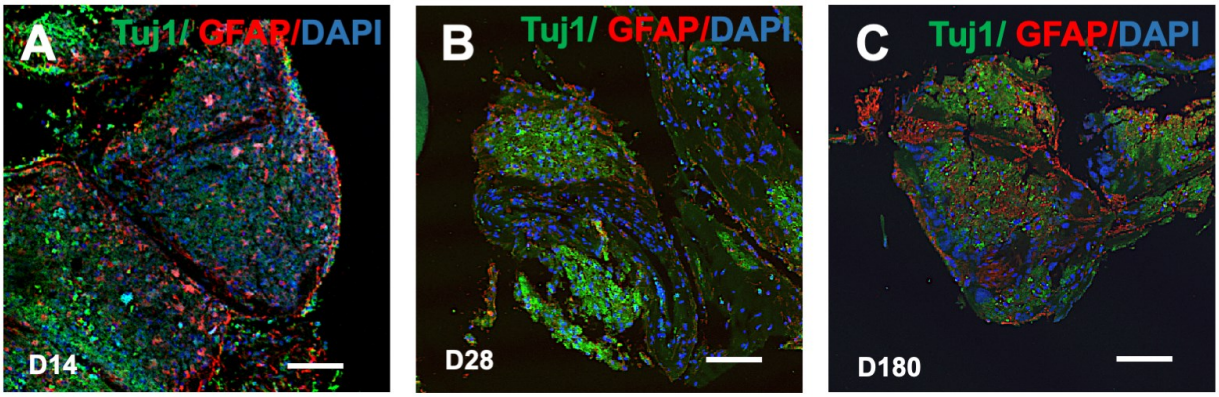

Figure 10. Differentiation of hBORGs in culture over time. hBORGs were harvested after 14 (A), 28 (B) or 180 days (C) post-differentiation, fixed and sectioned. Sections were immunostained with anti-Tuj-1 (green) and anti-GFAP (red) and imaged. Nucleus was stained with Dapi (blue). Scale bar is 100 µm.

3.3.4 HMC3 microglia can be incorporated into hBORGs to mimic multicellular crosstalk observed in HIV-1 neuropathology

The primary focus of developing the hBORG model is to study HIV-1 neuropathogenesis in a human representative system. An important component of HIV-1 neuropathology is the presence of virus-infected human macrophages and microglia, as observed in *post-mortem* brain tissues (109-111). Thus, we next incorporated microglia into the hBORGs as shown in **Fig. 11A**. Immortalized human microglial cells (HMC3) were infected with neurotropic HIV-1 NL(YU2-Env)-EGFP reporter virus in 2D cultures. Three days post infection, ~30% of HMC3 cells were infected (EGFP+) as detected by microscopy. To mimic the *in vivo* conditions, we incorporated mock- or HIV-1 infected HMC3 cells by placing them on top of the hBORGs cultures on day 15 post differentiation. Attachment of microglia to hBORGs and migration were monitored for another 15 days using confocal microscopy. Results indicate that by 24h post incorporation, more than 50% of microglia attached to the hBORGs **(Figure 11)** and both infected (green, arrowhead) and uninfected (red, asterisk) microglia continued to infiltrate into the hBORGs from day 1 (**Figure 11**, **insert a**) to day 7 (**Figure 11, insert b**).

Although microglia infiltration appeared most abundant surrounding the hBORGs (**Figure 11**) by day 3, many cells migrated into the hBORG layers and were completely embedded into it, as observed by z-stack reconstruction (**Figure 12**). Despite the fact both mock and infected microglia were membrane-labeled with fluorescent far-red dye, we observed that the EGFP signal was very strong due to the high level of expression of the EGFP-HIV-1 reporter virus in infected microglia cells, therefore overpowering the far-red membrane dye. Overall, these results suggest that both infected and uninfected microglia rapidly respond by migrating towards hBORGs similar to the migration of the immune cells from periphery into the CNS.

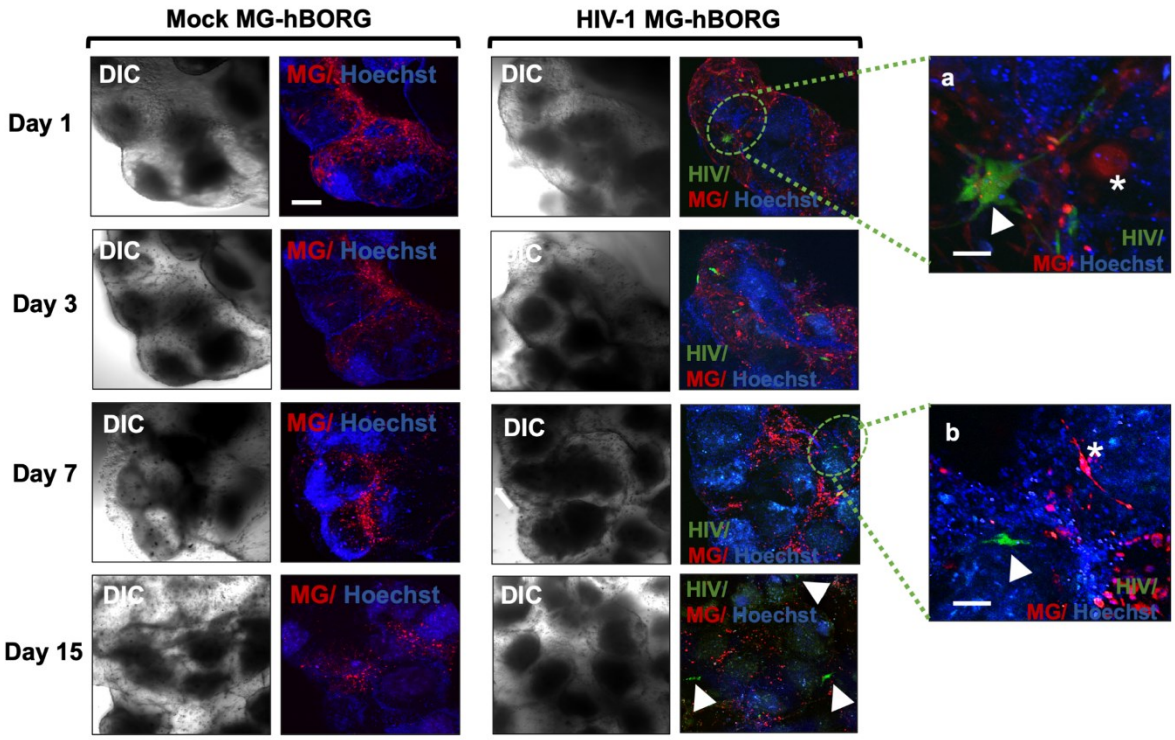

Figure 11. Incorporation of HMC3 human microglia into hBORGs. HMC3 microglia (1x 10^6 cells) were infected with HIV-1 (green) or mock-infected, membrane-labeled (red) and were added to hBORGs labeled with Hoechst-stained (blue). After 24 h, microglia incorporated-hBORGs were transferred to a new plate and maintained for an additional 15 days for further analyses. White arrowheads point to HIV-1 infected microglia (green) in insert a and b, and White asterisks in insert a and b point to uninfected microglia (red). Scale bar is 200 µm and 50 µm in inserts.

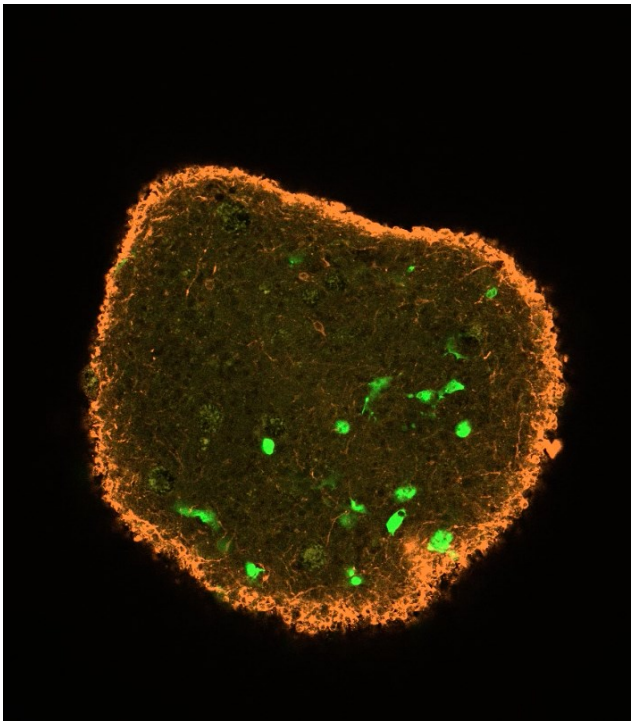

Figure 12. Microglia cells expressing EGFP incorporated into hBORGs 3 days post co-culture. MG-hBORGswere fixed and immunostained for MAP2 (orange). Movie depicts stacks through the entire organoid recorded as mp4 with an interval of 500 milliseconds between frames. Access the movie: https://pitt.box.com/s/aaox65y1d2so75vh8bu6k32hjp6qvgzb

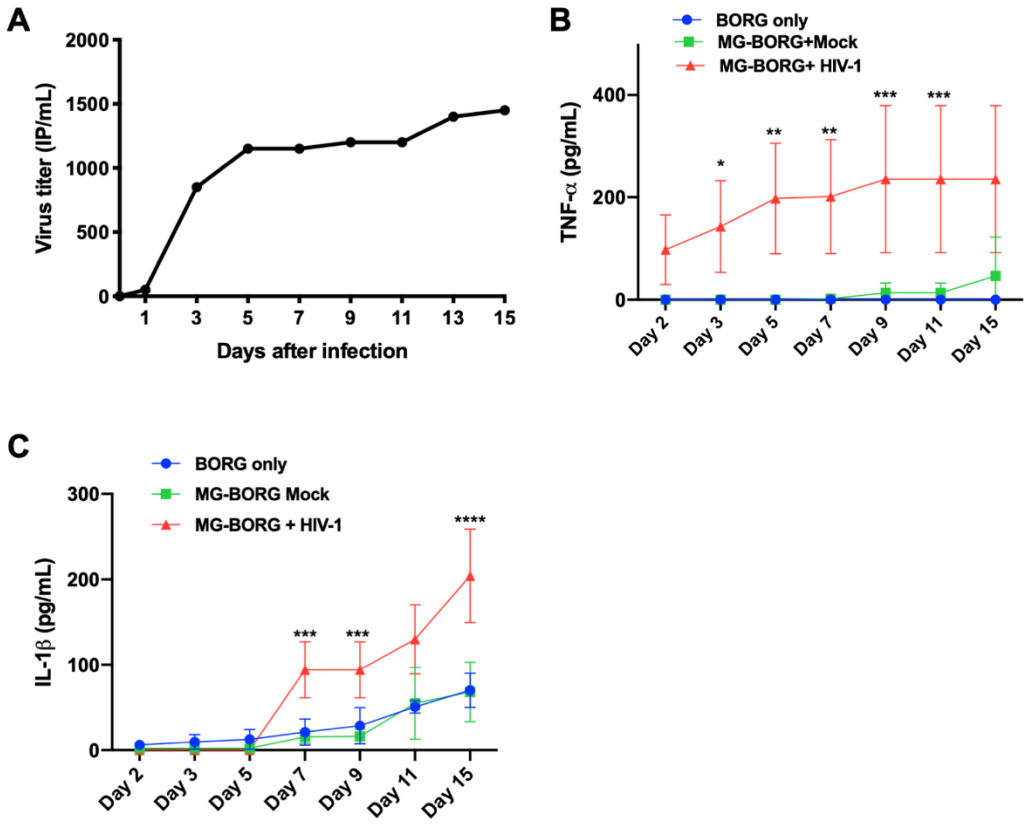

Figure 13. Microglial cell line HMC3 incorporated in hBORGs supports HIV-1 replication and exhibits inflammatory response to infection. (A) Cumulative virus titer in supernatants of MG-hBORGs generated from a representative organoid (N=3) containing HIV-1 infected HMC3 cells on day 15 post culture by RT-qPCR. Cumulative levels of TNF-α (B) and IL-1β (C) released from HIV-1 infected, mock infected MG-hBORGs and hBORGs measured by ELISA. Figure represents results from one of three independent experiments (N=3) from a representative NPC donor. *, $p<0.05$.

3.3.5 Human primary microglia incorporated into hBORGs support HIV-1 replication and alter the cytokine expression levels

We next investigated whether HIV-1 infected microglia incorporated hBORG (MG-hBORG) model can recapitulate some of the hallmarks of the HIV-1 CNS pathology in humans. Although the immortalized microglia cell line used in our studies demonstrated the physiological characteristics typical of human microglia such as migration into the hBORGs (**Figure 11 and 12**), viral replication, and secretion of TNF-α and IL-1β (**Figure 13**), these cells limited our studies to up to 15 days due to their rapid proliferation. To circumvent this limitation and to establish clinical relevance to our model, we incorporated primary human microglia from post-mortem adult human brain (infected or mock) into two independent sets of hBORGs following the protocol summarized in **Figure 14**. First, we incorporated primary microglia into hBORGs and imaged the infected (green) and uninfected (red) microglia (**Figure 14A, panel a**). The primary microglia infiltrated into hBORGs as early as 3 days (**Figure 14A, panel b**) similar to the activated phenotype observed for HMC3 cells (**Figure 11**). HIV-1 transcriptional activity was investigated by quantification of HIV-1 *gag* mRNA copy number in organoids through RT-qPCR (**Figure 14B**). Viral RNA transcripts were detectable in the two MG-hBORGs samples at day 15 post-infection (median 179,000 copies per 100ng of RNA; range 73,000–277,000 copies per 100ng of total RNA) suggesting high viral replication efficiency in organoids containing microglia. These results were further supported by the assessment of the viral titer in the conditioned media by measuring the infectious particles released into the supernatant. High levels of infectious virions were readily detected in the supernatants of HIV-1 infected MG-hBORGs as early as one day post incorporation and increased progressively throughout 30 days culture (**Figure 14C**) suggesting that MG-hBORGs supported active viral replication with potential to spread the infection to

bystander cells. Activated microglia and macrophages associated with HIV-1 neuropathogenesis are known to release various proinflammatory molecules. Among them, tumor necrosis factor (TNF-α) and interleukin-1 (IL-1β) play a central role in neuroinflammation(112-114). Hence, we measured cumulative levels of TNF-α and IL-1β in supernatants from MG-hBORGs by ELISA. Very low or below detectable levels of TNF-α and IL-1β were observed in hBORGs only and mock-infected MG-hBORG groups, as observed with HCM3 (**Figure 13**), whereas HIV-1 infected MG-hBORGs showed significantly higher levels of these two cytokines (**Figure 14D and 14E**). TNF-α levels were significantly elevated by 5.7-fold (1040±227.4 pg/mL) in HIV-1 infected MG-hBORGs compared to mock-infected (196.8±48.7 pg/mL) at early infection (day 3). TNF-α levels continued to increase up to 15 days after incorporation of infected MGs (**Figure 14D**), which directly correlated with the viral replication (**Figure 14C**). In contrast, increase in the IL-1β secretion occurred at later time points (after day 15 post MG incorporation) as reported by us in monocyte-derived macrophages earlier(102). IL-1β secretion was enhanced by 2.2-fold (134.5±24.3 pg/mL) in HIV-1 infected MG-hBORGs compared to mock MG-hBORGs (62.4±36.2 pg/mL) on day 15 (**Figure 14E**) and remained elevated up to 30 days of co-culture. The same trend was observed in the HMC3 incorporated organoids, that is, increased release of TNF-α and IL-1β (**Figure 13**). Together, these results confirm that our hBORGs are amenable for integration with primary adult human microglia, support chronic HIV-1 replication and recapitulate the neuroinflammatory milieu that is observed in HIV-1 infected brain.

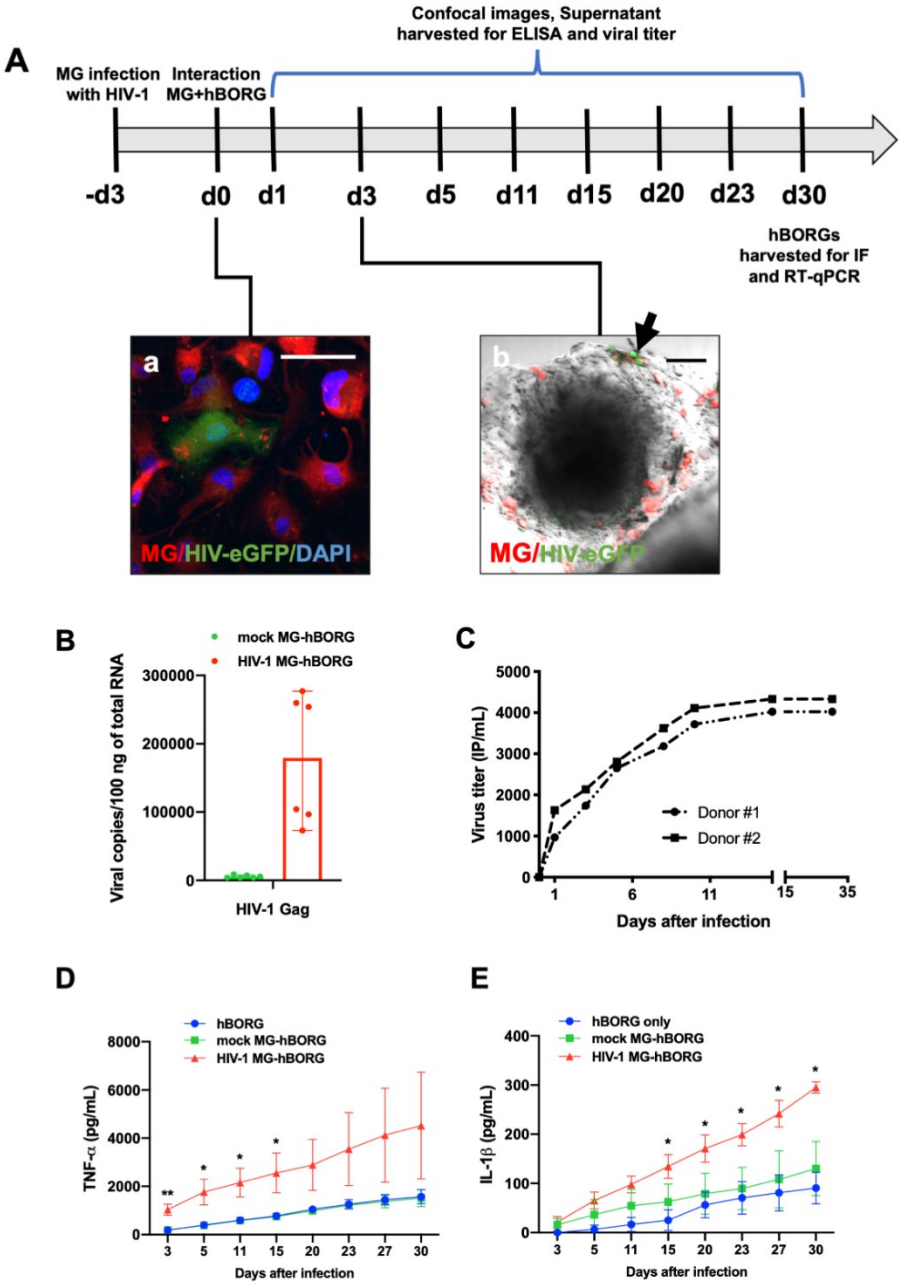

Figure 14. Human adult primary microglia recapitulate engagement with hBORGs, supports HIV-1 infection and produces inflammatory cytokines. (A) Schematic diagram of the experimental design is depicted. Primary adult brain microglia (0.5 x 10^6 cells) were infected with HIV-1 (panel a, green) or mock-infected, membrane-labeled (red) and were added to hBORGs for overnight. Scale is 100 μm. After 24 hrs, microglia incorporated-hBORGs were transferred to a new plate and maintained for an additional 30 days for further analyses. Image (panel b) depicts the

infiltration of primary adult brain microglia into hBORGs. Infected and uninfected microglia were membrane-labeled (red), incorporated into hBORGs and imaged by confocal microscopy. HIV-infected microglia (green, indicated with black arrow) and uninfected microglia (red) was incorporated in hBORGs on day 1 post coculture (panel b). Scale bar is 100 μm. (B) RT-qPCR assessment of HIV-1 gag mRNA copies in primary MG-hBORGs at day 30 post infection (N=3). (C) Representative cumulative HIV-1 virus titer in supernatants from HIV-infected MG-hBORGs where MG-hBORGs were developed using NPCs from two different donors. Kinetics of cumulative levels of (D) TNF-α and (E) IL-1β released from HIV-1 infected, mock-infected MG-hBORGs and BORGs without microglia during the course of infection measured by ELISA (N=4). **$p<0.01$, * $p<0.05$.

3.3.6 MG-hBORG model mimics HIV-1 CNS pathology signatures reported in *post-mortem* brain tissue of HIV-1 infected individuals.

We first sought to evaluate whether virus replication and chronic inflammatory condition in infected primary MG-hBORGs would have any effect on the viability of cells in hBORGs. To accomplish this goal, we assessed cell death in MG-hBORGs by staining with Calcein AM (live, green) and Ethidium homodimer (EthH, dead, red) (**Figure 15A**). In mock-infected MG-hBORGs, minimal level of cell death was detected, whereas HIV-1 infection gradually decreased the proportion of Calcein+ cells to the EthH+ cells in infected MG-hBORGs (**Figure 15B**). The results of viability from image analyses were further supported by measuring lactate dehydrogenase (LDH) released in the conditioned media from hBORGs-only cultures in comparison to both mock and infected groups as an indicator of cell injury (**Figure 15C**). Interestingly, incorporation of mock-infected microglia did not alter the basal level of cytotoxicity in hBORGs cultures. Notably, incorporation of HIV-1 infected primary microglia into hBORGs exhibited a 5-fold increase in cytotoxicity as early as day 11 of co-culture compared to mock-infected hBORGs (**Figure 15C**). Cytotoxicity peaked at day 15 of co-culture, exhibiting a 6-fold increase correlated with viral

expansion (**Figure 14C**) and suggesting potential loss of either neurons and/or astrocytes in HIV-1 infected MG-hBORGs. Since neurons are the most susceptible cells to damage due to HIV-1 (66,67), we tested whether the expression of neuronal marker βIII-Tubulin is altered in infected MG-hBORGs. Indeed, we observed 2.3-fold decrease in the βIII-Tubulin mRNA by RT-qPCR (**Figure 16A**), indicating neuronal loss in infected MG-hBORGs compared to mock-infected MG-hBORGs tested by day 15 post microglia incorporation. In contrast to the neuronal marker expression, the astrocyte marker (GFAP expression) is significantly increased by 18-fold in infected MG-hBORGs compared to mock-infected MG-hBORGs (**Figure 16B**) suggesting presence of astrocytosis. However, the expression of the microglial marker, (Iba1) was not significantly affected in HIV-1 infected microglia containing hBORGs (**Figure 16C**). Taken together, these results confirm that HIV-1 infection enhances loss of neurons and astrocytosis in hBORGs. Indeed, reactive morphology of astrocytes together with neurodegeneration are hallmarks of HIV-1 associated neuropathology in patients with severe HAND (115). To assess the synaptic damage due to HIV-1 infection in viable neurons, we further examined the intensity of staining of PSD-95 and Synaptophysin (SYN) immunolabeled puncta (**Figure 16D**) on day 30 of MG-hBORGs culture and plotted the mean intensity of each puncta as a fraction of Tuj-1 maximum intensity (**Figure 16E and 16F**). We observed a significant decline of 1.9-fold and 6.7-fold in PSD95+ and SYN+ areas, respectively, in the HIV-1-MG-hBORGs compared to mock-MG-hBORGs. The higher reduction in the pre-synaptic marker (SYN) may indicate that the pre-synaptic terminals are more susceptible to and hence, are preferentially compromised in HIV-1 infection. To consolidate this finding, we performed image analysis of synaptic contacts between PSD95+ and SYN+ neurons by assessing the mean intensity of the co-localized PSD95/SYN area in HIV-1 infected MG-hBORGs in comparison with the mock-infected MG-hBORGs (**Figure**

16G). Indeed, we observed a significant 10.6-fold decrease in the mean co-localization intensity of PSD95/SYN stained puncta in HIV-1-MG-hBORGs than mock-MG-hBORGs, further suggesting loss of synaptic integrity. Altogether, our data demonstrate the physiological relevance of the MG-hBORG system to study HIV-1-neuropathogenesis *in vitro*, and future applicability of this model to greatly improve our knowledge of mechanisms underlying initiation and progression of HIV-1-neuropathogenesis.

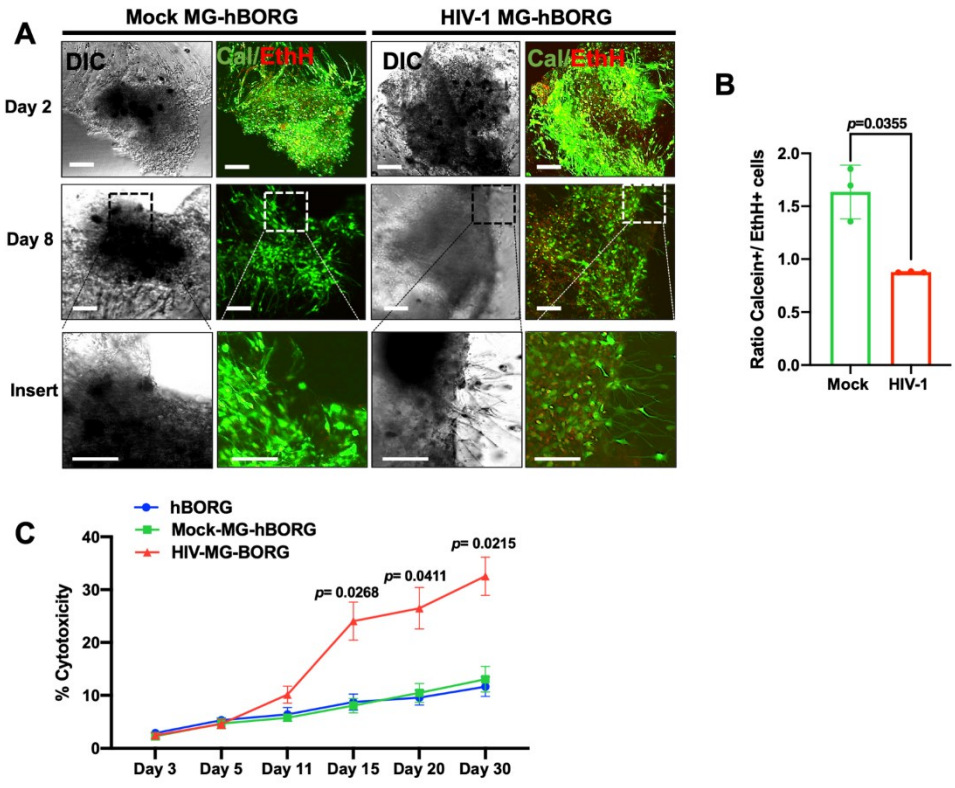

Figure 15. Characterization of viability and cytotoxicity induced by HIV-1 in primaery MG-hBORG model. (A) Mock-infected and HIV-1 infected MG-hBORGs were stained with LIVE/DEAD™ Cell imaging kit to determine the live and dead cells on days 3 and 8 post microglia incorporation. Calcein stains live cells (green) and ethidium homodimer stains nuclei of dead cells (red). Scale bars is 100 µm. (B) Calcein and ethidium homodimer positive cells were counted on day 8 and the corresponding ratio of live (calcein+) and dead (EthH+) cells were calculated. (C)

Cytotoxicity induced by HIV-1 infection was quantified in the supernatant of the HIV-1 infected, mock-infected MG-hBORGs and hBORGs by measuring LDH activity and % toxicity was determined (N=3).

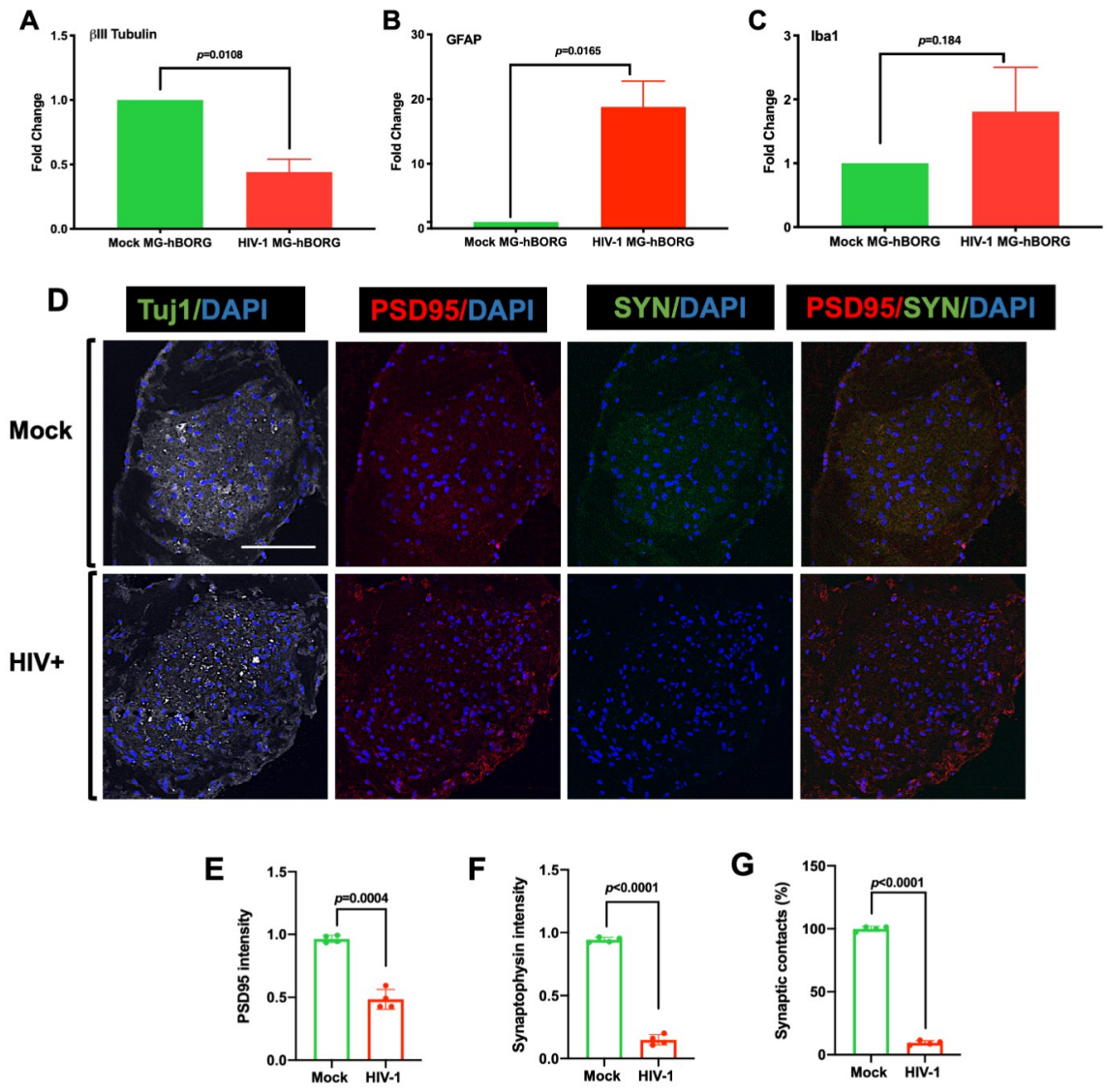

Figure 16. HIV-1 infection of MG-hBORGs causes reactive astrocytosis, decreased synaptic density, and neurodegeneration. Expression levels of βIII-Tubulin (A), GFAP (B) and Iba1 (C) in HIV-1 infected and mock - infected MG-BORGs were assessed on day 15. Fold change in HIV-1 infected MG-hBORGs was calculated using mock-infected MG-hBORGs as 1 (N=3). (D) Immunostaining of sections of MG-hBORGs for Tuj1(gray), PSD-95

(red) and SYN (green) were used to stain synapses (PSD95/SYN merged) in viable neurons in mock and HIV-1 infected organoids. Mean intensities PSD-95 (E) and SYN (F) were normalized to Tuj1 (maximum intensity). (G) The percentage of synaptic contacts (PSD-95/SYN co-localization intensity) in HIV-1 infected MG-hBORGs was calculated using the intensity of synaptic contacts in mock-infected MG-hBORGs as 100% (N=4). Statistical significance was calculated using unpaired Student's t-test.

3.4 Discussion

Here, to study HIV-1 neuropathogenesis, we developed a 3D *in vitro* brain organoid model derived from human neuroprogenitor cells that recapitulates the neurodegenerative microenvironment of human CNS pathology. We developed an efficient 3D culture system using a hydrogel microwell platform, which enables high throughput production of size-controlled neurospheres that can be differentiated into neurons and astrocytes to form multiple brain organoids simultaneously. We further incorporated HIV-1 infected microglia and demonstrated the utility of our system for modeling the major hallmarks of HIV-1 neuropathology.

Studying neurodegenerative diseases *in vitro* is challenging due to the complex nature of CNS biology involving multiple differentiated cell lineages(43). Attempts have been made to generate brain organoids using human induced pluripotent stem cell-derived neural stem cells (hiPSCs- derived NSCs) presenting remarkable progresses in this emerging field (83,116-120). Despite the fact that these systems require expensive techniques with complex protocols that are time-consuming, hiPSCs can be easily acquired, and cultured *in vitro* to study human diseases. On the other hand, genomic instability and variability in neural differentiation capacity have been reported and may compromise the functionality of iPSCs-derived systems(121),(122). Recently, other protocols have been established using human neuroprogenitor cells (NPCs) such as NTera-

2 (123), and ReN cells (124). NPCs are immortalized cell lines that have been modified to expand indefinitely and may differ from those found in the *in vivo* setting. Primary NPCs isolated from embryonic human brain tissue present a limited life span in culture. Studies may be hampered by limited tissue acquisition, and donor variability may pose a drawback. Additionally, fetal brain-derived primary NPCs should be collected within 18-20 weeks of gestation, since extended gestation period (within 18-20 weeks) may result in altered phenotypes and differentiation. Nevertheless, these cells have traditionally been used in 2D culture system, demonstrating efficient differentiation into functional neurons or glial cells and capturing the true heterogenicity akin to *in vivo* models (76,94). Hence, we chose fetal brain derived primary NPCs to develop hBORG model in this study.

We first employed a methodology to promote 2D mixed brain differentiation using embryonic NPCs by combining elements of already existing protocols to minimize preparation time and complexity (76,94,125). Next, we generated uniform size 3D neurospheres to be differentiated into neurons and astrocytes by employing the same customized mixed differentiation media. It has been shown that NPCs respond to the stiffness or resistance of the substrate in which they are embedded, directly affecting their differentiation to neural cells (126). In our system, the mechanical support was mimicked by the addition of matrigel that greatly improved our 3D system and hBORGs expressed neuronal and astrocytic markers in half of the time compared to the 2D mixed culture system.

Many of the available protocols are entirely focused on neurons and astrocytes and lack microglia or another inflammatory component (81,83,86). In contrast, we incorporated microglia into mature hBORGs mimicking invasion of microglia into the CNS during neurodevelopment (88). First, we incorporated the immortalized microglial cell line HMC3 in our model to

standardize our system. To mimic the adult HIV-1 patient's brain, we then tested the incorporation of human adult microglia isolated and cultured from *post-mortem* brain into hBORGs. Abud *et al.* (116,127,128) recently reported incorporation of immortalized or iPSC-induced microglia as inflammatory source in their models. However, none of these studies are reported in the context of HIV-1 infection, and primary human brain microglia were not included in these studies. Our study, on the other hand, is the first to report incorporation of HIV-1 infected primary human microglia into human brain organoids to more accurately recreate the human physiological microenvironment. Indeed, our results show that HIV-1 infected microglia can be incorporated into hBORGs that further support viral replication.

Another common and important feature associated with HIV-1 neuropathology is the release of inflammatory mediators (18,87,93). Microglia have been implicated as major producers of TNF-α in neurodegenerative diseases and CNS injuries (129,130). Not surprisingly, HIV-1 infection rapidly induced TNF-α release in our MG-hBORG system, which was directly correlated with the extent of virus replication. This finding is consistent with the early findings conducted in *post-mortem* tissue from HIV-1 infected individuals correlating both, viral replication and TNF-α transcription (131). Similarly, IL-1β is also elevated in the CNS during HIV-1 infection (112). In our study, we observed similar IL-1β release from HIV-1-infected MG-hBORG over the course of the culture consistent with previous work of our group showing variation of IL-1β expression and release by monocyte-derived macrophages throughout the course of HIV-1 infection (102). Of particular importance was the observation that IL-1β concentration increases with the viral production, suggesting that viral replication directly affects the release of this pro-inflammatory cytokine. Consistent with this assumption, Mamik and colleagues have shown that exposure to

recombinant Vpr protein induced transcription and release of IL-1β in human microglia in a dose-dependent manner (132).

It is possible to speculate that other pro-inflammatory cytokines released by infected cells can provoke an additive effect and exacerbate the inflammatory responses of the entire system regardless the level of infection. It is reported that astrocytes are infected by HIV-1 *in vivo* likely through cell-to-cell contact (133). However, we found no evidence of astrocyte infection during the period of study in our system based on image analysis of the entire organoid. Although astrocytes are unlikely to be major contributors of IL-1β within the brain, it is important to highlight that the contribution of astrocyte activation/infection to IL-1β peak release remains to be clarified (112). These cells outnumber microglia in the brain by 10-fold and have been shown to respond to LPS-activated microglia increasing TNF-α and IL-1β expression and release leading to a neurotoxic function (134). Nevertheless, ability of our MG-hBORG model to detect changes in TNF-α and IL-1β release in the conditioned media provides a significant advantage of our tri-culture system over most of the 2D cultures or current brain organoids devoid of microglia and prompts further investigation on the inflammatory response to HIV-1 infection in brain.

Neurotoxic soluble factors released by activated/infected microglia have been shown to contribute to neurodegeneration through different pathways (135-138). In our model, we observed decreased neuronal viability upon HIV-1 infection, which is in agreement with previous observations in HIV-1 infected *post-mortem* brain (12,18,73) . Although we have not determined the mechanisms involved, our ability to generate an organoid model that recapitulates HIV-1 neuropathology certainly enables the extended studies of the pathogenic cascade that culminate in neuronal damage.

Although it was not in the scope of this study to investigate a more extensive secretory profile, full examination of the conditioned media would broaden our knowledge in HIV-1 induced neuroinflammation. In addition, modulation of microglial responses is a potential therapeutic approach for treatment of HIV-1 neuropathology and other neurodegenerative diseases (139). Thus, future studies with infected MG-hBORG may give insights into the time course of microglial activation and polarization as well as unravel new molecular players that could be potentially targeted for therapies. Although not specifically studied in this report, the HIV-1 infected MG-hBORG model provides a physiologically relevant human-specific experimental system to further study the dynamics of viral latency and persistence in the absence or presence of antiretrovirals. It remains to be investigated if the cell damage observed in our study can be attenuated through suppression of viral replication. The effects of the combined antiretroviral therapy (ART) to the most severe neurologic manifestations of HIV-1 infection, correlate with a decrease in the prevalence of HIV-1 associated dementia in the post-ART era (10). Unfortunately, however, studies have reported high persistent rates of mild to moderate neurocognitive impairment in individuals under ART regimen, which neuropathology correlates to loss of synapses and dendritic simplification rather than substantial neurodegeneration (12). Detailed mechanistic studies on synaptodendritic damage by using MG-hBORG system in the presence of ART drugs deserves further investigation and may provide important insights.

Overall, hBORGs provide an alternative and physiologically relevant experimental model for investigating host-viral interactions and to assess molecular mechanisms underlying the progression of neuropathogenesis and the development of HAND. To the best of our knowledge, this is the first study to model HIV-1 neuropathology using hBORGs along with HIV-1 infected primary microglia. Our tri-culture model addresses key pathological features that are associated

with neuroinflammation by HIV-1, defined by the presence of activated microglia, reactive astrocytes and release of pro-inflammatory cytokines. The proposed model has great potential to serve as a human representative 3D model to boost our current knowledge about the molecular dynamics of HIV-1 neuropathogenesis and its progression.

4.0 Neurogranin Dysregulation and its Correlation to Synaptic Dysfunction and Loss and Dendrites in Early HIV-1 Neuropathogenesis

4.1 Introduction

HIV-1 associated neurocognitive disorder (HAND) remains the most prevalent HIV-1 related comorbidity, despite systemic viral suppression (10). The infectious microenvironment established upon viral entry in brain provokes changes in neuronal structure and function as dendritic simplification and synaptic loss, particularly in the frontal cortex (12,16). These structural changes are paired with deficits in memory and cognition, increasing the risk of poorer health outcomes in people living with HIV-1 under antiretroviral treatment. Currently, there is no treatment that can prevent or restore the neurodendritic damages. Therefore, it is critically important to understand the molecular and cellular mechanisms behind cognitive impairment upon HIV-1 infection of the brain.

Changes in neuronal function as the disruption of synaptic plasticity is widely thought to underlie the impaired cognitive function in people living with HIV-1. HIV-1 establishes infection in the brain primarily via the long-lived infected macrophages and microglia, however neurons are the most affected cell types in CNS (12,16,140). Both viral and host neuroinflammatory factors released from the infected cells are implicated in neuronal dysregulation (68). Studies using rat model have demonstrated disruption of one form of synaptic plasticity, the long-term potentiation (LTP) (44,48,141), after exposure to viral proteins Tat and gp120 which resulted in deficits in spatial learning tasks (142,143). Similarly, secreted proinflammatory factors released by HIV-1

infected macrophages also inhibited LTP, supporting HIV-1-induced impairment of synaptic plasticity (144). One of the proteins that regulates synaptic plasticity is neurogranin (50).

Neurogranin (Nrgn) is a small 7.5 kD protein, that is highly expressed in post-synaptic dendritic spines in the human cortex, hippocampus, amygdala and striatum (45,50). Through its calcium-dependent interaction with calmodulin, Nrgn acts as a potent regulator of postsynaptic signal transduction pathways and plays an important role in synaptic LTP (145-149). Although loss of neurogranin has been extensively associated with dysfunctional synaptic plasticity and impaired learning and memory, most of the recent studies have investigated Nrgn dysregulation only as a potential biomarker for the establishment and progression of Alzheimer's disease (150-154). Recently, our group have evaluated the Nrgn dysfunction in frontal cortex of HAND-positive samples and found reduced levels of Neurogranin compared to cognitively healthy controls (53).

In this study we sought to characterize cortical expression of Nrgn in HIV-1 positive individuals with and without cognitive impairment. Using RT-qPCR and immunohistochemistry, we assessed Nrgn levels in HIV-1 positive individuals with and without HAND in comparison to neurocognitively normal individuals. We further compared the expression pattern of Nrgn to the dendritic marker microtubule-associated protein 2 (MAP2) to verify whether Nrgn dysregulation correlates with dendritic simplification, but independent of changes in neuronal density. Additionally, we also examined the host and viral factors involved in Nrgn dysregulation *in vitro* and observed that, once infected, both perivascular macrophages and microglia can cause a selective loss of Nrgn mRNA levels in neurons in 2D and brain organoids. These findings led us to hypothesize that Nrgn loss is dependent on host and viral factors secreted by HIV-1 infected perivascular macrophages and microglia in the frontal cortex, and that these changes preceded dendritic simplification and neurodegeneration.

4.2 Materials and Methods

4.2.1 Study individuals

We obtained *postmortem* frontal cortex samples from HIV-1 positive individuals with cognitive impairment from National NeuroAIDS Tissue Consortium (NNTC) and Multicenter AIDS Cohort study (MACS). Frontal cortex samples from HIV-1 seronegative individuals, neurocognitive normal, age and sex matched, were obtained from Neurobiobank (NIH) and used as control. Only tissues for which a clear record of clinical information is available were considered for this study. Diagnosis of HAND was based on the clinical classification redefined in 2007 (72). All collected tissue samples were preserved frozen at −80°C until required.

4.2.2 Cells

HEK293T, U87MG, SH-SY5Y cells were grown in DMEM supplemented with 10% FCS, 1% glutamine and 1% penicillin-streptomycin. We induced differentiation of SH-SY5Y cells by adding 10 μM all-trans-retinoic acid (RA) to the growth medium 24 hours after plating, and RA-containing growth medium was replaced every day for 7 consecutive days. ReNCells VM were kindly provided by Dr. Amantha Thathiah, University of Pittsburgh. These cells were grown in ReN maintenance medium (Millipore) supplemented with 20 ng/mL of EGF and 20 ng/mL of bFGF (StemCELL) and were differentiated in plain ReN maintenance medium for 14 days. Primary adult human microglia were obtained from Dr. Changiz Geula from Northwestern University. Briefly, microglia were isolated from the prefrontal cortex of a 71-year-old Caucasian male (*postmortem* interval of 31 hours). Brain tissue from this patient was obtained from

Northwestern University Alzheimer's Disease Center Brain Bank (AG13854). Culture was maintained as previously published (101). Briefly, cells were seeded in PDL-coated plates and kept in complete microglia medium (ScienCell Research Laboratories). Experiments were conducted with passages between 8 to 10. All cell lines were kept in a humidified incubator at 37℃ and 5% CO_2.

4.2.3 Isolation of CD14+ monocytes and differentiation to macrophages (MDM)

Monocytes-derived macrophages (MDMs) were generated from normal peripheral blood mononuclear cells (PBMC). PBMCs from healthy donor were isolated by Ficoll-Hypaque gradient centrifugation. CD14+ monocytes were purified by positive selection using anti-CD14 monoclonal antibody-coated magnetic microbeads (Miltenyi Biotech, Auburn, CA) and differentiated in presence of 1 pg/ml M-CSF and 1×10^6 IU/ml GM-CSF (R&D Systems) as described previously (102). Half the volume of media was replaced every third day with fresh media containing GM-CSF and M-CSF for 7–8 days to differentiate them into MDMs.

4.2.4 Viral stocks and infection

HIV-1 viruses were generated using the neurotropic proviral construct pNLYU2-eGFP. HEK293T cells ($2x10^6$) were transfected with 3.5μg of proviral construct and 1.5 μg of vesicular stomatitis virus G (VSV-G) -Envelope expression plasmid using 15μL PolyJet™ transfection reagent (SignaGen Laboratories). The transfection mixture was gently vortexed and incubated for 20 min at room temperature to allow the formation of transfection complexes. The transfection mixture was then added dropwise to the cells and incubated at 37°C for 16 hrs. The medium-

containing transfection mixture was replaced using fresh complete medium, and after another 48 hour the supernatant containing viruses was removed, spun at 3000 g for 10 min and filtered to remove cell debris. Virus was collected by ultracentrifugation for 60 min at 20,000 rpm (4˚C) and stored at -80˚C until further use. Viruses were titrated onto the U87MG CD4+ CCR5+ permissive cells to determine the infectivity as infectious units/ml.

MDMs and adult primary microglia were infected with HIV-1 at a multiplicity of infection of 0.5 as described before (155). Mock infection was performed using equal amount of HEK293T culture supernatant. MDM supernatants were collected 8 to 12 days post infection and microglia supernatants were collected 3 to 14 days post infection. Supernatants were stored at -80℃ until use.

4.2.5 ELISA

IL-1β, TNF-α, IL-8 and IL-6 levels were measured in the supernatants from HIV-1 and mock infected MDMs and microglia by standard sandwich ELISA. We used human DuoSet ELISA kit (R&D Systems) following the manufacturer's protocol.

4.2.6 Lentiviruses production

Lentiviruses were packaged in HEK293T cells using Virapower lentiviral packaging mix (Invitrogen) per manufacturer's recommendations, with minor modifications. In brief, 2.75 µg of pLVX-Nrgn-mCherry (pNrgn-mCherry) vector, 1.0 µg of pLP1 (gag/pol), 0.50 µg of pLP2 (156) and 0.75µg of pLP/VSVg were cotransfected into 293T cells with the help of 15µL polyjet transfection reagent (polyjet, US). Forty-eight and 72 hours after transfection, supernatants were

removed and filtered (0.45-μm filter, Millipore). The virus-containing supernatant was titrated onto SH-SY5Y cells to determine the titers needed to transduce 95% of the cells (transduction units/ml). Mock virus was generated by the same procedure using empty vector.

4.2.7 Generation of brain organoids and histology

To generate size controlled neurospheres we followed the protocol previously established (157). Briefly, neuroprogenitor cells (20 x 10^6 cells/device/50 μL NPCs media) were seeded on top of microwell devices (1x1 cm^2) and were allowed to settle inside the microwells (30 min), followed by addition of NPC media. The devices were incubated at 37℃ and an atmosphere of 5% CO_2. When neurospheres were formed, the media was aspirated and 40 μL of matrigel (Corning) was applied on the top of devices to cover all the neurospheres (70-80/1x1 cm^2 device) and allowed to solidify by incubating for 30 min at 37˚C followed by addition of differentiation medium. Half of media was routinely replenished every other day until differentiation is complete.

Microglia (both mock and HIV-1 infected) were detached from the flasks and incubated with two-week old hBORGs, previously rinsed with PBS, as the ratio of 1 microglia cell to 20 NPCs. Microglia and hBORGs were incubated without agitation for 24h to allow attachment of microglia to the hBORG surface. The MG-hBORGs were then carefully transferred to a new plate with fresh differentiation media to remove unattached MGs and were maintained in culture in differentiation media for an additional 15 days.

MG-hBORGs were transferred from the original well followed by wash with PBS and fixation in 4% paraformaldehyde overnight at 4˚C. After fixation, MG-hBORGs were paraffin-embedded and sectioned at 10 mm on a microtome as described (104).

4.2.8 Immunohistochemistry (IHC)

Paraffin sections from frontal cortex slides and MG-BORGs were hydrated in a descending series of alcohol concentrations of 100, 95, and 70%, followed by PBS. Slides were then subjected to heat-induced epitope retrieval (HIER) utilizing citrate buffer at pH 6.0 in an electric pressure cooker at high heat for 15 min followed by a cooling down period prior to the initiation of IHC protocol. Sections were treated with hydrogen peroxide to block endogenous peroxidase activity as part of 3rd Generation IHC Detection Kit (Invitrogen, CA) followed by blocking with 10% normal goat serum for 15 min prior to incubation with primary antibody. Anti-human Nrgn antibody (EMD Millipore) was utilized at a 1:200 dilution, and the tissue sections were incubated at 4 °C overnight. The slides were developed utilizing the same 3rd Generation IHC Detection Kit, dehydrated, and mounted using permount.

4.2.9 Immunofluorescence staining

Deparaffinized sections from frontal cortex tissues and MG-BORGs were rehydrated by three washes of PBS and five washes of 0.5% bovine serum albumin (BSA) and circled with a Liquid Blocker Mini Pap Pen (Life Technologies). Sections were further permeabilized with 0.1% Triton-X-PBS for 15 min followed by blocking with 2% BSA for 1 h. Sections were incubated with primary antibodies against human Nrgn (1:1000) and microtubule-associated protein 2 (MAP2) (1:250) overnight at 4 °C. Cells were washed five times with 0.5% BSA in PBS and were further incubated with goat anti-mouse-IgG Alexa Flour 488 and anti-rabbit-Cy5 followed by five washes with 0.5% BSA in PBS, and the nuclei were stained with DAPI (1:1000).

Coverslips from treated and untreated ReN cells were fixed in 4% paraformaldehyde for 15 min, permeabilized and stained as previously described (104,157). Antibodies and concentrations were the same as described for the immunostaining of sections. Finally, slides were mounted, and images were taken using confocal microscope.

4.2.10 Confocal Microscopy and Image Analysis

Confocal imaging was carried out using a Z-stacking function on the Olympus FV1000 inverted confocal microscope using step size of 0.5-1.5 μm for coverslips and paraffin sections. Maximum intensity Z-projections were generated using Olympus Fluoview FV10-ASW 4.2 software. Images shown are representative of cultures generated from 3 independent experiments. processed using ImageJ 1.52q (National Institutes of Health, USA).

4.2.11 Total RNA extraction and quantitative real time PCR

RNA was isolated from tissue and cells using the MirVana kit (ThermoFisher) per manufacturer's recommendations. The concentration and purity of the RNA were measured by a NanoDrop 1000 spectrophotometer (Thermo Fisher Scientific). Purity was checked by the ratio of the OD_{260}/OD_{280} and OD_{260}/OD_{230}. The RNA was treated with DNase using a DNA-free Turbo DNase kit (Ambion). cDNA was prepared from 1 μg of total RNA using a high-capacity cDNA reverse transcription kit (ThermoFisher) in 20 μL total volume reaction. Quantitative real time PCR was performed using Taqman Universal PCR master mix (ThermoFisher) and the appropriate Taqman assays (ThermoFisher) or primers with 2 μL of the RT reaction mixture. Assays were conducted on an ABI 7000 real time PCR system in the following cycling conditions: activation

of Taq DNA polymerase at 95°C for 10 min, followed by 45 cycles of amplification at 95°C for 15 s and 60°C for 1 min. Results were normalized to the expression of Ribosomal Protein Lateral Stalk Subunit P0 (RPLP0).

4.2.12 Statistical analysis

RNA expression levels in tissues and cells relative to the control were calculated by the $2^{-\Delta\Delta Ct}$ formula and expressed as fold change to control. Statistical differences in gene expression levels were analyzed using Student's t-test, and correlations between lncRNA expression levels and Nrgn were analyzed using the non-parametric Mann-Whitney test. Statistical analysis was performed using GraphPad Prism, version 7 .0 (GraphPad Software, La Jolla, CA, USA). $P<0.05$ was considered to indicate a statistically significant difference.

4.3 Results

4.3.1 HIV-1 decreases Neurogranin (Nrgn) expression in human brain

Dysregulation of dendritic network and synaptic functions are neuropathological hallmarks of early HAND. Previous results have indicated that the post-synaptic protein, Nrgn is dysregulated in brains of HIV-1 infected individuals with HAND (53). Using immunohistochemistry (IHC), we evaluated the correlation between Nrgn expression and HIV-1 infection in the frontal cortex of human brain. we observed dramatic decrease of the staining of Nrgn in frontal cortex tissues of HIV-1 positive individuals compared to healthy control brain

tissues **(Fig. 17A)**. Loss of Nrgn was more evident in dendritic networks than in the neuronal body. Furthermore, the severity of cognitive impairment in HIV-1 positive individuals correlated with decreased Nrgn levels **(Fig. 17B and C)** and neuron atrophy **(Fig.17C)** which might reflect an Nrgn loss is an early stage of neurodegeneration.

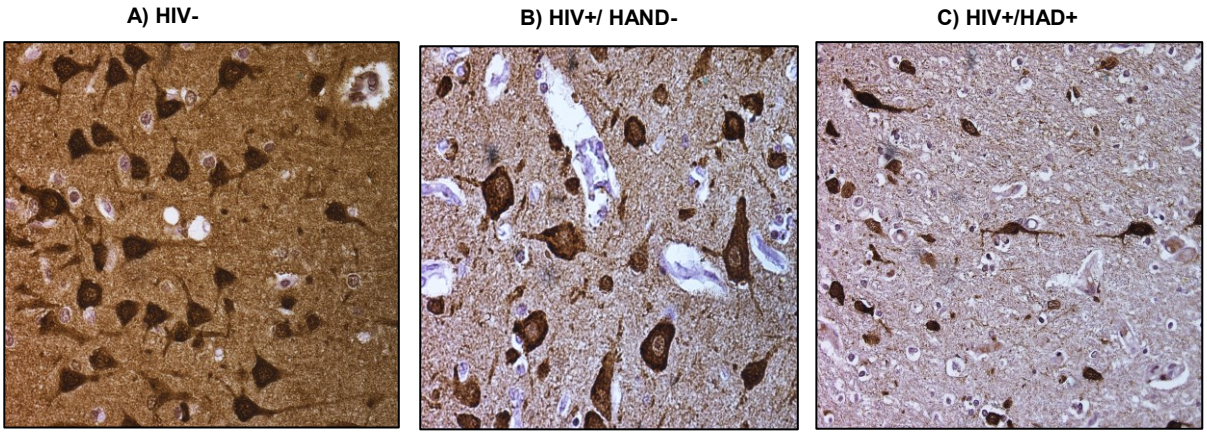

Figure 17. HIV-1 infection dysregulates Nrgn expression in human frontal cortex (FC) tissue. FC sections from (A) uninfected control, (B) HIV-1 +/HAND- and (C) HIV-1+/ HAD+ individuals were IHC-stained for Nrgn and counterstained with hematoxylin. Magnification: 40x.

We further assessed the relative expression level of Nrgn mRNA in 49 HIV-1-positive individuals and 22 age-matched control individuals brain tissues. Our preliminary results indicate that relative Nrgn mRNA level is significantly lower (by 2.5-fold) in HIV-1-positive individuals in 75.5% of cases (37 out of 49) **(Fig.18A)**. After grouping HIV-1 positive individuals in cognitively normal (HIV-1+/HAND-) and cognitively impaired individuals (HIV-1+/HAND+), we found similar trend towards decreased Nrgn in HIV-1+/HAND+ group compared to HIV-1+/HAND-, although not statistically significant (**Fig.18B**). Also, we assessed the copy number of Nrgn mRNA in brain tissue and found that Nrgn is significantly reduced (2.1-fold) in HIV-1+ individuals compared to HIV-1 individuals **(Fig.18C)** confirming that decreased levels in Nrgn

protein in frontal cortex of HIV-1 positive individuals is also associated with reduced amount of Nrgn mRNA.

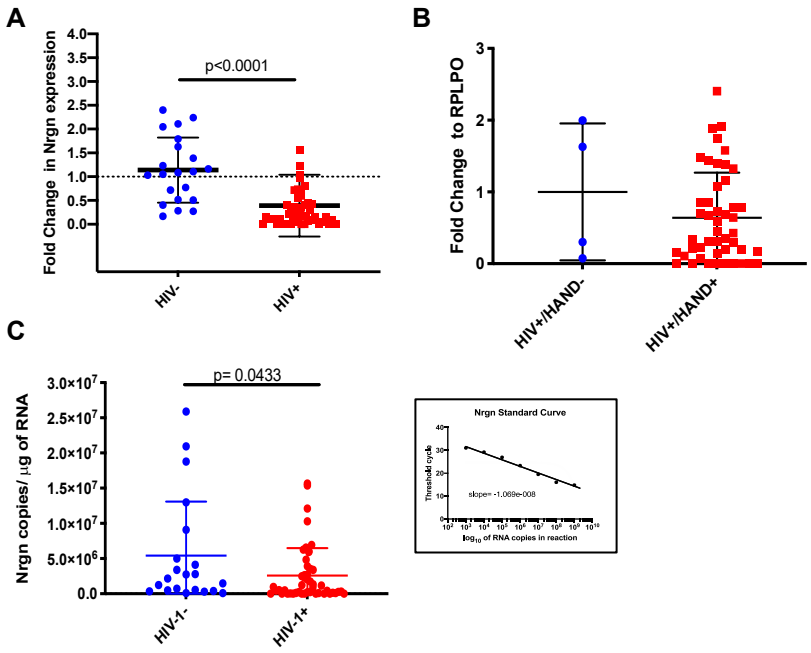

Figure 18. Scatterplots displaying Nrgn mRNA is downregulated upon HIV-1 infection. (A) Relative expression of Nrgn mRNA1 in *postmortem* frontal cortex brain samples from HIV-1 positive individuals (n=49) compared to control individuals (n=20) as assessed by RT-qPCR (B) Relative Nrgn expression indicates that Nrgn expression is lower HIV-1+/HAND+ individuals compared to HIV-1+/HAND- (C) Quantification of Nrgn mRNA1 copy number in frontal cortex brain samples of HIV-1 positive individuals compared to control individuals. A standard curve obtained from serial dilutions of full-length Nrgn construct as template for the RT-PCR reaction. Curve is shown in the insert.

4.3.2 Decrease in Nrgn expression precedes the synaptodendritic injury

Given that synaptodendritic damage rather than massive neuronal loss is more commonly observed in HIV-1 infected individuals (17), we next investigated the correlation between Nrgn

dysregulation and the dendritic integrity in brain. To accomplish that, we co-stained postmortem frontal cortex (FC) slices from HIV-1+/HAND- and HIV-1+/HAND+ individuals for Nrgn and microtubule associated protein 2 (MAP-2) and compared to brain sections from healthy individuals (control) through immunofluorescence. MAP-2 is one of the major components of neuronal cytoskeleton and is highly concentrated in dendrites, thus, it is considered a marker for dendritic integrity (158). As expected, Nrgn is enriched in neurons of healthy control samples and widely distributed throughout cell body and dendrites (**Fig. 19A**, yellow, overlay). Notably, a substantial loss of Nrgn in dendrites is observed in HIV-1+/HAND- and HIV-1+/HAND+ brain samples with accumulation of the protein in the perinuclear region of the neurons **(Fig. 19A)**. Image analysis of simultaneous fluorescence detection of Nrgn and MAP2 showed that the Nrgn/MAP-2 ratios of staining intensity is significantly reduced in HIV-1+/HAND- ($p=0.0009$) and HIV-1+/HAND+ ($p=0.0001$) samples compared to healthy control FC slices ($n=4$) (**Fig. 19B**). These results demonstrate that HIV-1 infection in the FC not only causes the decrease of Nrgn levels, but the selective loss of this protein in dendrites, where Nrgn exerts its main biological functions. This dendritic dysregulation of Nrgn (red) seems to be progressive and to precede the loss of dendrites (MAP-2+, green). Importantly, the marked decrease of Nrgn in the dendrites in cognitively normal HIV+ individuals (HIV-1+/HAND-) also suggests that Nrgn dysregulation occurs before the emergence of clinical symptoms of cognitive impairment.

Next, we evaluated the correlation of Nrgn and MAP-2 mRNA expression levels in postmortem brain tissue by RT-qPCR. We found out that Nrgn levels correlate positively with MAP2 levels with a positive correlation coefficient of 0.5658 **(Fig. 19C)**. It is the lower the Nrgn levels, the lower the MAP-2 levels, suggesting that the early loss of Nrgn may determine dendritic injury.

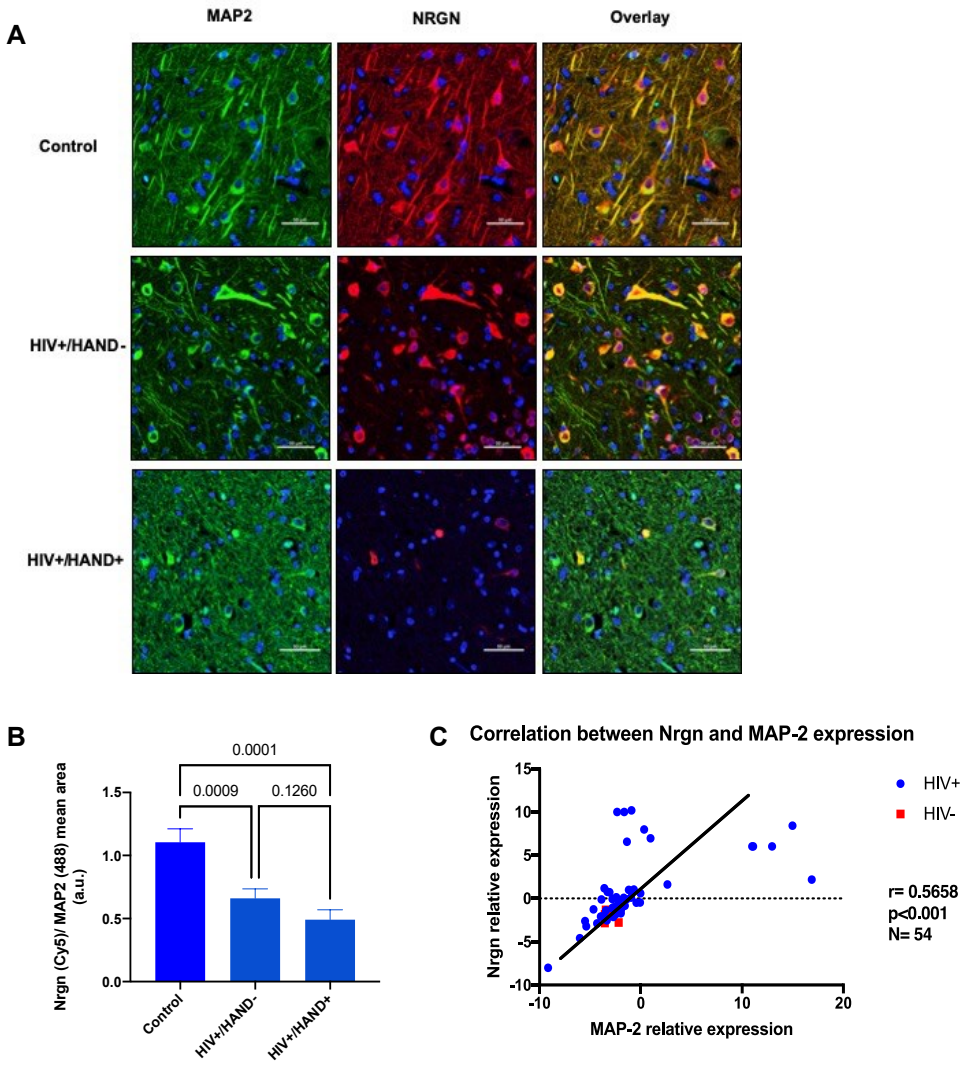

Figure 19. Distribution of Nrgn in frontal cortex and correlation with the dendritic integrity. Neurogranin was assessed by (A) immunostaining of brain sections from HIV-1 individuals and uninfected control for Nrgn (red) MAP-2 (dendritic marker, green) and nuclei (blue); (B) The ratio of the mean intensities of Nrgn and MAP2 staining in HIV-1 positive samples was calculated using the intensity of the colocalization (yellow) in healthy controls as 1 (N=4). Statistical significance was calculated using unpaired Student's t-test. (C) Nrgn expression correlates positively with MAP-2 expression as assessed by comparison between relative expression of Nrgn and MAP-2 mRNAs in frontal cortex.

4.3.3 Supernatant from HIV-1 infected macrophages/microglia alters Nrgn expression *in vitro*

It has been proposed that HIV-1 infected macrophages/microglia cause neuronal dysfunction through the inflammatory factors, neurotoxins and viral proteins that they release (4). In order to validate the indirect effect of HIV-1 infection in macrophages/microglia on Nrgn expression *in vitro*, we recapitulated the HIV-1 infected brain microenvironment by exposing differentiated neurons to mock-infected MDM and HIV-1 infected MDM supernatants (1:10 dilution). RNA from exposed was harvested at points 4, 6, 12 and 24 hrs post-exposure and Nrgn fold-change to mock was measured by RT-qPCR. Results from 2 different MDM donors (n=6) revealed that supernatants from infected MDM were able to induce 2-fold decrease in Nrgn mRNA as early as 12 hrs post-exposure **(Fig. 20A)**. Interestingly, Nrgn mRNA levels were restored to normal after 24 hrs post-exposure, suggesting that loss of Nrgn may actually be a reversible process, possibly due to the short window of time in which the viral and/or cellular factors released by MDMs are effective in the culture media.

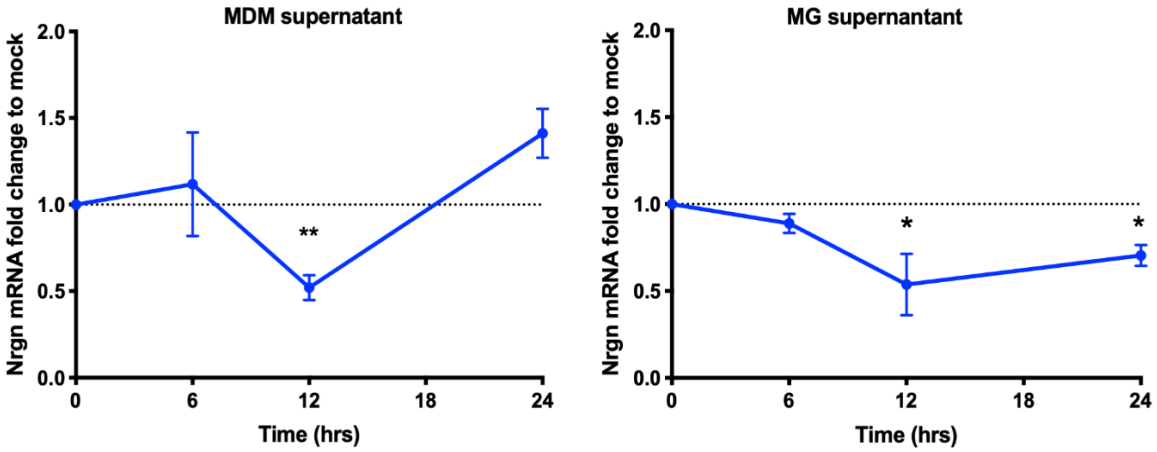

Figure 20. HIV-1 infection indirectly dysregulates Nrgn expression *in vitro*. SH-SY5Y cells were differentiated with RA for 7 days and exposed to HIV-1 or mock-infected MDM (A) or adult primary microglia (B). RNA was harvested at 6, 12 and 24 hrs and Nrgn expression level was assessed and compared to mock through RT-qPCR. Blue line represents the average. * $p<0.05$; ** $p<0.01$.

Microglia and macrophages are the major cell types that are productively infected by HIV-1 in the brain (63,64). However, in contrast to perivascular macrophages, microglia have the capacity for self-renewal and longevity. In addition, microglia interact directly with neurons and regulate cell survival and death as well as synaptogenesis (159). Since more neuronal cells are likely to interact anatomically with microglia than with macrophages, we asked whether microglia infection could trigger similar Nrgn dysregulation in neurons *in vitro*. To assess the timing and the contribution of HIV-1 infected microglia to Nrgn dysregulation, we exposed differentiated neurons to mock and HIV-1 infected microglia supernatants (1:10 dilution) and harvested cellular RNA 6, 12 and 24 hrs post exposure (**Fig. 20B**). A 2-fold Nrgn mRNA decrease ($p<0.05$) in neurons was observed upon exposure to HIV-1 infected microglia supernatant. These results indicate that HIV-

1 infection of either MDMs or microglia mediate Nrgn dysregulation in neurons, suggesting a common indirect mechanism.

4.3.4 Role of Host factor(s) on Nrgn dysregulation

The composition of products released from infected macrophages/microglia is complex and not fully known, however previous studies by us and others have identified several cytokines/chemokines that are known to have a role in neuropathogenesis (102,160-162). Thus, in order to identify the proinflammatory cytokines present in HIV-1 infected MDM and microglia supernatants that might contribute to loss of Nrgn in neurons, we selected and measured the levels of interleukin IL-1b, IL-6, tumor necrosis factor TNF-a, and IL-8 in the supernatants of HIV-1 and mock-infected MDMs (**Fig. 21A**) and microglia (**Fig. 21B**) by ELISA. As expected, HIV-1 infection overall increased the production and release of proinflammatory cytokines in both cell types. Among the pro-inflammatory cytokines tested, only IL-1b significantly increased upon HIV-1 infection in both MDM ($p=0.0210$) and microglia ($p=0.0356$) compared to mock infected. Collectively, our results suggest that IL-1b released by infected MDM/microglia might in part mediate Nrgn dysregulation in neurons.

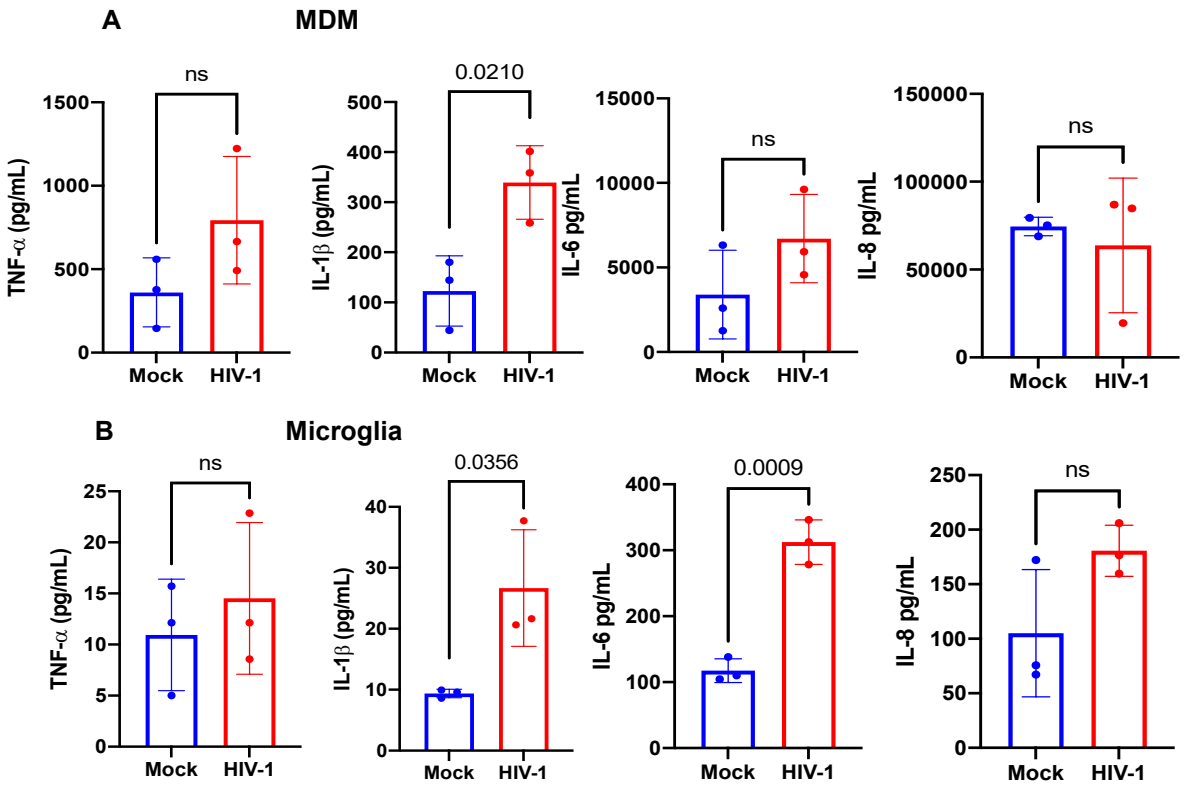

Figure 21. HIV-1 infection of MDM and microglia increase the release of pro-inflammatory cytokines. Healthy donors-derived macrophages were infected with HIV-1 NLYU2 at MOI=0.5 or mock-infected for 8-12 days (A). Levels of TNFα, IL-1β, IL-6 and IL-8 in supernatants harvested from mock and HIV-1-infected macrophages were measured by ELISA (N=3). Adult primary microglia were infected with HIV-1 NLYU2 at MOI=0.5 or mock-infected and supernatant harvested at day 3 post infection (B). Levels of TNFα, IL-1β, IL-6 and IL-8 in supernatants were measured by ELISA.

4.3.5 Viral factor(s) determinant on Nrgn downregulation

To determine the role of viral factors and to assess the relative contribution of each viral protein to Nrgn dysregulation, we infected MDMs using HIV-1 mutant viruses produced by proviral DNA constructs with EGFP reporter and compared to wild type HIV-1 for their ability to

induce changes in the levels of Nrgn and dendritic injury. The proviral constructs contain mutations in specific gene sequences that abolishes the expression of the following accessory genes of interest: Env, Vpr, Nef, and Vif, as these are all known to have cytotoxic effects to neurons. Hence, with this system we are able to assess the relative contribution of each viral protein to Nrgn dysregulation in a system physiologically more relevant than exposing cells to viral proteins alone. Differentiated neurons were exposed to supernatants (1:10 dilution) from macrophages infected with HIV-1 mutants and wild type viruses. RNA was harvested 12 hrs post incubation and Nrgn mRNA levels were assessed by RT-qPCR and compared to neurons exposed to supernatant from mock-infected cells. Results suggest that Viral protein R (Vpr) and the envelope (Env) proteins are more relevant to Nrgn loss after exposure to HIV-1 infected supernatant, since supernatant from MDMs infected with viruses lacking these two proteins reverted the Nrgn decrease in neuronal cells **(Fig. 22A)**. Nonetheless, macrophages infected with HIV-1 ΔEnv and HIV-1 ΔVpr secreted less IL-1b when compared to the levels of this pro-inflammatory cytokine secreted by MDMs infected with HIV-1 WT (**Fig. 22B**).

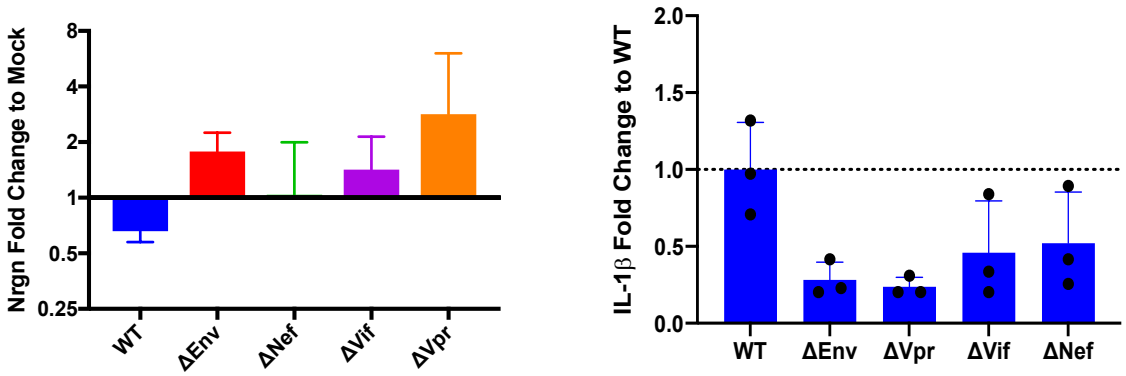

Figure 22. HIV-1 proteins role in Nrgn expression *in vitro*. SH-SY5Y cells were differentiated with RA for 7 days and exposed to HIV-1 wild-type, HIV-1 mutants, or mock-infected MDM supernatants for 12h. RNA was harvested and Nrgn expression was assessed by RT-qPCR (A). Values represent mean of fold change in Nrgn expression

compared to mock (N=2). (B) Fold-change variation of IL-1β levels in the supernatant of MDM infected with HIV-1 mutants compared to HIV-1 WT.

4.3.6 Loss of Nrgn by HIV-1 *in vivo* is recapitulated in 3D Brain organoids

To study Nrgn dysregulation in a more physiologically relevant model, we leveraged 3D brain organoid technology by incorporating infected microglia to better recapitulate the HIV-1infected brain microenvironment. Having previously established that the triculture brain organoid system is amenable to infection resulting in increased gliosis and neuroinflammation, we now wanted to discern the contribution of Nrgn dysregulation to the morphological and functional changes in neurons that precede neurodegeneration. As depicted in the schematic **(Fig. 23A)**, we infected primary adult brain microglia cells with HIV-1 YU2-EGFP (MOI of 0.5) and after 3 days of culture we incorporated infected and mock-infected microglia into fully mature brain organoids. We cultured the triculture organoids for up to 30 days, harvesting RNA at days 5 and 20 p.i for expression analysis, and intact organoids at days 10 and 30 p.i for subsequent immunostaining. We found that incorporation of HIV-1 infected microglia caused substantial decrease in Nrgn expression (2.7-fold, p=0.0056) as early as 5 days after infection and continued up to day 20 p.i. (2.5-fold, p=0.0005), compared to uninfected control **(Fig. 23B)**. In addition, the low expression of HIV-1 Gag at day 5 p.i. suggests that the rapid Nrgn mRNA dysregulation is happening before active viral replication and it was sustained thereafter. As expected, HIV-1 infection caused significant decrease of Nrgn immunostaining at 30 days p.i. **(Fig. 23C)**.

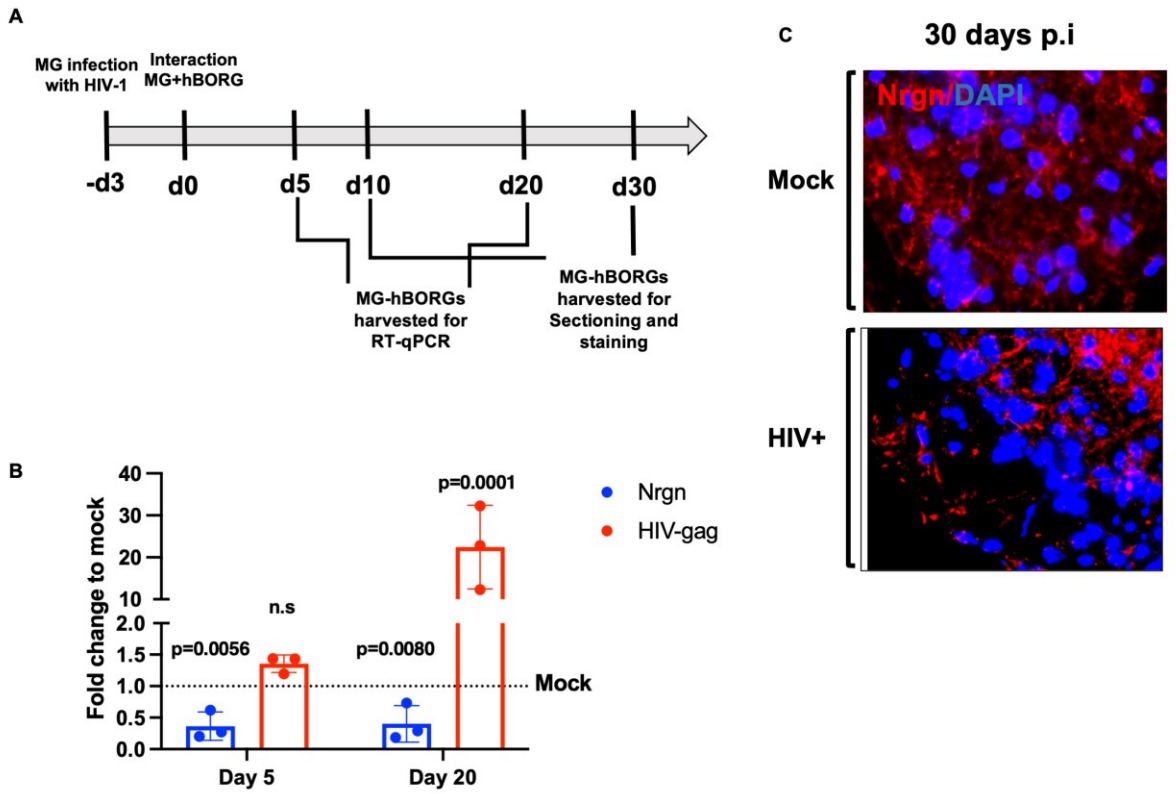

Figure 23. HIV-1 infection microenvironment causes Nrgn dysregulation in Brain organoids. (A) Schematic diagram of the experimental design is depicted. Primary adult brain microglia (0.5 x 10^6 cells) were infected with HIV-1 (panel a, green) or mock-infected and were added to brain organoids for overnight. Microglia-embedded organoids were harvested at days 5 and 20 p.i. for RNA extraction, and at days 10 and 30 p.i.for immunostaining. (B) Mean of fold change variation in Nrgn and HIV-1 Gag expression compared to mock assessed through RT-qPCR (N=3). (C) Immunostaining of infected Brain organoid for Nrgn (red) and nuclei (blue) compared to mock-infected organoid.

4.4 Discussion

The events underlying the functional and structural plasticity of neurons are widely thought to be the molecular basis of cognition. Dysruption of Neurogranin (Nrgn) is a post-synaptic protein abundant in dendrites in healthy brain and highly correlated to neuronal plasticity and cognitive performance (50). Therefore, we aimed to investigate Nrgn dysregulation in HAND. Herein, we have performed an extensive characterization of Nrgn in frontal cortex samples of HIV-1 positive individuals, with and without cognitive impairment, compared to aged-matched healthy control samples and quantified and compared the Nrgn expression pattern though immunohistochemistry, immunofluorescence and RT-qPCR. Using immunofluorescence and image analysis, we demonstrated that Nrgn is dysregulated in HIV-1 positive individuals before dendritic loss and neurodegeneration suggesting that Nrgn loss is an early molecular hallmark of HAND. Although our work mostly focused on the study of the intact brain tissue, further experiments by measuring the synaptic levels of Nrgn in the synaptic compartment will help to clarify the distribution of Nrgn in HIV-1 infected brain and whether total Nrgn is specifically dysregulated in the synaptosomes or is merely accumulated in the nucleus. Nevertheless, results account to a significant dysregulation of Nrgn mRNA expression, as well. Thus far, not much is known about the regulation of Nrgn expression other than thyroid hormone (TH) promotes its transcription (163-165). However, TH stimulus is ineffective in the upper layers of cortex and it is not likely that Nrgn downregulation in frontal cortex samples of HIV-1 positive individuals is due to TH deprivation (163). Neurogranin is also known to be locally translated in the dendrites (166,167). Other possibility that cannot be ruled out is that HIV-1 infection of brain somehow induces dendritic Nrgn mRNA destabilization in frontal cortex. If this is the case, future studies

investigating the spatial distribution of Nrgn mRNA in the context of HIV-1 infection may complement our results.

Our results support the notion that relevant pathways to neuronal injury in HAND are activated indirectly through the release of host/viral factors from infected macrophages/microglia (10,12). Under our experimental condition, neuronal treatment with conditioned media from either HIV-1 infected macrophages or microglia, led to a rapid significant decreased of Nrgn mRNA levels when compared to mock-infected cells. We did not detect neuronal death in these experiments. Indeed, Nrgn expression was transiently decreased in the first 12 hours of treatment and its expression levels seemed to recover afterwards. These observations indicate that Nrgn dysregulation is potentially reversible as a result of some compensatory mechanism for synapse or dendrites protection.

Additionally, this study suggests that immune responses may be involved in the Nrgn dysregulation in HAND. IL-1b is one of the many mediators released from glial cells involved in neurotoxicity (135,168,169). Interestingly, IL-1b was the only cytokine among those we tested which was highly abundant in supernatants from both HIV-1 infected MDM and HIV-1 infected microglia, suggesting an overlapping phenotype in response to viral infection. A growing body of evidence shows that increased IL-1b levels in brain is associated with long term plasticity impairment and cognitive decline (170-172). Thus, a key question is whether and how IL-1b signaling is involved in Nrgn dysregulation in neurons. Future studies treating neurons with physiological relevant concentration of the recombinant cytokine along with the neuronal IL-1b receptor antagonist (IL-ra) may help to tease out the direct contribution of this cytokine to Nrgn dysregulation. Another important question not addressed in this work is what the relative contribution of viral proteins to the loss of Nrgn in neurons. Although our preliminary assessment

suggests a differential contribution of the viral Envelope and Vpr to the downregulation of Nrgn in neurons, at least in part. However, it remains to be defined whether the effect of these viral proteins is indirect. Though some molecular pathway specifically activated in the infected cells, or if these proteins are shed in the conditioned media to exert its effect directly into neurons.

In summary, our results consolidated the characterization of Nrgn as an important molecular player in early HAND and added to the work available in the literature. Nrgn dysregulation at both mRNA and protein levels is evident in the frontal cortex of HIV-1 positive individuals even before the emergence of clinical symptoms of cognitive decline. This led us to speculate whether a greater expression of Nrgn can lead to a symptoms reversal or halt the disease progression, placing Nrgn on the spotlight as promising therapeutic target.

5.0 The role of non-coding RNA in Nrgn dysregulation in HIV-1 neuropathogenesis

5.1 Introduction

Mild forms of HIV-1 associated neurocognitive disorders (HAND) are globally prevalent in almost half of people living with HIV-1 (PLWH), despite the use of antiretrovirals (23,24). It is well stablished that HIV-1 neuropathology underlying the cognitive decline correlates with synaptodendritic damage triggered and exacerbated by multiple viral and host mediators, including inflammatory cytokines and chemokines (12,25,68). Among them, interleukin-1 beta (IL-1β) has been recognized as a key inflammatory mediator in the pathogenesis of HIV-1 in the human brain (53,87,173).

We have previously reported that Neurogranin (Nrgn), a post-synaptic protein, is decreased in the frontal cortex of *postmortem* brain of HIV-1 positive individuals and this reduction was associated with IL-1β and IL-8 expression (53). More recently, we have shown that Nrgn is also dysregulated at mRNA levels *in vivo* and *in vitro*, upon exposure to HIV-1 infected microglia supernatant enriched in IL-1β. Nrgn is highly abundant in healthy dendritic spines to modulate Ca^{2+}/Calmodulin signaling in synaptic plasticity and it has been extensively investigated in rodent models as a correlate of synaptic loss and cognitive impairment (147,149,154,174-178). Therefore, loss of Nrgn possibly contributes to establishment of the synaptodendritic damage underlying the cognitive deficits observed in HAND. However, not much is known about general regulation of Nrgn expression, and the mechanism involved in HIV-1 induced decrease of Nrgn levels remains to be elucidated. Thus, approaches to reverse Nrgn dysregulation in HAND could be of importance in restoring neuronal structure and function to alleviate cognitive deficits in PLWH.

A large proportion of the mammalian genome is broadly transcribed as noncoding RNAs. Long non-coding RNAs (lncRNAs) are a class of RNA transcripts longer than 200 nucleotides which do not have protein-coding potential but exert biological functions (179-181). For instance, lncRNAs contribute to gene expression by binding to several proteins, DNAs and RNAs to form functional complexes to regulate gene expression from epigenetic modifications and transcription to RNA processing, transport and translation (55). In recent years, thousands of lncRNAs have been annotated in human genome and the number of reports suggesting their functionality and implications to physiological and pathological processes are rapidly increasing (54,55,182-185). Additionally, a growing list of lncRNAs have also been reported to be altered in response to viral infections (182,186-189). Nevertheless, a limited number of long ncRNAs have been functionally characterized to date and have been found to be manipulated by HIV-1 (190-192).

A growing number of natural antisense transcripts, which is one of the class of the lncRNAs, have been recently reported and characterized as regulators of their sense mRNA expression (185,193,194). Antisense lncRNAs are transcribed from the strand opposite so that of the sense transcript of a protein-coding gene. Moreover, compared to other classes of lncRNAs as intergenic and intronic localized lncRNAs, antisense lncRNAs are more stable, which might be good indicators for their potential biological functions (195). Indeed, more than 30% of the annotated coding transcripts in the human genome have antisense transcription. Interestingly, we have identified a novel antisense lncRNA transcript (RP11-677M14.2) localized in the opposite strand of NRGN locus, which has not been yet functionally investigated.

Here, we investigate the potential role of RP11-677M14.2 antisense lncRNA in Nrgn expression in the context of HIV-1 infection of the brain. We found that RP11-677M14.2 transcript is significantly enriched in frontal cortex samples of HIV-1 positive individuals as compared to

age-matched cognitively normal individuals. *In vitro*, exposure of neurons to supernatant of HIV-1 infected macrophages recapitulated the discordant Nrgn-lncRNA regulation. Moreover, RP11-677M14.2 lncRNA was shown to be transcriptionally regulated by IL-1β present HIV-1 inflammatory millieu. Finally, overexpression of RP11-677M14.2 in neurons inhibited Nrgn expression through mechanisms other than Nrgn mRNA destabilization. Therefore, our discovery adds to the current understanding of Nrgn regulation and provides an important mechanistic link between IL-1β released by HIV-1 infected glial cells and the synaptodendritic damage in neurons via dysregulation of Nrgn expression in the brain.

5.2 Materials and Methods

5.2.1 Study individuals

We obtained from National NeuroAIDS Tissue Consortium (NNTC) and Multicenter AIDS Cohort study (MACS) frontal cortex samples from HIV-1 infected individuals with and without cognitive impairment. Frontal cortex samples from HIV-1 seronegative individuals, neurocognitive normal, age and sex matched, were obtained from Neurobiobank (NIH) and used as control. For this study, we will only use those tissues for which a clear record of clinical information is available. Diagnosis of HAND was based on the clinical classification redefined in 2007 (72). All collected tissue samples were preserved frozen at −80°C until required.

5.2.2 Viral stocks

HIV-1 viruses were generated using the neurotropic proviral construct pNLYU2-eGFP. HEK293T cells ($2x10^6$) were transfected with 3.5μg of proviral construct and 1.5 μg of vesicular stomatitis virus G (VSV-G) -Envelope expression plasmid using 15μL PolyJet™ transfection reagent (SignaGen Laboratories). The transfection mixture was gently vortexed and incubated for 20 min at room temperature to allow the formation of transfection complexes. The transfection mixture was then added dropwise to the cells and incubated at 37°C for 16 hr. The medium-containing transfection mixture was replaced using fresh complete medium, and after another 48 hour the supernatant containing viruses was removed, spun at 3000 g for 10 min and filtered to remove cell debris. Virus was collected by ultracentrifugation for 60 min at 20,000 rpm (4˚C) and stored at -80˚C until further use. Viruses were titrated onto the U87MG CD4+ CCR5+ permissive cells to determine the infectivity as infectious units/ml.

5.2.3 Cells

HEK293T, U87MG, SH-SY5Y cells were grown in DMEM supplemented with 10% FCS, 1% glutamine and 1% penicillin-streptomycin. We induced differentiation of SH-SY5Y cells by adding 10 μM all-trans-retinoic acid (RA) to the growth medium 24 hours after plating, and RA-containing growth medium was replaced every day for 7 consecutive days. All cell lines were kept in a humidified incubator at 37℃ and 5% CO_2.

5.2.4 Western Blot

Samples were lysed in RIPA lysis buffer supplemented with protease inhibitors (Roche) for 20 min on ice. Cellular debris was cleared by centrifugation at 10,000 x g for 15 min at 4℃. Protein concentrations were determined using the BCA Protein Assay kit (ThermoFisher) and a SpectraMAX Plus spectrophotometer (Molecular Devices). Equal amounts of proteins were diluted in RIPA buffer, supplemented with sampling buffer containing 250 mM Tris-HCl pH 6.8, 10% (wt/vol) sodium dodecyl sulphate, 30% (vol/vol) glycerol, 5% (vol/vol) -mercaptoethanol and 0.02% (wt/vol) bromophenol blue, and denatured for 5 min at 95℃. Protein lysates were resolved on 12% (wt/vol) SDS polyacrylamide gels and transferred to polyvinyl difluoride (PVDF) membranes (ThermoFisher) using the Trans-Blot Turbo transfer system (Biorad). Membranes were blocked for 60 min at room temperature (RT) in 5% (wt/vol) skim milk in Tris Buffered Saline (TBS) supplemented with 0.1% (vol/vol) Tween-20 (TBS-Tw). Primary antibodies used: rabbit anti-Nrgn (Millipore; 1:7,000), mouse anti-MAP-2 (Sigma; 1:1000), mouse anti-tubulin (Cell Signaling 1:2,500). Secondary antibodies conjugated to horseradish peroxidase (HRP) (Sigma) were diluted 1:3,000 in PBS-Tween and incubated for 60 min at RT. Protein bands were visualized by incubating membranes with enhanced chemiluminescence kit (Pierce) for 1 min at room temperature.

5.2.5 Plasmid construction and cell transfection

The cDNA encoding full length RP11-677M14.2 was PCR-amplified and subcloned into pcDNA3.1 vector (Invitrogen). The empty pcDNA3.1 vector was used as the control. All plasmids

were isolated using a Thermo Maxiprep kit and the specific clones were confirmed by DNA sequencing of at least 5 colonies.

5.2.6 Total RNA extraction and quantitative real time PCR

RNA was isolated from tissue and cells using the MirVana kit (ThermoFisher) per manufacturer's recommendations. The concentration and purity of the RNA were measured by a NanoDrop 1000 spectrophotometer (Thermo Fisher Scientific). Purity was checked by the ratio of the OD_{260}/OD_{280} and OD_{260}/OD_{230}. The RNA was treated with DNase using a DNA-free Turbo DNase kit (Ambion). cDNA was prepared from 1 µg of total RNA using a high-capacity cDNA reverse transcription kit (ThermoFisher) in 20 µL total volume reaction. Quantitative real time PCR was performed using Taqman Universal PCR master mix (ThermoFisher) and the appropriate Taqman assays (ThermoFisher) or primers with 2 µL of the RT reaction mixture. Assays were conducted on an ABI 7000 real time PCR system in the following cycling conditions: activation of Taq DNA polymerase at 95°C for 10 min, followed by 45 cycles of amplification at 95°C for 15 s and 60°C for 1 min. Results were normalized to the expression of Ribosomal Protein Lateral Stalk Subunit P0 (RPLP0)

5.2.7 Subcellular fractionation

The separation of nuclear and cytosolic fractions was performed using a PARIS Kit (Life Technologies) according to the manufacturer's instructions.

5.3 Results

5.3.1 Identification of candidate lncRNA

Long non-coding RNAs (lncRNAs) by definition are RNA molecules longer than 200 nucleotides without protein coding potential. To identify putative lncRNAs with potential role in neurogranin dysregulation, we utilized the University of California Santa Cruz (UCSC) Genome Browser (genome.ucsc.edu) to investigate the genomic landscape of human NRGN gene. We have identified one transcript (RP11-677M14.2) of 1,704 base pair length, which is localized in the antisense strand in NRGN locus in chromosome 11 (-strand, hg38) that remains to be characterized **(Figure 24, red arrow)**. Moreover, in Ensembl (http://www.ensembl.org) browser this transcript corresponds to a 3 exons antisense RNA with no protein-coding potential, being classified as a long non-coding RNA. RP11-677M14.2 arises from independent promoter and its promoter region co-aligns to epigenetic markers of active transcription **(Figure 24, red circle, H3K27Ac mark)**. Analysis of the promoter activity from the same cell lines **(Figure 24, Regulatory build track, thick red blocks)** corroborates to this analysis, showing that when the Nrgn promoter is inactive (grey boxes on left), the RP11-677M14.2 promoter is active (red blocks on right). Additionally, gene expression data in 53 tissues from GTEx RNA-seq track revealed that RP11-677M14.2 is particularly abundant in human brain regions where Nrgn is also abundant, as hippocampus and frontal **(Figure 24, yellow track)** (50). Therefore, these data suggest the potential functional role of RP11-677M14.2 in mediating Nrgn expression. Importantly, in Ensembl (http://www.ensembl.org) browser this transcript corresponds to a 3 exons antisense RNA with no protein-coding potential.

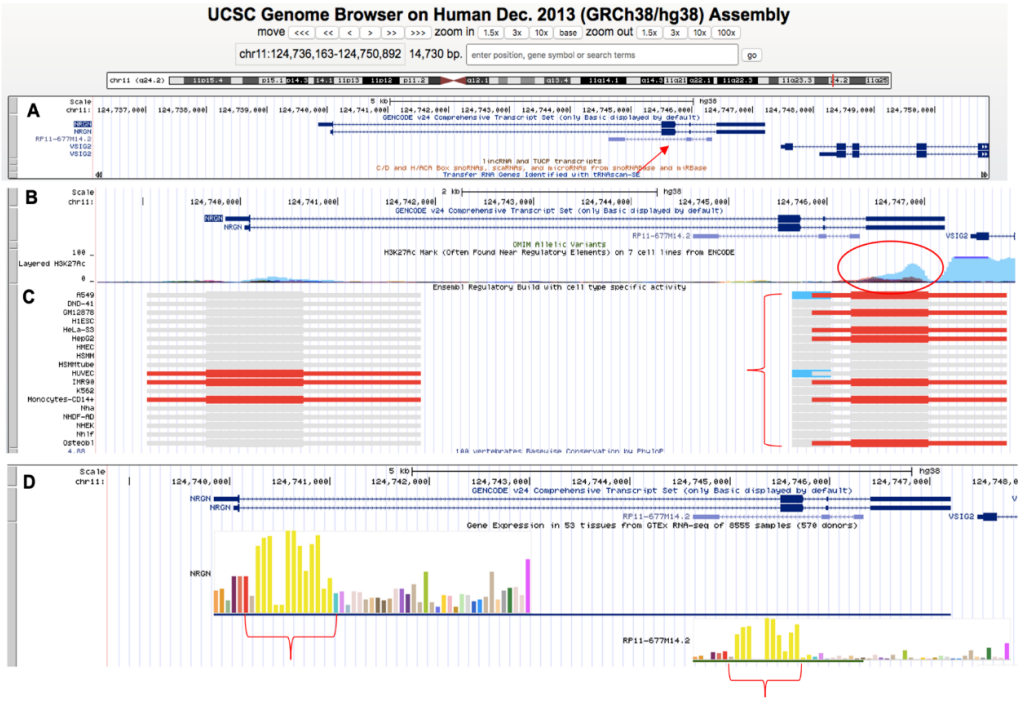

Figure 24. Identification and characterization of RP11-677M14.2 on Genome Browser. (A) Genome Browser view of human NRGN locus on chromosome 11 is shown. The first two dark blue lines represent the two isoforms of Nrgn mRNA. RP11-677M14.2, shown in light blue, is transcribed from the opposite strand (red arrow). (B) ChIP-sequencing of the NRGN locus for H3K27Ac show active transcription co-aligning with RP11-677M14.2 promoter region (red circle) in several cell lines. (C) Expanded ChiP-seq data of the NRGN locus per cell line. (D) Nrgn mRNA and RP11-677M14.2 levels measured in 53 different human tissues. In yellow is highlighted the levels of these two transcripts in different brain sections.

5.3.2 RP11-677M14.2 expression is elevated in brain of HIV-1 positive individuals and inversely correlates with Neurogranin expression

To investigate if RP11-677M14.2 is dysregulated in HAND, we detected the lncRNA expression levels in frontal cortex tissues from 49 HIV-1-positive individuals and age and sex-matched 22 non-infected control tissues by using RT-qPCR. The levels of RP11-677M14.2 were aberrantly up-regulated (>12.000 average fold-change, p=0.0046) in 61.2% (30 of 49) HIV-1 positive tissues compared with HIV-1-negative tissues (**Figure 25A**). Comparison between HIV-1 positive individuals without any degree of cognitive impairment (HIV-1+/HAND-) with HIV-1 positive individuals diagnosed with some level of cognitive impairment (HIV-1+/HAND+) also revealed a statistically significant increase in the RP11-677M14.2 levels **(Figure 25B)**. Moreover, the relationship between RP11-677M14.2 expression and clinical stages of HAND was analyzed. Although not statistically significant, we can point out a trend of increased RP11-677M14.2 levels as HAND progresses from the less severe form (asymptomatic neurocognitive impairment, ANI) to the most severe form of disease (HIV-1- associated dementia, HAD) **(Figure 25C)**.

Finally, we examined the correlation of Nrgn expression level with RP11-677M14.2 expression level in frontal cortex. As shown in **Figure 25D**, higher levels of RP11-677M14.2 were significantly correlated with lower levels of Nrgn in frontal cortex with a correlation coefficient of -0.3065 (p=0.0322). These findings led us to speculate whether this antisense lncRNA exerts a silencing effect on the Nrgn mRNA or corresponding protein abundance.

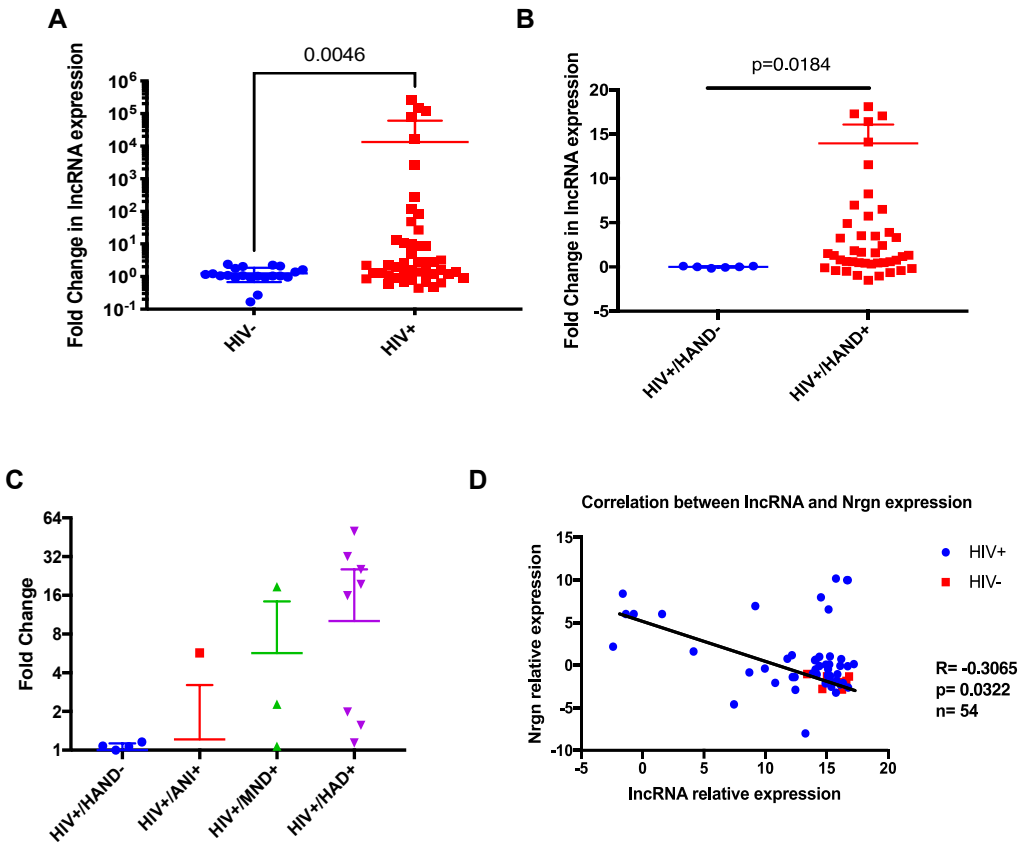

Figure 25. Expression analysis of RP11-677M14.2 in frontal cortex tissues. (A) Relative expression of RP11-677M14.2 in brain from HIV-1 positive individuals (N=49) compared with control HIV-1 negative tissue (N=22) was analyzed by RT-qPCR. (B) Relative expression of RP11-677M14.2 in HIV-1+/HAND+ individuals (N=6) compared to HIV-1+/HAND- individuals (N=43). (C) Comparison of RP11-677M14.2 expression in different stages of HAND (D) relative expression of Nrgn mRNA in frontal cortex compared to relative expression of RP11-677M14.2 in the same tissue assessed by RT-qPCR.

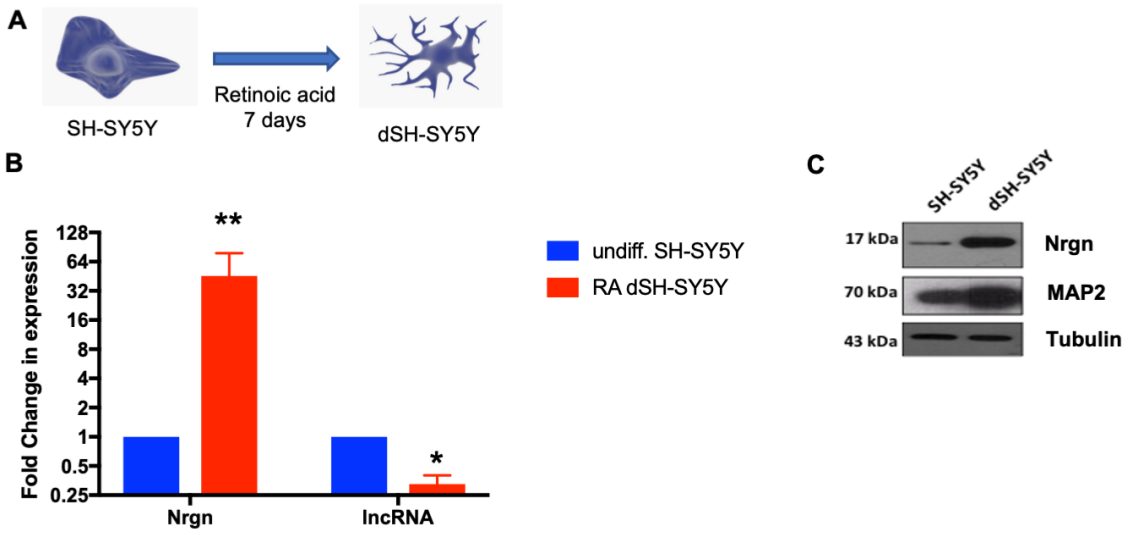

Figure 26. Transcriptional activation of Nrgn is associated with repression of lncRNA. (A) Schematic of SH-SY5Y differentiation with retinoic acid (RA) treatment. (B) Assessment of Nrgn mRNA and RP11-677M14.2 transcript through RT-qPCR. (C) Assessment of Nrgn protein levels after SH-SY5Y differentiation by Western blot. *p<0.05, **p<0.01

5.3.3 Overexpression of RP11-677M14.2 inhibits Neurogranin expression and dysregulates synaptic integrity

The overlap between sense and antisense transcripts may regulate expression at the transcriptional level (via transcriptional interference) and/or post-transcriptional level (196). To investigate the potential regulation of Nrgn by RP11-677M14.2, we treated SH-SY5Y cells with all-trans retinoic acid (RA) for 7 days **(Figure 26A)** and performed RT-qPCR. During the differentiation process with RA treatment, Nrgn mRNA and protein levels are known to increase **(Figure 26B and 26C) (163,165)**. Interestingly, our data reveals that while the expression of Nrgn

increased, RP11-677M14.2 sharply declined upon the induction of differentiation **(Figure 26B)**. This observation suggests that Nrgn levels may be regulated by its anti-sense lncRNA in a discordant manner upon certain stimuli, as recently shown for other sense-antisense pairs (196,197)

To test the prediction of a discordant regulation of RP11-677M14.2 and Nrgn mRNA, we have cloned full-length RP11-677M14.2 transcript into pCDNA3.1 expression vector (InVitrogen) to overexpress this lncRNA. Nrgn mRNA and protein levels were assessed by transiently transfecting the RP11-677M14.2 construct in SHSY-5Y cells, which express low expression levels of endogenous RP11-677M14.2 and high levels of Nrgn under normal conditions. The Nrgn mRNA and protein expression levels were normalized to cells transfected with empty vector (negative control). Our results show that Nrgn mRNA was decreased by 50% in neuronal cells overexpressing RP11-677M14.2 **(Figure 27A)**. To confirm the mRNA results, we further assessed protein levels of Nrgn by ELISA immunoassay. Similar results were obtained when we measured the protein levels of Nrgn, being observed an average decrease of 4.7-fold in neuronal cells overexpressing RP11-677M14.2 in comparison to cells transfected with empty plasmid as control. These results suggest that the overexpression of the lncRNA directly or indirectly affects Nrgn mRNA expression resulting in lower protein levels. In order to investigate the effects of RP11-677M14.2 on the synaptodendritic damage, we also examined the expression levels of selected synaptodendritic integrity markers: the dendritic marker MAP-2, the pre-synaptic markers GAP43, Synapsin and SNAP25, and the post-synaptic proteins Calmodulin, CAMK2, and calcineurin (PP3CA). We observed a significant decreased of expression of MAP-2 ($p=0.016377$), SNAP25 ($p=0.0128$) and CAMK2 ($p=0.003930$) indicating that inhibition of Nrgn

expression induced by overexpression of the lncRNA caused dysruption in the synaptodendritic integrity, widely thought to be the neuropathological correlate to the cognitive decline.

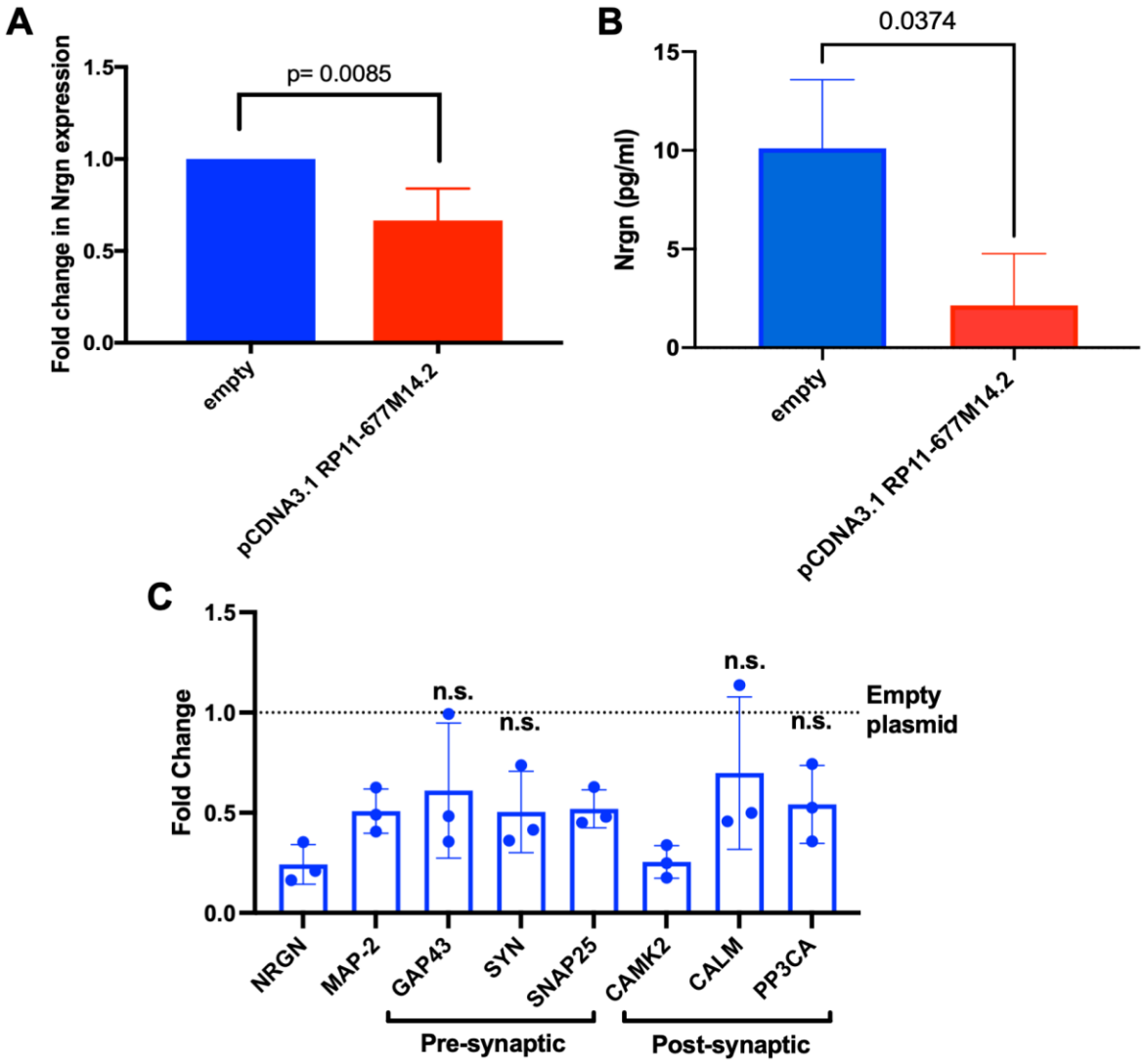

Figure 27. Overexpression of RP11-677M14.2 inhibit Nrgn expression. (A) Levels of Nrgn mRNA and (B) protein were assessed by RT-qPCR and Nrgn ELISA respectively upon transient transfection of SH-SY5Y with pCDNA3.1 RP11-677M14.2 compared to empty plasmid. (C) Assessment of synaptodendritic markers levels upon transient transfection of SH-SY5Y with pCDNA3.1 RP11-677M14.2 compared to empty plasmid (red): Nrgn (p=0.005641),

MAP-2 (dendritic marker, p= 0.016377), GAP43 (pre-synaptic, p= 0.183997), SYN (pre-synaptic, p=0.051), SNAP25 (pre-synaptic, p=0.0128), CAMK2 (post-synaptic, p=0.003930), CALM (post-synaptic, p=0.3029) and PP3CA (post-synaptic, p= 0.054975).

5.3.4 RP11-677M14.2 is predominantly localized in the nucleus

LncRNAs have been separated into several broad classes in terms of their mechanisms of regulation of mRNA transcription and translation: decoys, regulators of translation, enhancers and modular scaffolds that guide chromatin modifying enzymes to specific genomic loci. Those lncRNAs localized within the nucleus, have been previously linked to the epigenetic control of transcriptional regulation through several different mechanisms, whereas, cytoplasmic lncRNAs are involved essentially in post-transcriptional mechanisms, subcellular localization and regulation of translation (198).

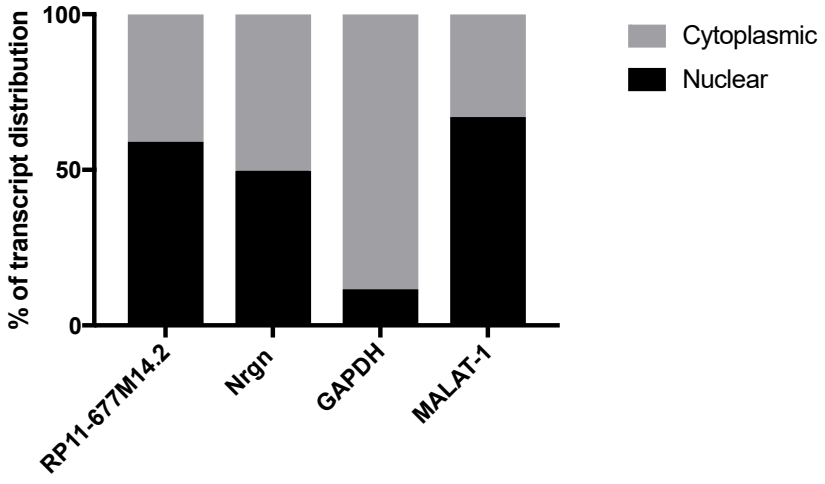

Figure 28. RP11-677M14.2 is enriched in the nucleus. Relative RP11-677M14.2 and Nrgn mRNA levels in cytoplasm or nucleus of SH-SY5Y were detected by RT-qPCR. GAPDH was used as cytoplasm control and Malat1

was used as nucleus control. Distribution of RP11-677M14.2 transcript was presented as average percentage rate of total RNA (N=3).

To dissect the function of RP11-677M14.2 in Nrgn regulation we first examined the distribution of this lncRNA in SH-SY5Y cells. Cell fractionation followed by RT-qPCR showed that almost 60% of the RP11-677M14.2 transcript resides in the nucleus **(Figure 28)**. Nrgn mRNA, in turn, is equally distributed between these two subcellular compartments. According to the distribution of glyceraldehyde-3-phosphate dehydrogenase (GAPDH) and Malat1, the nucleus/cytoplasm separation was successful **(Figure 28)**. Notably, Malat1, a lncRNA with nuclear function, is also distributed across both compartments, however, is enriched in the nucleus. Our results, although not conclusive, suggest that lncRNA is slightly accumulated in the nucleus and may be involved in the epigenetic regulation of Nrgn transcription.

5.3.5 IL-1β released from HIV-1 infected macrophages/microglia mediate RP11-677M14.2 dysregulation in neurons *in vitro*

We next investigated whether HIV-1 infection can affect RP11-677M14.2 transcript levels as it affects Nrgn mRNA levels *in vitro*. To accomplish that, neuronal cells were exposed for 12h to supernatant of MDM and microglia cells infected with HIV-1 YU2 MOI 0.5 or mock-infected, as previously described, to mimic the impact of HIV-1 induced inflammatory factors, toxins and/or viral proteins in these cells.

The effect of these factors on sense and antisense transcripts levels was assessed by RT-qPCR at different time-points **(Figure 29A)**. We found that exposure of cells to supernatant of MDM infected cells peaked at 12 hrs post-exposure resulting in a 1.8-fold decrease of Nrgn mRNA and a 6.8-fold increase of RP11-677M14.2 transcript levels, whereas exposure to supernatant of

infected microglia (**Figure 29B**) resulted in 1.9-fold decrease of Nrgn mRNA and 4.7-fold increase of RP11-677M14.2. Interestingly, our results show that both transcripts alter at the same time (between 6 and 12h post-exposure) and these alterations seem to be reversible as the stress factor degrades in the culture media (~24h post-exposure). These results suggest that both viral proteins and/or inflammatory factors released by infected macrophages can affect antisense transcript levels.

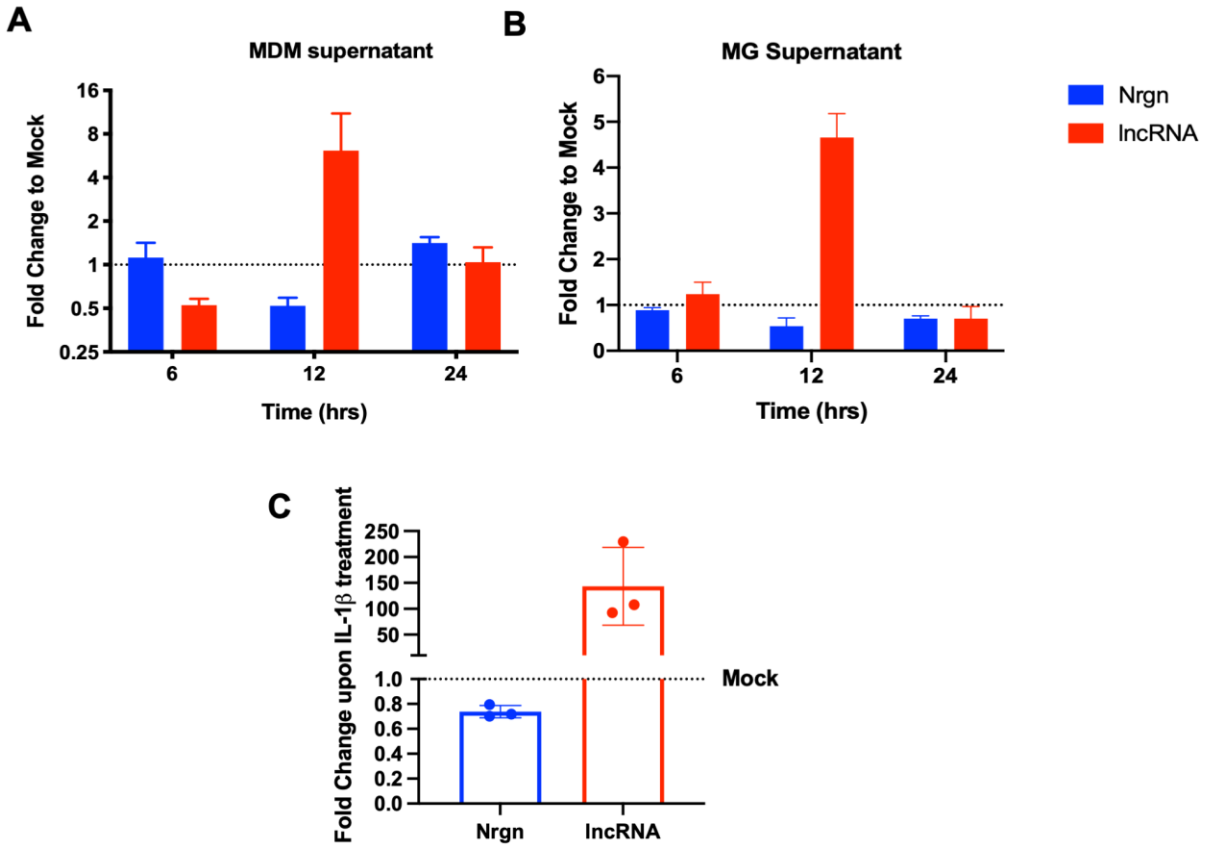

Figure 29. HIV-1 infection indirectly dysregulates Nrgn expression *in vitro*. SH-SY5Y cells were differentiated with RA for 7 days and (A) exposed to supernatant from HIV-1-infected or mock-infected MDM or (B) Microglia (N=3). RNA was harvested at, 6, 12 and 24hrs of incubation. (C) SH-SY5Y cells were differentiated with RA for 7

days and exposed to 0.1 ng of recombinant IL-1β for 1 hr and RNA was harvested. Nrgn and RP11-677M14.2 transcript expression level was assessed and compared to mock-treated neurons through RT-qPCR. Dotted lines represent the mock-treated neurons expression, blue bars represent average Nrgn fold change in expression whereas red bars represent the average lncRNA fold change in expression.

Based on previous results on Nrgn dysregulation, we anticipated that IL-1β, an important proinflammatory factor induced and secreted by HIV-1 infected macrophages/microglia, might have a role on RP11-677M14.2 dysregulation as well. To explore the role of IL-1β in lncRNA overexpression, we exposed differentiated SH-SY5Y cells with recombinant IL-1β for 1 hr and examined the lncRNA expression in comparison to mock treated. Analysis of sense and anti-sense expression revealed that a 143-fold increase in RP11-677M14.2 transcript expression ($p=0.0123$), whereas Nrgn expression decreased by 1.35-fold compared to untreated neurons (**Figure 29B**). This suggests that activation of an intracellular cascade downstream to IL-1β leads to transcriptional activation of RP11-677M14.2 which in turn downregulates Nrgn mRNA.

5.3.6 *In silico* analysis of RP11-677M14.2 promoter region predicts regulatory network for lncRNA overexpression in neurons

In order to obtain insights on how HIV-1 mediated factors might affect up-regulation of RP11-677M14.2, we performed *in silico* analysis to examine all the putative transcription factors binding sites present in the promoter regions of Nrgn sense and anti-sense transcripts by using the TRANSFAC platform (199). We predicted 15 transcription factors that putatively interact with lncRNA promoter region only, 19 that interact with Nrgn promotor region only and 48 transcription factors that interact with both promotor regions (**Figure 30A**). Interestingly, we

found that lncRNA promoter region contains the cAMP response element (CRE), which has been found to be activated in neurons through IL-1β-dependent phosphorylation of CRE-binding protein (CREB) (**Figure 30B, highlighted in red**). Further experiments will help us to better define the regulatory networks linking IL-1β and CRE-driven RP11-677M14.2 overexpression in HIV-1 neuropathogenesis.

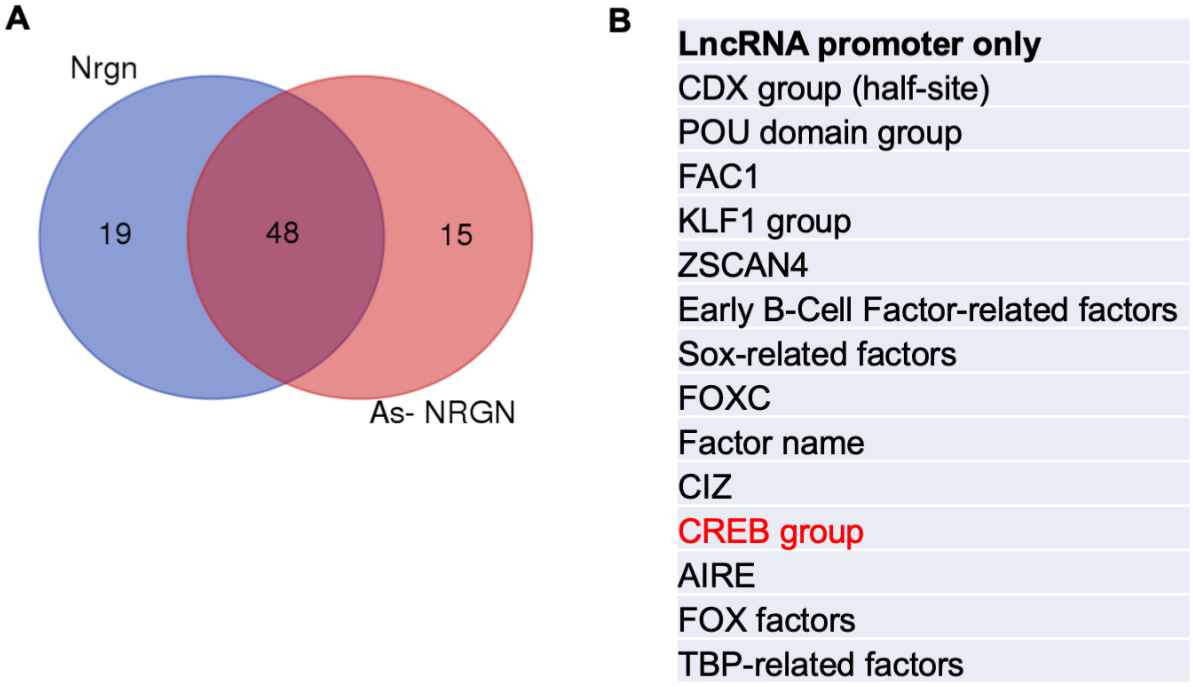

Figure 30. TRANSFAC analysis of lncRNA and Nrgn promoter region. (A) Venn diagram depicting the overlap between sets of potential transcriptional regulators predicted by TRANSFAC platform and (B) list of predicted transcription factors that target lncRNA promoter region only.

5.4 Discussion

There is a clear correlation between Nrgn levels and cognitive function (47,49). We have recently demonstrated that Nrgn mRNA is dysregulated in frontal cortex of people living with HIV-1 suggesting that Nrgn loss might be an early target in the onset of HIV-1 associated cognitive disorder (HAND). Currently, there is no effective treatment to alleviate or restore cognitive deficits in HAND. Therefore, is critically important to elucidate the molecular mechanisms underlying Nrgn dysregulation followed by learning and memory impairment. LncRNAs are emerging as key players in regulating important cellular functions and a large volume of studies have linked the aberrant lncRNAs expression to a diverse number of human diseases (200). However, only a couple were linked to HIV-1 infection and virtually none to development or progression of HIV-1 associated neurocognitive disorder (HAND) (190,191).

Here we present a novel lncRNA antisense transcript, named RP11-677M14.2, which function has not yet been identified. Because the expression of this lncRNA is increased in frontal cortex samples of HIV-1 positive individuals and its levels negatively correlated with Nrgn mRNA levels, we predicted that this lncRNA might be of particular relevance to the Nrgn dysregulation in HAND. Thus, based on the *in silico* and *in vivo* evidence of a discordant regulation of the expression of sense and anti-sense transcripts, we hypothesized that RP11-677M14.2 functions to suppress Nrgn expression.

Supporting our hypothesis, the transient overexpression of RP11-677M14.2 in SH-SY5Y cells, led to significant decrease in Nrgn mRNA expression. Moreover, overexpression of this lncRNA seemed to specifically reduce Nrgn expression. Remains to be investigated however, if treatment to silence RP11-677M14.2 transcript would restore Nrgn levels in the neurons. Ideally, an effective therapeutic agent should preferentially increase Nrgn levels without disturbing the

essential basal expression levels. Future transcriptome analysis of cells endogenously overexpressing RP11-677M14.2 and cells silencing RP11-677M14.2 expression will clarify how specific is this anti-sense regulatory mechanism. Interestingly, our results showing discordant expression levels of sense and antisense before and after SH-SY5Y differentiation, suggests that RP11-677M14.2 acts as a temporal regulator since in physiological conditions the lncRNA is abundant in neuroprogenitor cells but suppressed soon after the neuronal differentiation is initiated.

Our work further demonstrated that RP11-677M14.2 transcript is distributed throughout the cells but slightly enriched in the nucleus as several other lncRNAs recently identified. Subcellular localization of lncRNAs generally indicates their putative physiological roles. LncRNAs accumulated in the cytoplasm usually interacts with mRNAs to either stabilize the transcript for translation or target it to degradation. Alternatively, lncRNAs accumulated in the nucleus usually mediate transcriptional repression or activation of specific genes. Further RNA FISH experiments will reveal the precise localization of RP11-677M14.2 transcript to support our preliminary findings and future mechanistic studies.

According to the prevailing consensus, neurons are damaged as a result of a combination of both, direct exposure to shed viral factors and from pro-inflammatory factors released by HIV-infected macrophages/microglia in the brain (25). We demonstrated that RP11-677M14.2 transcript is upregulated in response to treatment with conditioned medium from HIV-1 infected macrophages/microglia. In our experimental setting, we observed a timely coordinated discordant regulation of Nrgn mRNA and RP11-677M14.2 lncRNA. While we cannot be certain that the Nrgn dysregulation upon exposure to supernatant of HIV-1 infected glial cells is due only to the up-regulation of RP11-677M14.2 lncRNA expression, these results provide preliminary evidence for a role to RP11-677M14.2 transcript in HIV-1 neuropathogenesis. Moreover, these observations

suggest that the inflammatory factors released by infected macrophages might be in part responsible for Nrgn dysregulation through its anti-sense transcript (RP11-677M14.2). Our finding that recombinant IL-β treatment of neurons enhances the lncRNA expression *in vitro* strongly suggests that this transcript is one of the mechanistic links between neuroinflammation and the neuronal dysfunction underlying the cognitive decline. It will be worth studying the downstream signaling pathways in neurons modulated by IL-β treatment to provide experimental evidence to our *in silic*o analysis. Furthermore, these supernatants also contain virus particles that have not been separated or inactivated. Future experiments will tease out the individual contribution of inflammatory factors, virus particles and viral proteins.

Although our study was limited to the brain, investigation of differential expression of RP11-677M14.2 in plasma and/or CSF may also have an utility as a new biomarker for HAND as recently demonstrated for other antisense lncRNA (201).

In summary, we have employed cellular and molecular approaches to investigate the role of RP11-677M14.2 lncRNA in dysregulating Nrgn. We have demonstrated that upregulation of the lncRNA in HAND may be partially determinant to Nrgn loss in neurons with potential implications to the onset and progression of the neuropathogenesis. The insights obtained from this study will further advance our understanding of the molecular mechanisms underlying HIV-1 neuropathogenesis.

6.0 Overall Conclusions and Future Directions

6.1 Summary of Findings

Studying neurodegenerative diseases *in vitro* is challenging due to the complex nature of CNS biology involving multiple differentiated cell lineages (43). Three-dimensional brain models using primarily human induced pluripotent stem cells (hiPSCs), the so called "brain organoids", have emerged as a whole new field in neuroscience and neuropathogenesis presenting remarkable progresses (83,116-120). However, most of the available protocols are entirely focused on neurons and astrocytes and lack microglia or another inflammatory component (81,83,86). To circumvent this issue, we incorporated microglia into mature human brain organoid (hBORG) mimicking the invasion of microglia into the CNS during neurodevelopment (88). To mimic the adult HIV-1 positive patient's brain, we tested the incorporation of human adult microglia isolated and cultured from *post-mortem* brain into hBORGs and generated MG-hBORGs as a physiologically relevant tool to study HIV-1 neuropathogenesis.

Once the triculture and the protocol of infection were established, we used techniques as RT-qPCR for gene expression analysis, immunofluorescence for protein expression and ELISA for cytokines measurement to test different features associated with HIV-1 neuropathology. An important feature associated with HIV-1 neuropathology is the release of inflammatory mediators (18,87,93). Several early studies conducted in *postmortem* brain tissue from HIV-1 infected individuals correlating both, viral replication and TNF-α transcription (131). Similarly, IL-1β is also elevated in the CNS during HIV-1 infection (112). Consistent with these findings, HIV-1 infection rapidly induced TNF-α and IL-1β release in our MG-hBORG system, which was directly

correlated with the extent of virus replication. Of particular importance was the observation that IL-1β concentration increases with the viral production, suggesting that viral replication directly affects the release of this pro-inflammatory cytokine. Thus, the capacity to detect changes in TNF-α and IL-1β release in the conditioned media of our MG-hBORG model provides a significant advantage of our tri-culture system over most of the 2D cultures or current brain organoids devoid of microglia and prompts further investigation on the inflammatory response to HIV-1 infection in brain.

Overall, MG-hBORGs provide an alternative and physiologically relevant experimental model that has great potential to boost our current knowledge about the molecular dynamics of HIV-1 neuropathogenesis and its progression. Notably, Our MG-hBORG model recapitulated all the most important hallmarks of HIV-1 neuropathology widely documented in postmortem brain (12,18,73). Although we have not focused to determine the mechanisms involved, our ability to generate an organoid model that recapitulated neuroinflammation, synaptodendritic damage, astrogliosis, neurodegeneration, certainly enables the extended studies of the pathogenic cascade that culminate in neuronal damage.

As mentioned in Chapter 2, dendrites simplification and synaptic loss, also known as synaptodendritic damage, are the pathological hallmark of early cognitive decline. Neurogranin (Nrgn) is a post-synaptic protein abundant in dendrites in healthy brain. Interestingly, Nrgn is only expressed in excitatory neurons in the specific brain regions such as cortex and hippocampus, the neuronal type and brain regions most affected by HIV-1 in HIV-1 neuropathogenesis. Dysregulation of neurogranin expression is associated with cognitive impairment and higher risk of developing neurodegenerative and psychiatric disorders, highlighting the critical function of

neurogranin in maintaining normal brain activities (50). Therefore, we investigated Nrgn expression dysregulation in HAND.

Herein, we have assessed Nrgn levels in frontal cortex samples of HIV-1 positive individuals, with and without cognitive impairment, through immunohistochemistry, immunofluorescence and RT-qPCR, and compared to aged-matched healthy control samples. Our protein data indicated that Nrgn is dysregulated in HIV-1 positive individuals before dendritic loss and neurodegeneration. Additionally, our results point to a significant dysregulation of Nrgn mRNA expression in the frontal cortex samples from HIV-1 positive individuals, suggesting that Nrgn loss may be an early "molecular hallmark" of HAND.

To examine the indirect effect of HIV-1 infection on neurogranin dysregulation, we set up infection of macrophages and microglia and collected the conditioned media for further exposure of neurons. A significant decrease of Nrgn mRNA was observed from 6 to 12 hours after exposure to HIV-1 infected macrophage/microglia supernatant, supporting the notion that relevant pathways to neuronal injury in HAND are activated indirectly through the release of host/viral factors from infected macrophages/microglia (10,12). Even though we have not thoroughly investigated the immune profile of the conditioned media, we quantitated the levels of four proinflammatory cytokines present in the conditioned media from infected MDM and primary microglia compared to mock-infected supernatants. These four cytokines were shortlisted from previous works from our group (53,173). Among those cytokines tested, IL-1b was the only cytokine among those we tested which was highly abundant in supernatants from both HIV-1 infected MDM and HIV-1 infected microglia, suggesting an overlapping phenotype in response to viral infection. Altogether, our results suggested that immune responses may be involved in the Nrgn dysregulation in HAND.

Intrigued by the dysregulation of Nrgn mRNA in brain and by our in vitro results indicating that this mechanism may be reversible, we decided to examine possible mechanisms involved in Nrgn gene regulation. Currently, there is no effective treatment to alleviate or restore cognitive deficits in HAND. Therefore, is critically important to elucidate the molecular mechanisms behind Nrgn. We then identified in silico a lncRNA named RP11-677M14.2, localized in the antisense strand of NRGN locus which function has not yet been identified. We then hypothesized that this lncRNA might be of particular relevance to the Nrgn dysregulation in HAND. We addressed this hypothesis by employing *in silico*, cellular and molecular approaches to investigate the role of RP11-677M14.2 lncRNA in dysregulating Nrgn.

Next, we generated a plasmid expression construct using the spliced sequence of RP11-677M14.2 under regulation of a mammalian cell promoter to overexpress this lncRNA in SH-SY5Y cells and observed a significant decrease in Nrgn mRNA expression. Our work further demonstrated that RP11-677M14.2 transcript is distributed throughout the cells but slightly enriched in the nucleus. As the subcellular localization of lncRNAs generally indicates their putative physiological roles we speculate that RP11-677M14.2 mediate Nrgn transcriptional repression rather than mRNA destabilization in the cytoplasm. Because the expression of this lncRNA is increased in frontal cortex samples of HIV-1 positive individuals and its levels negatively correlated with Nrgn mRNA levels,

Finally, we demonstrated that RP11-677M14.2 transcript is upregulated in response to treatment with conditioned medium from HIV-1 infected macrophages/microglia. In our experimental setting, we observed a timely coordinated dysregulation of Nrgn mRNA and RP11-677M14.2 lncRNA supporting our hypothesis of a discordant regulation. In summary, we have demonstrated that upregulation of the lncRNA in HAND may be partially responsible for loss of

Nrgn in neurons with potential implications to the onset and progression of the neuropathogenesis. The insights obtained from this study will further advance our understanding of the molecular mechanisms underlying HIV-1 neuropathogenesis.

6.2 Public health Relevance

Despite the success of the antiretroviral therapy on controlling viral replication and even reducing viral transmission, HIV-1 is still one of the leading causes of death and a health threat to millions worldwide. There are currently 38 million adults and children living with the HIV-1 and in 2019 ART coverage reached 67%. Nevertheless, approximately 690,000 people died of AIDS-related causes.

While the efforts to control the epidemic by treatment and prevention services are accelerated, the viral spread still continue with more than 1.7 million newly HIV-1 infections in 2019. Unfortunately, there is no cure for HIV-1 and vaccination still remains elusive. Although ART prolongs life and prevents AIDS-related complications, people living with HIV-1 have a disproportionate risk of developing comorbidities compared to HIV-1 negative people. Cardiovascular diseases, cancer and chronic diseases driven by liver, bone and kidney complications have been described as common comorbidities associated with HIV-1, including the individuals receiving ART. Among these complications that still impact the health and quality of life of people living with HIV-1, HIV-1 associated neurocognitive disorders (HAND) pose unique challenges. Despite the prevalence of HIV-1 associated dementia due to HIV-1 infection has markedly reduced since the advent of ART, less severe forms continue to increase. It has been suggested that as many as 70% of HIV-1 infected individuals might have some degree of cognitive

impairment despite long term ART usage. Because the precise pathogenesis surrounding these disorders is still unclear and effective diagnostic and treatment options for HAND are limited, accelerated efforts to better understand the mechanisms underlying neurodegeneration in HAND are paramount in the improvement of HIV-1 therapy. Here we sought to contribute to such effort by offering an alternative *in vitro* model to study HIV-1 neuropathogenesis and by investigating new molecular targets that can be dysregulated in human brain upon HIV-1 infection.

6.3 Future Directions

To the best of our knowledge, this was the first study to model HIV-1 neuropathology using brain organoids along with HIV-1 infected primary microglia. Our triculture model addressed key pathological features that are associated with neuroinflammation by HIV-1, defined by the presence of activated microglia, reactive astrocytes and release of pro-inflammatory cytokines. Because human triculture brain organoids (MG-hBORGs) more accurately recreate the human brain physiological microenvironment, their utilization in HIV-1 neuropathogenesis could open up whole new lines of investigation on molecular mechanisms underlying the onset and progression of HAND.

Although it was not in the scope of our study to investigate a more extensive secretory profile of the infected MG-hBORGs, full examination of the conditioned media during the course of infection could be performed either through multiplex technologies or proteomics analysis. It is also possible to speculate that other pro-inflammatory cytokines than the ones investigated in our study released by infected cells can provoke an additive effect and exacerbate the inflammatory responses of the entire system regardless the level of infection. Thus, in the future, analysis of

cytokines/chemokines present in conditioned media from infected MG-hBORGs in the presence or absence of antiretrovirals would substantially broaden our knowledge in HIV-1 induced neuroinflammation.

Despite the controversy, it is reported that astrocytes are infected by HIV-1 *in vivo* likely through cell-to-cell contact (133). In our preliminary investigation based on image analysis of the entire organoid, we found no evidence of productive astrocytes infection during the period of our study. It might be possible that longer periods of infection and the use of improved techniques, for instance immunostaining of histological sections, will help to clarify the mechanisms of astrocytes infection and the contribution of these cells to latency.

Although astrocytes are unlikely to be major contributors of IL-1β within the brain, it is important to highlight that the contribution of astrocyte activation/infection to IL-1β peak release remains to be clarified (112). These cells outnumber microglia in the brain by 10-fold and have been shown to respond to LPS-activated microglia increasing TNF-α and IL-1β expression and release leading to a neurotoxic function (134). Therefore, a thorough investigation using MG-hBORGs as tools will certainly contribute to a better understanding of the activated astrocytes contribution to neuroinflammation.

In addition, modulation of microglial responses is a potential therapeutic approach for treatment of HIV-1 neuropathology and other neurodegenerative diseases (139). Thus, future studies with infected MG-hBORG may give insights into the time course of microglial activation and polarization as well as unravel new molecular players that could be potentially targeted for therapies. Although not specifically studied in this report, the HIV-1 infected MG-hBORG model provides a physiologically relevant human-specific experimental system to further study the dynamics of viral latency and persistence in the absence or presence of antiretrovirals. It remains

to be investigated if the cell damage observed in our study can be attenuated through suppression of viral replication. The effects of the combined antiretroviral therapy (ART) to the most severe neurologic manifestations of HIV-1 infection, correlate with a decrease in the prevalence of HIV-1 associated dementia in the post-ART era (10). Unfortunately, however, studies have reported high persistent rates of mild to moderate neurocognitive impairment in individuals under ART regimen, which neuropathology correlates to loss of synapses and dendritic simplification rather than substantial neurodegeneration (12). Detailed mechanistic studies on synaptodendritic damage by using MG-hBORG system in the presence of ART drugs deserves further investigation and may provide important insights.

We have demonstrated in this study that Nrgn mRNA is dysregulated in frontal cortex of people living with HIV-1. Because there is a clear correlation between Nrgn levels and cognitive function (47,49), we speculate that Nrgn loss might be an early event in the onset of HAND.

Thus far, not much is known about the regulation of Nrgn expression other than thyroid hormone (TH) promotes its transcription (163-165). However, TH stimulus is ineffective in the upper layers of cortex and it is not likely that Nrgn downregulation in frontal cortex samples of HIV-1 positive individuals is due to TH deprivation (163). Importantly, Nrgn is known to be locally translated in the dendrites (166,167). Other possibility that cannot be ruled out is that HIV-1 infection somehow induces dendritic Nrgn mRNA destabilization in frontal cortex. If this is the case, future studies investigating the spatial distribution of Nrgn mRNA in the context of HIV-1 infection may complement our results. In addition, measurement of the synaptic levels of Nrgn in the synaptic compartment will help to clarify the regional distribution of Nrgn in HIV-1 infected brain and whether total Nrgn is specifically dysregulated in the synaptosomes or it is accumulated in the nucleus.

Since neurons do not seem to be infected by HIV-1, we next asked if exposure of neurons to conditioned media from infected glial cells would reproduce the Nrgn dysregulation observed in brain samples. Indeed, Nrgn expression was transiently decreased *in vitro* in the first 12 hours of treatment and its expression levels seemed to recover afterwards. These observations indicate that Nrgn dysregulation is potentially reversible as a result of some compensatory mechanism for synapse or dendrites protection. Further mechanistic studies will help to identify signaling pathways that contribute to Nrgn rebound in neurons.

IL-1b is one of the many mediators released from glial cells involved in neurotoxicity (135,168,169) and cognitive decline (170-172). Thus, a key question is whether and how IL-1b signaling is involved in Nrgn dysregulation in neurons. Future studies treating neurons with physiological relevant concentration of the recombinant cytokine along with the neuronal IL-1b receptor antagonist (IL-ra) may help to tease out the direct contribution of this cytokine to Nrgn dysregulation. Another important question not addressed in this work is what the relative contribution of viral proteins to the loss of Nrgn in neurons. Although our preliminary assessment suggests a differential contribution of the viral Envelope and Vpr to the downregulation of Nrgn in neurons, at least in part. However, it remains to be defined whether the effect of these viral proteins is indirect through some molecular pathway specifically activated in the infected cells, or if these proteins are shed in the conditioned media to exert its effect directly into neurons.

In this study we showed that Nrgn dysregulation at both mRNA and protein levels is evident in the frontal cortex of HIV-1 positive individuals even before the emergence of clinical symptoms. This led us to speculate whether a greater expression of Nrgn can lead to a symptoms reversal or halt the disease progression, placing Nrgn on the spotlight as promising therapeutic target. To address this hypothesis, it would be interesting to leverage the organoid technology

established in this study to overexpress Nrgn in neurons in a more physiologically relevant system. Results from this experiment would help to depict whether neurons overexpressing Nrgn will become resistant to synaptodendritic damage or will be able to restore synaptodendritic integrity upon HIV-1 infection.

Furthermore, we have identified and characterized a possible role for the RP11-677M14.2 lncRNA transcript in Nrgn transcriptional regulation. Future gain and loss-of-function experiments followed by whole transcriptome analysis will clarify how specific is anti-sense regulatory mechanism mediated by RP11-677M14.2. Additionally, treatments to silence the RP11-677M14.2 transcript, for instance, by delivering antisense oligos (202) to cells, would help to restore Nrgn levels in the neurons. Once more, leveraging the brain organoid tool developed in this study to target this lncRNA for silencing could perhaps reverse Nrgn loss and so pave the way to therapeutically explore RP11-677M14.2 in cognitively impaired individuals.

While we cannot be certain that the up-regulation of RP11-677M14.2 lncRNA expression is the only factor involved in Nrgn dysregulation in frontal cortex and *in vitro* upon exposure to supernatant of HIV-1 infected glial cells, the results included in this dissertation provide preliminary evidence for a role to RP11-677M14.2 transcript in HIV-1 neuropathogenesis. In addition, these observations suggest that the inflammatory factors released by infected macrophages might be in part responsible for Nrgn dysregulation through its anti-sense transcript (RP11-677M14.2). Furthermore, these supernatants also contain virus particles that have not been separated or inactivated. Future experiments will tease out the individual contribution of inflammatory factors, virus particles and viral proteins on the upregulation of RP11-677M14.2.

Bibliography

1. Chivero, E. T., Guo, M. L., Periyasamy, P., Liao, K., Callen, S. E., and Buch, S. (2017) HIV-1 Tat Primes and Activates Microglial NLRP3 Inflammasome-Mediated Neuroinflammation. *J Neurosci* **37**, 3599-3609
2. WHO. (2018) Unaids-Global Aids update.
3. Cohen, M. S., Hellmann, N., Levy, J. A., DeCock, K., and Lange, J. (2008) The spread, treatment, and prevention of HIV-1: evolution of a global pandemic. *J Clin Invest* **118**, 1244-1254
4. Herbein, A. K. a. G. (2014) The macrophage: a therapeutic target in HIV-1 infection. *Molecular and Celular Therapies* **2**, 15
5. POST F.A. , W. R. a. M. G. (1996) CD4 and total lymphocyte counts as predictors of HIV disease progression. *Q J Med* **89**, 4
6. De Cock, K. M., Jaffe, H. W., and Curran, J. W. (2011) Reflections on 30 Years of AIDS. *Emerging Infectious Diseases* **17**, 1044-1048
7. Gallant, J., Hsue, P., Budd, D., and Meyer, N. (2018) Healthcare utilization and direct costs of non-infectious comorbidities in HIV-infected patients in the USA. *Curr Med Res Opin* **34**, 13-23
8. Gallant, J., Hsue, P. Y., Shreay, S., and Meyer, N. (2017) Comorbidities Among US Patients With Prevalent HIV Infection-A Trend Analysis. *J Infect Dis* **216**, 1525-1533
9. Lerner, A. M., Eisinger, R. W., and Fauci, A. S. (2019) Comorbidities in Persons With HIV: The Lingering Challenge. *JAMA*
10. Saylor, D., Dickens, A. M., Sacktor, N., Haughey, N., Slusher, B., Pletnikov, M., Mankowski, J. L., Brown, A., Volsky, D. J., and McArthur, J. C. (2016) HIV-associated neurocognitive disorder--pathogenesis and prospects for treatment. *Nat Rev Neurol* **12**, 234-248
11. Tedaldi, E. M., Minniti, N. L., and Fischer, T. (2015) HIV-associated neurocognitive disorders: the relationship of HIV infection with physical and social comorbidities. *Biomed Res Int* **2015**, 641913
12. Ellis, R., Langford, D., and Masliah, E. (2007) HIV and antiretroviral therapy in the brain: neuronal injury and repair. *Nat Rev Neurosci* **8**, 33-44
13. Carne CA, S. A., Erkington SG, Preston FE, Tedder RS, Sutherland S, Daly HM, Craske J. (1985) Acute Encephalopathy Coincident with Seroconversion for Anti-HTLV-III. *The Lancet*, 3
14. Hellmuth J, F. J., Valcour, V, Kroon E, Ananworanich J, Intasan J, Lerdlum S, Narvid J, Pothisri M, Allen I, Krebs SJ, Slike B, Pruksakaew P, Jagodzinski LL, Puttamaswin S, Phanuphak N, Spudich S. (2016) Neurologic signs and symptoms frequently manifest in acute HIV infection. *Neurology* **87**, 7
15. Gray F, L. M., Keohane C, Paraire F, Marc B, Durigon M, Gherardi R. (1992) Early Brain Changes in HIV infection: Neuropathological Study of 11 HIV Seropositive, Non-AIDS Cases. *Journal of Neuropathology and Experimental Neurology* **51**, 9

16. Everall IP, H. R., Marcotte TD, Ellis RJ, McCutchan JA, Atkinsin JH, Grant I, Mallory M, Masliah E (1999) Cortical Synaptic Density is Reduced in Mild to Moderate Human Immunodeficiency Virus Neurocognitive Disorder *Brain Pathology* **9**, 9
17. Masliah E, H. R., Marcotte TD, Ellis RJ, Wiley CA, Mallory M, Achim CL, McCutchan JA, Nelson JA, Atkinson JH, Grant I. (1997) Dendritic Injury Is a Pathological Substrate for Human Immunodeficiency Virus-Related Cognitive Disorders *Annals of Neurology* **42**, 10
18. Kaul, M., and Lipton, S. A. (2006) Mechanisms of neuroimmunity and neurodegeneration associated with HIV-1 infection and AIDS. *J Neuroimmune Pharmacol* **1**, 138-151
19. Nightingale, S., Winston, A., Letendre, S., Michael, B. D., McArthur, J. C., Khoo, S., and Solomon, T. (2014) Controversies in HIV-associated neurocognitive disorders. *The Lancet Neurology* **13**, 1139-1151
20. Green, M. V., Raybuck, J. D., Zhang, X., Wu, M. M., and Thayer, S. A. (2019) Scaling Synapses in the Presence of HIV. *Neurochem Res* **44**, 234-246
21. Ru, W., and Tang, S. J. (2017) HIV-associated synaptic degeneration. *Mol Brain* **10**, 40
22. Qian, X., Nguyen, H. N., Song, M. M., Hadiono, C., Ogden, S. C., Hammack, C., Yao, B., Hamersky, G. R., Jacob, F., Zhong, C., Yoon, K. J., Jeang, W., Lin, L., Li, Y., Thakor, J., Berg, D. A., Zhang, C., Kang, E., Chickering, M., Nauen, D., Ho, C. Y., Wen, Z., Christian, K. M., Shi, P. Y., Maher, B. J., Wu, H., Jin, P., Tang, H., Song, H., and Ming, G. L. (2016) Brain-Region-Specific Organoids Using Mini-bioreactors for Modeling ZIKV Exposure. *Cell* **165**, 1238-1254
23. Wang, Y., Liu, M., Lu, Q., Farrell, M., Lappin, J. M., Shi, J., Lu, L., and Bao, Y. (2020) Global prevalence and burden of HIV-associated neurocognitive disorder: A meta-analysis. *Neurology* **95**, e2610-e2621
24. Heaton, R. K., Clifford, D. B., Franklin, D. R., Jr., Woods, S. P., Ake, C., Vaida, F., Ellis, R. J., Letendre, S. L., Marcotte, T. D., Atkinson, J. H., Rivera-Mindt, M., Vigil, O. R., Taylor, M. J., Collier, A. C., Marra, C. M., Gelman, B. B., McArthur, J. C., Morgello, S., Simpson, D. M., McCutchan, J. A., Abramson, I., Gamst, A., Fennema-Notestine, C., Jernigan, T. L., Wong, J., Grant, I., and Group, C. (2010) HIV-associated neurocognitive disorders persist in the era of potent antiretroviral therapy: CHARTER Study. *Neurology* **75**, 2087-2096
25. Zayyad, Z., and Spudich, S. (2015) Neuropathogenesis of HIV: from initial neuroinvasion to HIV-associated neurocognitive disorder (HAND). *Curr HIV/AIDS Rep* **12**, 16-24
26. Gannon, P., Khan, M. Z., and Kolson, D. L. (2011) Current understanding of HIV-associated neurocognitive disorders pathogenesis. *Curr Opin Neurol* **24**, 275-283
27. MP, H. N. M. (2002) Calcium Dysregulation and Neuronal Apoptosis by the HIV-1 Porteins Tat and gp120. *JAIDS* **31**, 7
28. Baxter, A. E., Niessl, J., Fromentin, R., Richard, J., Porichis, F., Charlebois, R., Massanella, M., Brassard, N., Alsahafi, N., Delgado, G. G., Routy, J. P., Walker, B. D., Finzi, A., Chomont, N., and Kaufmann, D. E. (2016) Single-Cell Characterization of Viral Translation-Competent Reservoirs in HIV-Infected Individuals. *Cell Host Microbe* **20**, 368-380
29. Ferdin, J., Goricar, K., Dolzan, V., Plemenitas, A., Martin, J. N., Peterlin, B. M., Deeks, S. G., and Lenassi, M. (2018) Viral protein Nef is detected in plasma of half of HIV-infected adults with undetectable plasma HIV RNA. *PLoS One* **13**, e0191613

30. Rychert, J., Strick, D., Bazner, S., Robinson, J., and Rosenberg, E. (2010) Detection of HIV gp120 in plasma during early HIV infection is associated with increased proinflammatory and immunoregulatory cytokines. *AIDS Res Hum Retroviruses* **26**, 1139-1145
31. Nath, A. (2002) Human immunodeficiency virus (HIV) proteins in neuropathogenesis of HIV dementia. *J Infect Dis* **186 Suppl 2**, S193-198
32. Vignoli, A. L., Martini, I., Haglid, K. G., Silvestroni, L., Augusti-Tocco, G., and Biagioni, S. (2000) Neuronal glycolytic pathway impairment induced by HIV envelope glycoprotein gp120. *Mol Cell Biochem* **215**, 73-80
33. Louboutin, J. P., Agrawal, L., Reyes, B. A., van Bockstaele, E. J., and Strayer, D. S. (2012) Gene delivery of antioxidant enzymes inhibits human immunodeficiency virus type 1 gp120-induced expression of caspases. *Neuroscience* **214**, 68-77
34. Nath, A., Padua, R. A., and Geiger, J. D. (1995) HIV-1 coat protein gp120-induced increases in levels of intrasynaptosomal calcium. *Brain Res* **678**, 200-206
35. Zheng, J., Thylin, M. R., Ghorpade, A., Xiong, H., Persidsky, Y., Cotter, R., Niemann, D., Che, M., Zeng, Y. C., Gelbard, H. A., Shepard, R. B., Swartz, J. M., and Gendelman, H. E. (1999) Intracellular CXCR4 signaling, neuronal apoptosis and neuropathogenic mechanisms of HIV-1-associated dementia. *J Neuroimmunol* **98**, 185-200
36. Dreyer, E. B., Kaiser, P. K., Offermann, J. T., and Lipton, S. A. (1990) HIV-1 coat protein neurotoxicity prevented by calcium channel antagonists. *Science* **248**, 364-367
37. Kaiser, P. K., Offermann, J. T., and Lipton, S. A. (1990) Neuronal injury due to HIV-1 envelope protein is blocked by anti-gp120 antibodies but not by anti-CD4 antibodies. *Neurology* **40**, 1757-1761
38. Patel, C. A., Mukhtar, M., and Pomerantz, R. J. (2000) Human immunodeficiency virus type 1 Vpr induces apoptosis in human neuronal cells. *J Virol* **74**, 9717-9726
39. Jones, G. J., Barsby, N. L., Cohen, E. A., Holden, J., Harris, K., Dickie, P., Jhamandas, J., and Power, C. (2007) HIV-1 Vpr causes neuronal apoptosis and in vivo neurodegeneration. *J Neurosci* **27**, 3703-3711
40. Magnuson, D. S., Knudsen, B. E., Geiger, J. D., Brownstone, R. M., and Nath, A. (1995) Human immunodeficiency virus type 1 tat activates non-N-methyl-D-aspartate excitatory amino acid receptors and causes neurotoxicity. *Ann Neurol* **37**, 373-380
41. Maragos, W. F., Tillman, P., Jones, M., Bruce-Keller, A. J., Roth, S., Bell, J. E., and Nath, A. (2003) Neuronal injury in hippocampus with human immunodeficiency virus transactivating protein, Tat. *Neuroscience* **117**, 43-53
42. Sabatier, J. M., Vives, E., Mabrouk, K., Benjouad, A., Rochat, H., Duval, A., Hue, B., and Bahraoui, E. (1991) Evidence for neurotoxic activity of tat from human immunodeficiency virus type 1. *J Virol* **65**, 961-967
43. Wang, H. (2018) Modeling Neurological Diseases With Human Brain Organoids. *Front Synaptic Neurosci* **10**, 15
44. Stuchlik, A. (2014) Dynamic learning and memory, synaptic plasticity and neurogenesis: an update. *Front Behav Neurosci* **8**, 106
45. Dominguez-Gonzalez, I., Vazquez-Cuesta, S. N., Algaba, A., and Diez-Guerra, F. J. (2007) Neurogranin binds to phosphatidic acid and associates to cellular membranes. *Biochem J* **404**, 31-43

46. Hoffman, L., Chandrasekar, A., Wang, X., Putkey, J. A., and Waxham, M. N. (2014) Neurogranin alters the structure and calcium binding properties of calmodulin. *J Biol Chem* **289**, 14644-14655
47. Kubota, Y., Putkey, J. A., and Waxham, M. N. (2007) Neurogranin controls the spatiotemporal pattern of postsynaptic Ca2+/CaM signaling. *Biophys J* **93**, 3848-3859
48. Huang, F. L., Huang, K. P., Wu, J., and Boucheron, C. (2006) Environmental enrichment enhances neurogranin expression and hippocampal learning and memory but fails to rescue the impairments of neurogranin null mutant mice. *J Neurosci* **26**, 6230-6237
49. Pak JH, H. F., Li J, Balschun D, Reymann KG, Chiang C, Westphal H and Huang KP. (2000) Involvement of neurogranin in the modulation of calcium calmodulin-dependent protein kinase II, synaptic plasticity, and spatial learning: A study with knockout mice. *PNAS* **97**, 6
50. Diez-Guerra, F. J. (2010) Neurogranin, a link between calcium/calmodulin and protein kinase C signaling in synaptic plasticity. *IUBMB Life* **62**, 597-606
51. Garrido-Garcia, A., de Andres, R., Jimenez-Pompa, A., Soriano, P., Sanz-Fuentes, D., Martinez-Blanco, E., and Diez-Guerra, F. J. (2019) Neurogranin Expression Is Regulated by Synaptic Activity and Promotes Synaptogenesis in Cultured Hippocampal Neurons. *Mol Neurobiol* **56**, 7321-7337
52. Alvarez-Bolado, G., Rodriguez-Sanchez, P., Tejero-Diez, P., Fairen, A., and Diez-Guerra, F. J. (1996) Neurogranin in the development of the rat telencephalon. *Neuroscience* **73**, 565-580
53. Guha, D., Wagner, M. C. E., and Ayyavoo, V. (2018) Human immunodeficiency virus type 1 (HIV-1)-mediated neuroinflammation dysregulates neurogranin and induces synaptodendritic injury. *J Neuroinflammation* **15**, 126
54. Barry, G. (2014) Integrating the roles of long and small non-coding RNA in brain function and disease. *Mol Psychiatry* **19**, 410-416
55. Briggs, J. A., Wolvetang, E. J., Mattick, J. S., Rinn, J. L., and Barry, G. (2015) Mechanisms of Long Non-coding RNAs in Mammalian Nervous System Development, Plasticity, Disease, and Evolution. *Neuron* **88**, 861-877
56. Massone S., V. I., Fiorino G, Castelnuovo M, Barbieri F, Borghi R, Tabaton M, Robello M, Gatta E, Russo C, Florio T, Dieci G, Cancedda R, Pagano A. (2011) 17A, a novel non-coding RNA, regulates GABA B alternative splicing and signaling in response to inflammatory stimuli and in Alzheimer disease. *Neurobiology of Disease* **41**, 10
57. Faghihi, M. A., Modarresi, F., Khalil, A. M., Wood, D. E., Sahagan, B. G., Morgan, T. E., Finch, C. E., St Laurent, G., 3rd, Kenny, P. J., and Wahlestedt, C. (2008) Expression of a noncoding RNA is elevated in Alzheimer's disease and drives rapid feed-forward regulation of beta-secretase. *Nat Med* **14**, 723-730
58. Johnson, R., Richter, N., Jauch, R., Gaughwin, P. M., Zuccato, C., Cattaneo, E., and Stanton, L. W. (2010) Human accelerated region 1 noncoding RNA is repressed by REST in Huntington's disease. *Physiol Genomics* **41**, 269-274
59. Millar JK, W.-A. J., Anderson S, Christie S, Taylor MS, Semple CA, Devon RS, St Clair DM, Muir WJ, Blackwood DH, Porteous DJ. (2000) Disruption of two novel genes by a translocation co-segregating with schizophrenia. **9**, 9
60. Lisa Chakrabarti, M. H., Marie-Annick Maire, Rosemay Vazeux, Dominique Dormont, Luc Montagnier and Bruno Hurtrel. (1991) Early Viral Replication in the Brain of SIV-infected Rhesus Monkeys. *American Journal of Pathology* **139**, 8

61. Tourtellotte, L. R. J. R. B. P. S. a. W. W. (1988) Early penetration of blood-brain-barrier by HIV. *Neurology* **38**, 9
62. Masliah, E., Ge, N., Achim, C. L., Hansen, L. A., and Wiley, C. A. (1992) Selective neuronal vulnerability in HIV encephalitis. *J Neuropathol Exp Neurol* **51**, 585-593
63. Wiley, C. A., Achim, C. L., Christopherson, C., Kidane, Y., Kwok, S., Masliah, E., Mellors, J., Radhakrishnan, L., Wang, G., and Soontornniyomkij, V. (1999) HIV mediates a productive infection of the brain. *AIDS* **13**, 2055-2059
64. Churchill, M. J., Gorry, P. R., Cowley, D., Lal, L., Sonza, S., Purcell, D. F., Thompson, K. A., Gabuzda, D., McArthur, J. C., Pardo, C. A., and Wesselingh, S. L. (2006) Use of laser capture microdissection to detect integrated HIV-1 DNA in macrophages and astrocytes from autopsy brain tissues. *J Neurovirol* **12**, 146-152
65. Everall, I. P., Heaton, R. K., Marcotte, T. D., Ellis, R. J., McCutchan, J. A., Atkinson, J. H., Grant, I., Mallory, M., and Masliah, E. (1999) Cortical synaptic density is reduced in mild to moderate human immunodeficiency virus neurocognitive disorder. HNRC Group. HIV Neurobehavioral Research Center. *Brain Pathol* **9**, 209-217
66. Ketzler, S., Weis, S., Haug, H., and Budka, H. (1990) Loss of neurons in the frontal cortex in AIDS brains. *Acta Neuropathol* **80**, 92-94
67. Weis, S., Haug, H., & Budka, H. (1993) Neuronal damagein the cerebral cortex of AIDS brains: a morphometric study. *Acta Neuropathol* **85**, 5
68. Rao, V. R., Ruiz, A. P., and Prasad, V. R. (2014) Viral and cellular factors underlying neuropathogenesis in HIV associated neurocognitive disorders (HAND). *AIDS Res Ther* **11**, 13
69. Thompson, P. M., Dutton, R. A., Hayashi, K. M., Toga, A. W., Lopez, O. L., Aizenstein, H. J., and Becker, J. T. (2005) Thinning of the cerebral cortex visualized in HIV/AIDS reflects CD4+ T lymphocyte decline. *Proc Natl Acad Sci U S A* **102**, 15647-15652
70. Masliah E, H. R., Marcotte TD, Ellis RJ, Wiley CA, Mallory M, Achim CL, McCutchan JA, Nelson JA, Atkinson JH, Grant I. (1997) Dendritic Injury Is a Pathological Substrate for Human Immunodeficiency Virus-Related Cognitive Disorders. *Annals of Neurology* **42**, 10
71. Robertson KR, S. M., Parsons TD, Wu K, Bosch RJ, Wu J, McArthur JC, Collier AC, Evans SR and Ellis RJ. (2007) The prevalence and incidence of neurocognitive impairment in the HAART era. *AIDS* **21**, 7
72. Antinori, A., Arendt, G., Becker, J. T., Brew, B. J., Byrd, D. A., Cherner, M., Clifford, D. B., Cinque, P., Epstein, L. G., Goodkin, K., Gisslen, M., Grant, I., Heaton, R. K., Joseph, J., Marder, K., Marra, C. M., McArthur, J. C., Nunn, M., Price, R. W., Pulliam, L., Robertson, K. R., Sacktor, N., Valcour, V., and Wojna, V. E. (2007) Updated research nosology for HIV-associated neurocognitive disorders. *Neurology* **69**, 1789-1799
73. Archibald SL, M. E., Fennema-Notestine C, Marcotte TD, Ellis RJ, McCutchan JA, Heaton RK,, and Grant I, M. M., Miller A, et al. (2004) Correlation of In Vivo Neuroimaging Abnormalities With Postmortem Human Immunodeficiency Virus Encephalitis and Dendritic Loss. *Archives of Neurology* **61**, 7
74. Hirsch, P. R. J. V. M. (1992) SIV infection of macaques as a model for AIDS pathogenesis. *Intern. Rev. Immunol* **8**, 9
75. Beck, S. E., Queen, S. E., Metcalf Pate, K. A., Mangus, L. M., Abreu, C. M., Gama, L., Witwer, K. W., Adams, R. J., Zink, M. C., Clements, J. E., and Mankowski, J. L. (2018)

An SIV/macaque model targeted to study HIV-associated neurocognitive disorders. *J Neurovirol* **24**, 204-212
76. Hammond R.R, I. S., Achim C.L., Hearn S., Nassif J., Wiley C.A. . (2002) A reliable primary human CNS culture protocol for morphological studies of dendritic and synaptic elements. *Journal of Neuroscience Methods*, 10
77. Green, M. V., and Thayer, S. A. (2016) NMDARs Adapt to Neurotoxic HIV Protein Tat Downstream of a GluN2A-Ubiquitin Ligase Signaling Pathway. *J Neurosci* **36**, 12640-12649
78. Kim, H. J., Martemyanov, K. A., and Thayer, S. A. (2008) Human immunodeficiency virus protein Tat induces synapse loss via a reversible process that is distinct from cell death. *J Neurosci* **28**, 12604-12613
79. Shin, A. H., and Thayer, S. A. (2013) Human immunodeficiency virus-1 protein Tat induces excitotoxic loss of presynaptic terminals in hippocampal cultures. *Mol Cell Neurosci* **54**, 22-29
80. Zhang, X., Green, M. V., and Thayer, S. A. (2019) HIV gp120-induced neuroinflammation potentiates NMDA receptors to overcome basal suppression of inhibitory synapses by p38 MAPK. *J Neurochem* **148**, 499-515
81. Pasca, S. P. (2018) The rise of three-dimensional human brain cultures. *Nature* **553**, 437-445
82. Amin, N. D., and Pasca, S. P. (2018) Building Models of Brain Disorders with Three-Dimensional Organoids. *Neuron* **100**, 389-405
83. Lancaster, M. A., and Knoblich, J. A. (2014) Generation of cerebral organoids from human pluripotent stem cells. *Nat Protoc* **9**, 2329-2340
84. Yakoub, A. M. (2019) Cerebral organoids exhibit mature neurons and astrocytes and recapitulate electrophysiological activity of the human brain. *Neural Regen Res* **14**, 757-761
85. Watanabe, M., Buth, J. E., Vishlaghi, N., de la Torre-Ubieta, L., Taxidis, J., Khakh, B. S., Coppola, G., Pearson, C. A., Yamauchi, K., Gong, D., Dai, X., Damoiseaux, R., Aliyari, R., Liebscher, S., Schenke-Layland, K., Caneda, C., Huang, E. J., Zhang, Y., Cheng, G., Geschwind, D. H., Golshani, P., Sun, R., and Novitch, B. G. (2017) Self-Organized Cerebral Organoids with Human-Specific Features Predict Effective Drugs to Combat Zika Virus Infection. *Cell Rep* **21**, 517-532
86. Pamies, D., Barreras, P., Block, K., Makri, G., Kumar, A., Wiersma, D., Smirnova, L., Zang, C., Bressler, J., Christian, K. M., Harris, G., Ming, G. L., Berlinicke, C. J., Kyro, K., Song, H., Pardo, C. A., Hartung, T., and Hogberg, H. T. (2017) A human brain microphysiological system derived from induced pluripotent stem cells to study neurological diseases and toxicity. *ALTEX* **34**, 362-376
87. Katuri, A., Bryant, J., Heredia, A., and Makar, T. K. (2019) Role of the inflammasomes in HIV-associated neuroinflammation and neurocognitive disorders. *Exp Mol Pathol* **108**, 64-72
88. Kettenmann, H., Hanisch, U. K., Noda, M., and Verkhratsky, A. (2011) Physiology of microglia. *Physiol Rev* **91**, 461-553
89. Salter, M. W., and Stevens, B. (2017) Microglia emerge as central players in brain disease. *Nat Med* **23**, 1018-1027

90. Xavier, A. L., Menezes, J. R., Goldman, S. A., and Nedergaard, M. (2014) Fine-tuning the central nervous system: microglial modelling of cells and synapses. *Philos Trans R Soc Lond B Biol Sci* **369**, 20130593
91. Mittelbronn, M., Dietz, K., Schluesener, H. J., and Meyermann, R. (2001) Local distribution of microglia in the normal adult human central nervous system differs by up to one order of magnitude. *Acta Neuropathol* **101**, 249-255
92. Fernandez-Arjona, M. D. M., Grondona, J. M., Granados-Duran, P., Fernandez-Llebrez, P., and Lopez-Avalos, M. D. (2017) Microglia Morphological Categorization in a Rat Model of Neuroinflammation by Hierarchical Cluster and Principal Components Analysis. *Front Cell Neurosci* **11**, 235
93. Gonzalez-Scarano, F., and Martin-Garcia, J. (2005) The neuropathogenesis of AIDS. *Nat Rev Immunol* **5**, 69-81
94. Lu, J., Delli-Bovi, L. C., Hecht, J., Folkerth, R., and Sheen, V. L. (2011) Generation of neural stem cells from discarded human fetal cortical tissue. *J Vis Exp*
95. Singh, M., Warita, K., Warita, T., Faeder, J. R., Lee, R. E. C., Sant, S., and Oltvai, Z. N. (2018) Shift from stochastic to spatially-ordered expression of serine-glycine synthesis enzymes in 3D microtumors. *Scientific Reports* **8**, 9388
96. Singh, M., Tian, X. J., Donnenberg, V. S., Watson, A. M., Zhang, J., Stabile, L. P., Watkins, S. C., Xing, J., and Sant, S. (2019) Targeting the Temporal Dynamics of Hypoxia-Induced Tumor-Secreted Factors Halts Tumor Migration. *Cancer research* **79**, 2962-2977
97. Singh, M., Mukundan, S., Jaramillo, M., Oesterreich, S., and Sant, S. (2016) Three-Dimensional Breast Cancer Models Mimic Hallmarks of Size-Induced Tumor Progression. *Cancer research* **76**, 3732-3743
98. Singh, M., Close, D. A., Mukundan, S., Johnston, P. A., and Sant, S. (2015) Production of Uniform 3D Microtumors in Hydrogel Microwell Arrays for Measurement of Viability, Morphology, and Signaling Pathway Activation. *Assay Drug Dev Technol* **13**, 570-583
99. Singh, M., Venkata Krishnan, H., Ranganathan, S., Kiesel, B., Beumer, J. H., Sreekumar, S., and Sant, S. (2017) Controlled three-dimensional tumor microenvironments recapitulate phenotypic features and differential drug response in early vs. advanced stage breast cancer. *ACS Biomaterials Science & Engineering*
100. Hubner, R., Schmole, A. C., Liedmann, A., Frech, M. J., Rolfs, A., and Luo, J. (2010) Differentiation of human neural progenitor cells regulated by Wnt-3a. *Biochem Biophys Res Commun* **400**, 358-362
101. Guo, L., Rezvanian, A., Kukreja, L., Hoveydai, R., Bigio, E. H., Mesulam, M. M., El Khoury, J., and Geula, C. (2016) Postmortem Adult Human Microglia Proliferate in Culture to High Passage and Maintain Their Response to Amyloid-beta. *J Alzheimers Dis* **54**, 1157-1167
102. Guha D, N. P., Redinger C, Srinivasan A, Schatten GP and Ayyavoo V. (2012) Neuronal apoptosis by HIV-1 Vpr: contribution of proinflammatory molecular networks from infected target cells. *Journal of Neuroinflammation* **9**, 15
103. Lawson, L. J., Perry, V. H., Dri, P., and Gordon, S. (1990) Heterogeneity in the distribution and morphology of microglia in the normal adult mouse brain. *Neuroscience* **39**, 151-170
104. Worsdorfer, P., Dalda, N., Kern, A., Kruger, S., Wagner, N., Kwok, C. K., Henke, E., and Ergun, S. (2019) Generation of complex human organoid models including vascular networks by incorporation of mesodermal progenitor cells. *Sci Rep* **9**, 15663

105. Bystron, I., Blakemore, C., and Rakic, P. (2008) Development of the human cerebral cortex: Boulder Committee revisited. *Nat Rev Neurosci* **9**, 110-122
106. Sardar, A. M., Hutson, P. H., and Reynolds, G. P. (1999) Deficits of NMDA receptors and glutamate uptake sites in the frontal cortex in AIDS. *Neuroreport* **10**, 3513-3515
107. Haughey, N. J., Nath, A., Mattson, M. P., Slevin, J. T., and Geiger, J. D. (2001) HIV-1 Tat through phosphorylation of NMDA receptors potentiates glutamate excitotoxicity. *J Neurochem* **78**, 457-467
108. Potter, M. C., Figuera-Losada, M., Rojas, C., and Slusher, B. S. (2013) Targeting the glutamatergic system for the treatment of HIV-associated neurocognitive disorders. *J Neuroimmune Pharmacol* **8**, 594-607
109. Wallet, C., De Rovere, M., Van Assche, J., Daouad, F., De Wit, S., Gautier, V., Mallon, P. W. G., Marcello, A., Van Lint, C., Rohr, O., and Schwartz, C. (2019) Microglial Cells: The Main HIV-1 Reservoir in the Brain. *Front Cell Infect Microbiol* **9**, 362
110. Ko, A., Kang, G., Hattler, J. B., Galadima, H. I., Zhang, J., Li, Q., and Kim, W. K. (2019) Macrophages but not Astrocytes Harbor HIV DNA in the Brains of HIV-1-Infected Aviremic Individuals on Suppressive Antiretroviral Therapy. *J Neuroimmune Pharmacol* **14**, 110-119
111. Wheeler, E. D., Achim, C. L., and Ayyavoo, V. (2006) Immunodetection of human immunodeficiency virus type 1 (HIV-1) Vpr in brain tissue of HIV-1 encephalitic patients. *J Neurovirol* **12**, 200-210
112. John G Walsh, S. N. R., Manmeet K Mamik, Brienne A McKenzie, Ferdinand Maingat, William G Branton, David I Broadhurst and Christopher Power. (2014) Rapid inflammasome activation in microglia contributes to brain disease in HIV/AIDS. *Retrovirology* **11**, 18
113. Garden, G. A. (2002) Microglia in human immunodeficiency virus-associated neurodegeneration. *Glia* **40**, 240-251
114. Achim, C. L., Heyes, M. P., and Wiley, C. A. (1993) Quantitation of human immunodeficiency virus, immune activation factors, and quinolinic acid in AIDS brains. *J Clin Invest* **91**, 2769-2775
115. Ton, H., and Xiong, H. (2013) Astrocyte Dysfunctions and HIV-1 Neurotoxicity. *J AIDS Clin Res* **4**, 255
116. Abud, E. M., Ramirez, R. N., Martinez, E. S., Healy, L. M., Nguyen, C. H. H., Newman, S. A., Yeromin, A. V., Scarfone, V. M., Marsh, S. E., Fimbres, C., Caraway, C. A., Fote, G. M., Madany, A. M., Agrawal, A., Kayed, R., Gylys, K. H., Cahalan, M. D., Cummings, B. J., Antel, J. P., Mortazavi, A., Carson, M. J., Poon, W. W., and Blurton-Jones, M. (2017) iPSC-Derived Human Microglia-like Cells to Study Neurological Diseases. *Neuron* **94**, 278-293 e279
117. Sloan, S. A., Andersen, J., Pasca, A. M., Birey, F., and Pasca, S. P. (2018) Generation and assembly of human brain region-specific three-dimensional cultures. *Nat Protoc* **13**, 2062-2085
118. Birey, F., Andersen, J., Makinson, C. D., Islam, S., Wei, W., Huber, N., Fan, H. C., Metzler, K. R. C., Panagiotakos, G., Thom, N., O'Rourke, N. A., Steinmetz, L. M., Bernstein, J. A., Hallmayer, J., Huguenard, J. R., and Pasca, S. P. (2017) Assembly of functionally integrated human forebrain spheroids. *Nature* **545**, 54-59

119. Lancaster, M. A., Corsini, N. S., Wolfinger, S., Gustafson, E. H., Phillips, A. W., Burkard, T. R., Otani, T., Livesey, F. J., and Knoblich, J. A. (2017) Guided self-organization and cortical plate formation in human brain organoids. *Nat Biotechnol* **35**, 659-666
120. Yoon, S. J., Elahi, L. S., Pasca, A. M., Marton, R. M., Gordon, A., Revah, O., Miura, Y., Walczak, E. M., Holdgate, G. M., Fan, H. C., Huguenard, J. R., Geschwind, D. H., and Pasca, S. P. (2019) Reliability of human cortical organoid generation. *Nat Methods* **16**, 75-78
121. Peterson, S. E., and Loring, J. F. (2014) Genomic instability in pluripotent stem cells: implications for clinical applications. *J Biol Chem* **289**, 4578-4584
122. Hu, B. Y., Weick, J. P., Yu, J., Ma, L. X., Zhang, X. Q., Thomson, J. A., and Zhang, S. C. (2010) Neural differentiation of human induced pluripotent stem cells follows developmental principles but with variable potency. *Proc Natl Acad Sci U S A* **107**, 4335-4340
123. Terrasso, A. P., Pinto, C., Serra, M., Filipe, A., Almeida, S., Ferreira, A. L., Pedroso, P., Brito, C., and Alves, P. M. (2015) Novel scalable 3D cell based model for in vitro neurotoxicity testing: Combining human differentiated neurospheres with gene expression and functional endpoints. *J Biotechnol* **205**, 82-92
124. Jorfi, M., D'Avanzo, C., Tanzi, R. E., Kim, D. Y., and Irimia, D. (2018) Human Neurospheroid Arrays for In Vitro Studies of Alzheimer's Disease. *Sci Rep* **8**, 2450
125. Balmiki Ray, N. C., Justin M Long and debomoy K Lahiri. (2014) Human primary mixed brain cultures: preparation, differentiation, characterization and application to neuroscience research. *Molecular Brain* **7**, 15
126. Murphy, A. R., Laslett, A., O'Brien, C. M., and Cameron, N. R. (2017) Scaffolds for 3D in vitro culture of neural lineage cells. *Acta Biomater* **54**, 1-20
127. Muffat, J., Li, Y., Omer, A., Durbin, A., Bosch, I., Bakiasi, G., Richards, E., Meyer, A., Gehrke, L., and Jaenisch, R. (2018) Human induced pluripotent stem cell-derived glial cells and neural progenitors display divergent responses to Zika and dengue infections. *Proc Natl Acad Sci U S A* **115**, 7117-7122
128. Abreu, C. M., Gama, L., Krasemann, S., Chesnut, M., Odwin-Dacosta, S., Hogberg, H. T., Hartung, T., and Pamies, D. (2018) Microglia Increase Inflammatory Responses in iPSC-Derived Human BrainSpheres. *Front Microbiol* **9**, 2766
129. Hanisch, U. K. (2002) Microglia as a source and target of cytokines. *Glia* **40**, 140-155
130. Welser-Alves, J. V., and Milner, R. (2013) Microglia are the major source of TNF-alpha and TGF-beta1 in postnatal glial cultures; regulation by cytokines, lipopolysaccharide, and vitronectin. *Neurochem Int* **63**, 47-53
131. G.J. Nuovo, F. G., P. MacConnell and A. Braun. (1994) In Situ Detection of Polymerase Chain Reaction-Amplified HIV-1 Nucleic Acids and Tumor Necrosis Factor-a RNA inthe Central

Nervous System. *American Journal of Pathology* **144**, 8

132. Mamik, M. K., Hui, E., Branton, W. G., McKenzie, B. A., Chisholm, J., Cohen, E. A., and Power, C. (2017) HIV-1 Viral Protein R Activates NLRP3 Inflammasome in Microglia: implications for HIV-1 Associated Neuroinflammation. *J Neuroimmune Pharmacol* **12**, 233-248
133. Russell, R. A., Chojnacki, J., Jones, D. M., Johnson, E., Do, T., Eggeling, C., Padilla-Parra, S., and Sattentau, Q. J. (2017) Astrocytes Resist HIV-1 Fusion but Engulf Infected Macrophage Material. *Cell Rep* **18**, 1473-1483

134. Liddelow, S. A., Guttenplan, K. A., Clarke, L. E., Bennett, F. C., Bohlen, C. J., Schirmer, L., Bennett, M. L., Munch, A. E., Chung, W. S., Peterson, T. C., Wilton, D. K., Frouin, A., Napier, B. A., Panicker, N., Kumar, M., Buckwalter, M. S., Rowitch, D. H., Dawson, V. L., Dawson, T. M., Stevens, B., and Barres, B. A. (2017) Neurotoxic reactive astrocytes are induced by activated microglia. *Nature* **541**, 481-487
135. Di Filippo, M., Sarchielli, P., Picconi, B., and Calabresi, P. (2008) Neuroinflammation and synaptic plasticity: theoretical basis for a novel, immune-centred, therapeutic approach to neurological disorders. *Trends Pharmacol Sci* **29**, 402-412
136. Hickman, S., Izzy, S., Sen, P., Morsett, L., and El Khoury, J. (2018) Microglia in neurodegeneration. *Nat Neurosci* **21**, 1359-1369
137. Ransohoff, R. M. (2016) How neuroinflammation contributes to neurodegeneration. *Science* **353**, 7
138. Lecours, C., Bordeleau, M., Cantin, L., Parent, M., Paolo, T. D., and Tremblay, M. E. (2018) Microglial Implication in Parkinson's Disease: Loss of Beneficial Physiological Roles or Gain of Inflammatory Functions? *Front Cell Neurosci* **12**, 282
139. K. A. Frankola, N. H. G., W. Luo and D. Tweedie. (2011) Targeting TNF-alpha to elucidate and ameliorate neuroinflammation in neurodegenerative diseases. *CNS Neurol Disord Drug Targets* **10**, 13
140. Bissel, S. J., and Wiley, C. A. (2004) Human immunodeficiency virus infection of the brain: pitfalls in evaluating infected/affected cell populations. *Brain Pathol* **14**, 97-108
141. Whitlock JR, H. A., Shuler MG, Bear MF. (2006) Learning Induces Long-Term Potentiation in the Hippocampus. *Science* **313**, 5
142. Behnisch T, F. W., Sanna PP. (2004) HIV secreted protein Tat prevents long-term potentiation in the hippocampal CA1 region. *Brain Res* **1012**, 3
143. Dong, J., and Xiong, H. (2006) Human immunodeficiency virus type 1 gp120 inhibits long-term potentiation via chemokine receptor CXCR4 in rat hippocampal slices. *J Neurosci Res* **83**, 489-496
144. Xiong, H., Zeng YC, Zheng J, Thylin M and Gendelman HE. (1999) Soluble HIV-1 infected macrophage secretory products mediate blockade of long-term potentiation: a mechanism for cognitive dysfunction in HIV-1-associated dementia. *Journal of Neurovirology* **5**, 10
145. Rodriguez-Sanchez, P., Tejero-Diez, P., and Diez-Guerra, F. J. (1997) Glutamate stimulates neurogranin phosphorylation in cultured rat hippocampal neurons. *Neurosci Lett* **221**, 137-140
146. Huang, K. P., Huang, F. L., Jager, T., Li, J., Reymann, K. G., and Balschun, D. (2004) Neurogranin/RC3 enhances long-term potentiation and learning by promoting calcium-mediated signaling. *J Neurosci* **24**, 10660-10669
147. Jones, K. J., Templet, S., Zemoura, K., Kuzniewska, B., Pena, F. X., Hwang, H., Lei, D. J., Haensgen, H., Nguyen, S., Saenz, C., Lewis, M., Dziembowska, M., and Xu, W. (2018) Rapid, experience-dependent translation of neurogranin enables memory encoding. *Proc Natl Acad Sci U S A* **115**, E5805-E5814
148. Miyakawa, T., Yared, E., Pak, J. H., Huang, F. L., Huang, K. P., and Crawley, J. N. (2001) Neurogranin null mutant mice display performance deficits on spatial learning tasks with anxiety related components. *Hippocampus* **11**, 763-775
149. Pak, J. H., Huang, F. L., Li, J., Balschun, D., Reymann, K. G., Chiang, C., Westphal, H., and Huang, K. P. (2000) Involvement of neurogranin in the modulation of

calcium/calmodulin-dependent protein kinase II, synaptic plasticity, and spatial learning: a study with knockout mice. *Proc Natl Acad Sci U S A* **97**, 11232-11237
150. De Vos, A., Struyfs, H., Jacobs, D., Fransen, E., Klewansky, T., De Roeck, E., Robberecht, C., Van Broeckhoven, C., Duyckaerts, C., Engelborghs, S., and Vanmechelen, E. (2016) The Cerebrospinal Fluid Neurogranin/BACE1 Ratio is a Potential Correlate of Cognitive Decline in Alzheimer's Disease. *J Alzheimers Dis* **53**, 1523-1538
151. Hellwig, K., Kvartsberg, H., Portelius, E., Andreasson, U., Oberstein, T. J., Lewczuk, P., Blennow, K., Kornhuber, J., Maler, J. M., Zetterberg, H., and Spitzer, P. (2015) Neurogranin and YKL-40: independent markers of synaptic degeneration and neuroinflammation in Alzheimer's disease. *Alzheimers Res Ther* **7**, 74
152. Kester, M. I., Teunissen, C. E., Crimmins, D. L., Herries, E. M., Ladenson, J. H., Scheltens, P., van der Flier, W. M., Morris, J. C., Holtzman, D. M., and Fagan, A. M. (2015) Neurogranin as a Cerebrospinal Fluid Biomarker for Synaptic Loss in Symptomatic Alzheimer Disease. *JAMA Neurol* **72**, 1275-1280
153. Kvartsberg, H., Duits, F. H., Ingelsson, M., Andreasen, N., Ohrfelt, A., Andersson, K., Brinkmalm, G., Lannfelt, L., Minthon, L., Hansson, O., Andreasson, U., Teunissen, C. E., Scheltens, P., Van der Flier, W. M., Zetterberg, H., Portelius, E., and Blennow, K. (2015) Cerebrospinal fluid levels of the synaptic protein neurogranin correlates with cognitive decline in prodromal Alzheimer's disease. *Alzheimers Dement* **11**, 1180-1190
154. Thorsell, A., Bjerke, M., Gobom, J., Brunhage, E., Vanmechelen, E., Andreasen, N., Hansson, O., Minthon, L., Zetterberg, H., and Blennow, K. (2010) Neurogranin in cerebrospinal fluid as a marker of synaptic degeneration in Alzheimer's disease. *Brain Res* **1362**, 13-22
155. LIU, Y., JONES M, HINGTGEN CM, BU G, LARIBEE N, TANZ RE, MOIR RD, NATH A & HE JJ. (2000) Uptake of HIV-1 Tat protein mediated by low-density lipoprotein receptor-related protein disrupts the neuronal metabolic balance of the receptor ligands. *Nature Medicine* **6**, 8
156. Barzon, L., Trevisan, M., Sinigaglia, A., Lavezzo, E., and Palu, G. (2016) Zika virus: from pathogenesis to disease control. *FEMS Microbiol Lett* **363**
157. Dos Reis, R. S., Sant, S., Keeney, H., Wagner, M. C. E., and Ayyavoo, V. (2020) Modeling HIV-1 neuropathogenesis using three-dimensional human brain organoids (hBORGs) with HIV-1 infected microglia. *Sci Rep* **10**, 15209
158. Matesic, D. F., and Lin, R. C. S. (1994) Microtubule-Associated Protein-2 as an Early Indicator of Ischemia-Induced Neurodegeneration in the Gerbil Forebrain. *Journal of Neurochemistry* **63**, 1012-1020
159. Yin, J., Valin, K. L., Dixon, M. L., and Leavenworth, J. W. (2017) The Role of Microglia and Macrophages in CNS Homeostasis, Autoimmunity, and Cancer. *J Immunol Res* **2017**, 5150678
160. Hadi, K., Walker, L. A., Guha, D., Murali, R., Watkins, S. C., Tarwater, P., Srinivasan, A., and Ayyavoo, V. (2014) Human immunodeficiency virus type 1 Vpr polymorphisms associated with progressor and nonprogressor individuals alter Vpr-associated functions. *J Gen Virol* **95**, 700-711
161. Venkatachari, N. J., Jain, S., Walker, L., Bivalkar-Mehla, S., Chattopadhyay, A., Bar-Joseph, Z., Rinaldo, C., Ragin, A., Seaberg, E., Levine, A., Becker, J., Martin, E., Sacktor, N., and Ayyavoo, V. (2017) Transcriptome analyses identify key cellular factors associated with HIV-1-associated neuropathogenesis in infected men. *AIDS* **31**, 623-633

162. Yoshioka M, B. W., Shapshak P, Nagano I, Stewart RV, Xin KQ, Srivastava AK, Nakamura S. . (1995) Role of immune activation and cytokine expression in HIV-l-associated neurologic diseases *Advances in Neuroimmunology* **5**, 24
163. Guadano-Ferraz, A., Escamez, M. J., Morte, B., Vargiu, P., and Bernal, J. (1997) Transcriptional induction of RC3/neurogranin by thyroid hormone: differential neuronal sensitivity is not correlated with thyroid hormone receptor distribution in the brain. *Brain Res Mol Brain Res* **49**, 37-44
164. Iniguez, M. A., De Lecea, L., Guadano-Ferraz, A., Morte, B., Gerendasy, D., Sutcliffe, J. G., and Bernal, J. (1996) Cell-specific effects of thyroid hormone on RC3/neurogranin expression in rat brain. *Endocrinology* **137**, 1032-1041
165. Iniguez, M. A., Rodriguez-Pena, A., Ibarrola, N., Morreale de Escobar, G., and Bernal, J. (1992) Adult rat brain is sensitive to thyroid hormone. Regulation of RC3/neurogranin mRNA. *J Clin Invest* **90**, 554-558
166. Gao, Y., Tatavarty, V., Korza, G., Levin, M. K., and Carson, J. H. (2008) Multiplexed dendritic targeting of alpha calcium calmodulin-dependent protein kinase II, neurogranin, and activity-regulated cytoskeleton-associated protein RNAs by the A2 pathway. *Mol Biol Cell* **19**, 2311-2327
167. Schuman, E. M., Dynes, J. L., and Steward, O. (2006) Synaptic regulation of translation of dendritic mRNAs. *J Neurosci* **26**, 7143-7146
168. Minghetti, L. (2005) Role of inflammation in neurodegenerative diseases. *Curr Opin Neurol* **18**, 315-321
169. Minghetti, L., Ajmone-Cat, M. A., De Berardinis, M. A., and De Simone, R. (2005) Microglial activation in chronic neurodegenerative diseases: roles of apoptotic neurons and chronic stimulation. *Brain Res Brain Res Rev* **48**, 251-256
170. Lynch, M. A. (1998) Age-related impairment in long-term potentiation in hippocampus: a role for the cytokine, interleukin-1 beta? *Prog Neurobiol* **56**, 571-589
171. Trompet, S., de Craen, A. J., Slagboom, P., Shepherd, J., Blauw, G. J., Murphy, M. B., Bollen, E. L., Buckley, B. M., Ford, I., Gaw, A., Macfarlane, P. W., Packard, C. J., Stott, D. J., Jukema, J. W., Westendorp, R. G., and Group, P. (2008) Genetic variation in the interleukin-1 beta-converting enzyme associates with cognitive function. The PROSPER study. *Brain* **131**, 1069-1077
172. Youm, Y. H., Grant, R. W., McCabe, L. R., Albarado, D. C., Nguyen, K. Y., Ravussin, A., Pistell, P., Newman, S., Carter, R., Laque, A., Munzberg, H., Rosen, C. J., Ingram, D. K., Salbaum, J. M., and Dixit, V. D. (2013) Canonical Nlrp3 inflammasome links systemic low-grade inflammation to functional decline in aging. *Cell Metab* **18**, 519-532
173. Guha, D., Nagilla, P., Redinger, C., Srinivasan, A., Schatten, G. P., and Ayyavoo, V. (2012) Neuronal apoptosis by HIV-1 Vpr: contribution of proinflammatory molecular networks from infected target cells. *J Neuroinflammation* **9**, 138
174. Krug, A., Krach, S., Jansen, A., Nieratschker, V., Witt, S. H., Shah, N. J., Nothen, M. M., Rietschel, M., and Kircher, T. (2013) The effect of neurogranin on neural correlates of episodic memory encoding and retrieval. *Schizophr Bull* **39**, 141-150
175. Petersen, A., and Gerges, N. Z. (2015) Neurogranin regulates CaM dynamics at dendritic spines. *Sci Rep* **5**, 11135
176. Zhabotinsky, A. M., Camp, R. N., Epstein, I. R., and Lisman, J. E. (2006) Role of the neurogranin concentrated in spines in the induction of long-term potentiation. *J Neurosci* **26**, 7337-7347

177. Zhong, L., Cherry, T., Bies, C. E., Florence, M. A., and Gerges, N. Z. (2009) Neurogranin enhances synaptic strength through its interaction with calmodulin. *EMBO J* **28**, 3027-3039
178. Zhong, L., and Gerges, N. Z. (2012) Neurogranin targets calmodulin and lowers the threshold for the induction of long-term potentiation. *PLoS One* **7**, e41275
179. Derrien, T., Johnson, R., Bussotti, G., Tanzer, A., Djebali, S., Tilgner, H., Guernec, G., Martin, D., Merkel, A., Knowles, D. G., Lagarde, J., Veeravalli, L., Ruan, X., Ruan, Y., Lassmann, T., Carninci, P., Brown, J. B., Lipovich, L., Gonzalez, J. M., Thomas, M., Davis, C. A., Shiekhattar, R., Gingeras, T. R., Hubbard, T. J., Notredame, C., Harrow, J., and Guigo, R. (2012) The GENCODE v7 catalog of human long noncoding RNAs: analysis of their gene structure, evolution, and expression. *Genome Res* **22**, 1775-1789
180. Djebali, S., Davis, C. A., Merkel, A., Dobin, A., Lassmann, T., Mortazavi, A., Tanzer, A., Lagarde, J., Lin, W., Schlesinger, F., Xue, C., Marinov, G. K., Khatun, J., Williams, B. A., Zaleski, C., Rozowsky, J., Roder, M., Kokocinski, F., Abdelhamid, R. F., Alioto, T., Antoshechkin, I., Baer, M. T., Bar, N. S., Batut, P., Bell, K., Bell, I., Chakrabortty, S., Chen, X., Chrast, J., Curado, J., Derrien, T., Drenkow, J., Dumais, E., Dumais, J., Duttagupta, R., Falconnet, E., Fastuca, M., Fejes-Toth, K., Ferreira, P., Foissac, S., Fullwood, M. J., Gao, H., Gonzalez, D., Gordon, A., Gunawardena, H., Howald, C., Jha, S., Johnson, R., Kapranov, P., King, B., Kingswood, C., Luo, O. J., Park, E., Persaud, K., Preall, J. B., Ribeca, P., Risk, B., Robyr, D., Sammeth, M., Schaffer, L., See, L. H., Shahab, A., Skancke, J., Suzuki, A. M., Takahashi, H., Tilgner, H., Trout, D., Walters, N., Wang, H., Wrobel, J., Yu, Y., Ruan, X., Hayashizaki, Y., Harrow, J., Gerstein, M., Hubbard, T., Reymond, A., Antonarakis, S. E., Hannon, G., Giddings, M. C., Ruan, Y., Wold, B., Carninci, P., Guigo, R., and Gingeras, T. R. (2012) Landscape of transcription in human cells. *Nature* **489**, 101-108
181. Morris, K. V., and Mattick, J. S. (2014) The rise of regulatory RNA. *Nat Rev Genet* **15**, 423-437
182. Earls, L. R., Westmoreland, J. J., and Zakharenko, S. S. (2014) Non-coding RNA regulation of synaptic plasticity and memory: implications for aging. *Ageing Res Rev* **17**, 34-42
183. Kung, J. T., Colognori, D., and Lee, J. T. (2013) Long noncoding RNAs: past, present, and future. *Genetics* **193**, 651-669
184. Rinn, J. L., and Chang, H. Y. (2012) Genome regulation by long noncoding RNAs. *Annu Rev Biochem* **81**, 145-166
185. Salta, E., and De Strooper, B. (2017) Noncoding RNAs in neurodegeneration. *Nat Rev Neurosci* **18**, 627-640
186. Barichievy, S., Naidoo, J., and Mhlanga, M. M. (2015) Non-coding RNAs and HIV: viral manipulation of host dark matter to shape the cellular environment. *Front Genet* **6**, 108
187. Duskova K, N. P., Le HS, Iyer P, Thalamuthu A, Martinson J, Bar-Joseph Z, Buchanan W, Rinaldo C, Ayyavoo V. (2013) MicroRNA regulation and its effects on cellular transcriptome in Human Immunodeficiency Virus-1 (HIV-1) infected individuals with distinct viral load and CD4 cell counts. *BMC Infectious Diseases* **13**, 18
188. Ojha, C. R., Rodriguez, M., Dever, S. M., Mukhopadhyay, R., and El-Hage, N. (2016) Mammalian microRNA: an important modulator of host-pathogen interactions in human viral infections. *J Biomed Sci* **23**, 74
189. Qureshi, I. A., and Mehler, M. F. (2011) Non-coding RNA networks underlying cognitive disorders across the lifespan. *Trends Mol Med* **17**, 337-346

190. Imam, H., Bano, A. S., Patel, P., Holla, P., and Jameel, S. (2015) The lncRNA NRON modulates HIV-1 replication in a NFAT-dependent manner and is differentially regulated by early and late viral proteins. *Sci Rep* **5**, 8639
191. Zhang, Q., Chen, C. Y., Yedavalli, V. S., and Jeang, K. T. (2013) NEAT1 long noncoding RNA and paraspeckle bodies modulate HIV-1 posttranscriptional expression. *MBio* **4**, e00596-00512
192. Torkzaban, B., Natarajaseenivasan, K., Mohseni Ahooyi, T., Shekarabi, M., Amini, S., Langford, T. D., and Khalili, K. (2020) The lncRNA LOC102549805 (U1) modulates neurotoxicity of HIV-1 Tat protein. *Cell Death Dis* **11**, 835
193. Carrieri, C., Cimatti, L., Biagioli, M., Beugnet, A., Zucchelli, S., Fedele, S., Pesce, E., Ferrer, I., Collavin, L., Santoro, C., Forrest, A. R., Carninci, P., Biffo, S., Stupka, E., and Gustincich, S. (2012) Long non-coding antisense RNA controls Uchl1 translation through an embedded SINEB2 repeat. *Nature* **491**, 454-457
194. Faghihi, M. A., and Wahlestedt, C. (2009) Regulatory roles of natural antisense transcripts. *Nat Rev Mol Cell Biol* **10**, 637-643
195. Clark, M. B., Johnston, R. L., Inostroza-Ponta, M., Fox, A. H., Fortini, E., Moscato, P., Dinger, M. E., and Mattick, J. S. (2012) Genome-wide analysis of long noncoding RNA stability. *Genome Res* **22**, 885-898
196. Pelechano, V., and Steinmetz, L. M. (2013) Gene regulation by antisense transcription. *Nat Rev Genet* **14**, 880-893
197. Modarresi, F., Faghihi, M. A., Lopez-Toledano, M. A., Fatemi, R. P., Magistri, M., Brothers, S. P., van der Brug, M. P., and Wahlestedt, C. (2012) Inhibition of natural antisense transcripts in vivo results in gene-specific transcriptional upregulation. *Nat Biotechnol* **30**, 453-459
198. Ma, H., Hao, Y., Dong, X., Gong, Q., Chen, J., Zhang, J., and Tian, W. (2012) Molecular mechanisms and function prediction of long noncoding RNA. *ScientificWorldJournal* **2012**, 541786
199. Qian, J., Lin, J., Luscombe, N. M., Yu, H., and Gerstein, M. (2003) Prediction of regulatory networks: genome-wide identification of transcription factor targets from gene expression data. *Bioinformatics* **19**, 1917-1926
200. Niland, C. N., Merry, C. R., and Khalil, A. M. (2012) Emerging Roles for Long Non-Coding RNAs in Cancer and Neurological Disorders. *Front Genet* **3**, 25
201. Feng, L., Liao, Y. T., He, J. C., Xie, C. L., Chen, S. Y., Fan, H. H., Su, Z. P., and Wang, Z. (2018) Plasma long non-coding RNA BACE1 as a novel biomarker for diagnosis of Alzheimer disease. *BMC Neurol* **18**, 4
202. Hamel, R., Dejarnac, O., Wichit, S., Ekchariyawat, P., Neyret, A., Luplertlop, N., Perera-Lecoin, M., Surasombatpattana, P., Talignani, L., Thomas, F., Cao-Lormeau, V. M., Choumet, V., Briant, L., Despres, P., Amara, A., Yssel, H., and Misse, D. (2015) Biology of Zika Virus Infection in Human Skin Cells. *J Virol* **89**, 8880-8896